# CAPP's High Mass Axion Searches and Heterodyne-Based Variance Method

Junu Jeong

Center for Axion and Precision Physics Research, Institute for Basic Science

ChatGPT: physicists discussing near a hotel at Busan Haeundae Beach in winter

CAPP
Center for Axion and Precision Physics Research

KAIST

부산대학교 PUSAN NATIONAL UNIVERSITY

ibs Institute for Basic Science

PNU-IBS workshop on Axion Physics : Search for axions, Dec 6th 2023 (Haeundae, Busan, South Korea)

# Outline

- Search for Dark Matter Axion
- CAPP’s High Mass Axion Searches
- Heterodyne-Based Variance Method

# What is Axion?

## Neutron

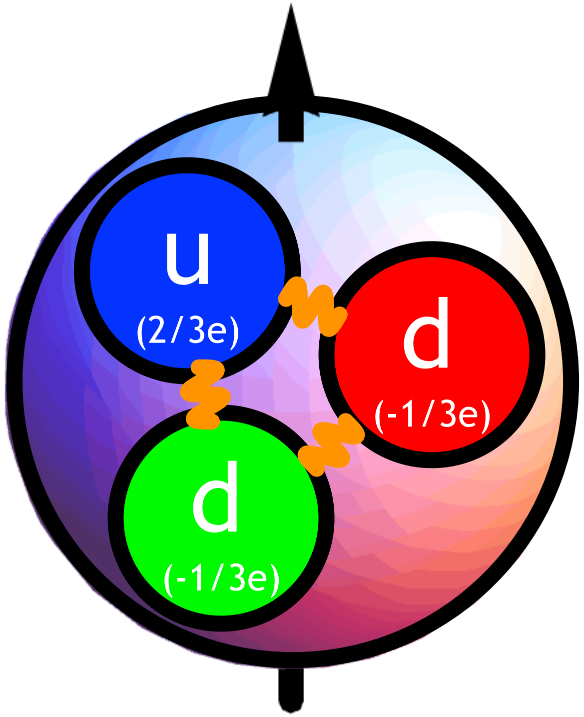


**CP-violating Lagrangian**

$$\mathcal{L}_\theta = \frac{g^2 \bar{\theta}}{32\pi^2} G^a_{\mu\nu} \tilde{G}^{a\mu\nu}$$

## Why no EDM for neutron and proton?

⇒ Spontaneous symmetry breaking of global U(1)

⇒ pesudo-Nambu-Goldstone Boson, **Axion**

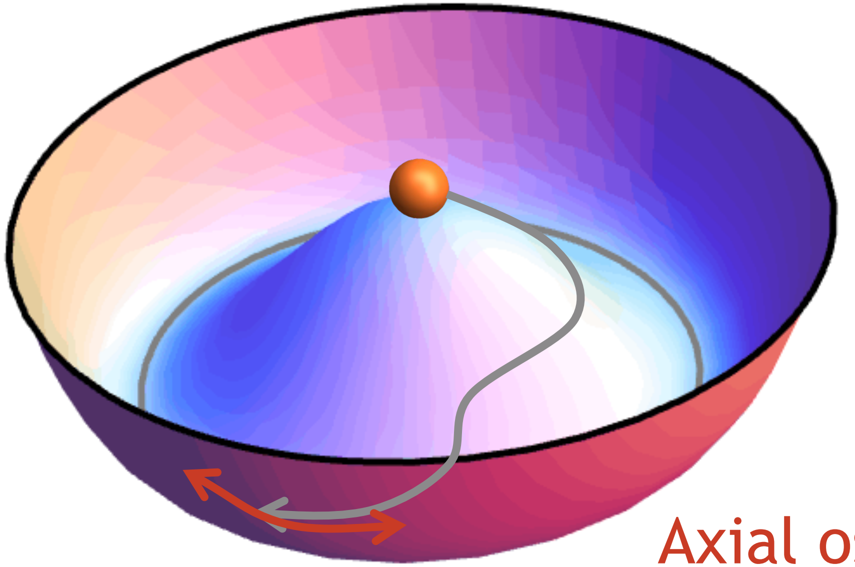

Axial oscillation

Titled Mexican-Hat Potential

# Dark Matter Axion

**Invisible axion** (KSVZ or DFSZ, mass less than meV)

- Feebly interacts with standard particles
- Non-relativistic in sufficient quantities

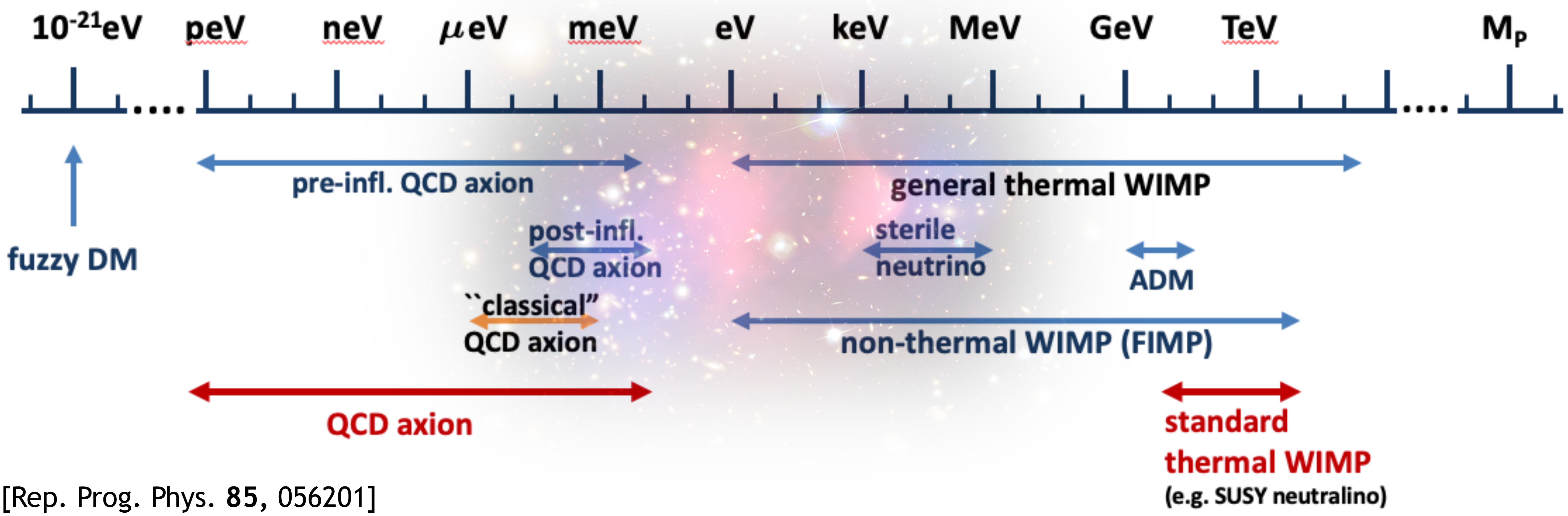


[Rep. Prog. Phys. **85**, 056201]

# Search for Dark Matter Axion

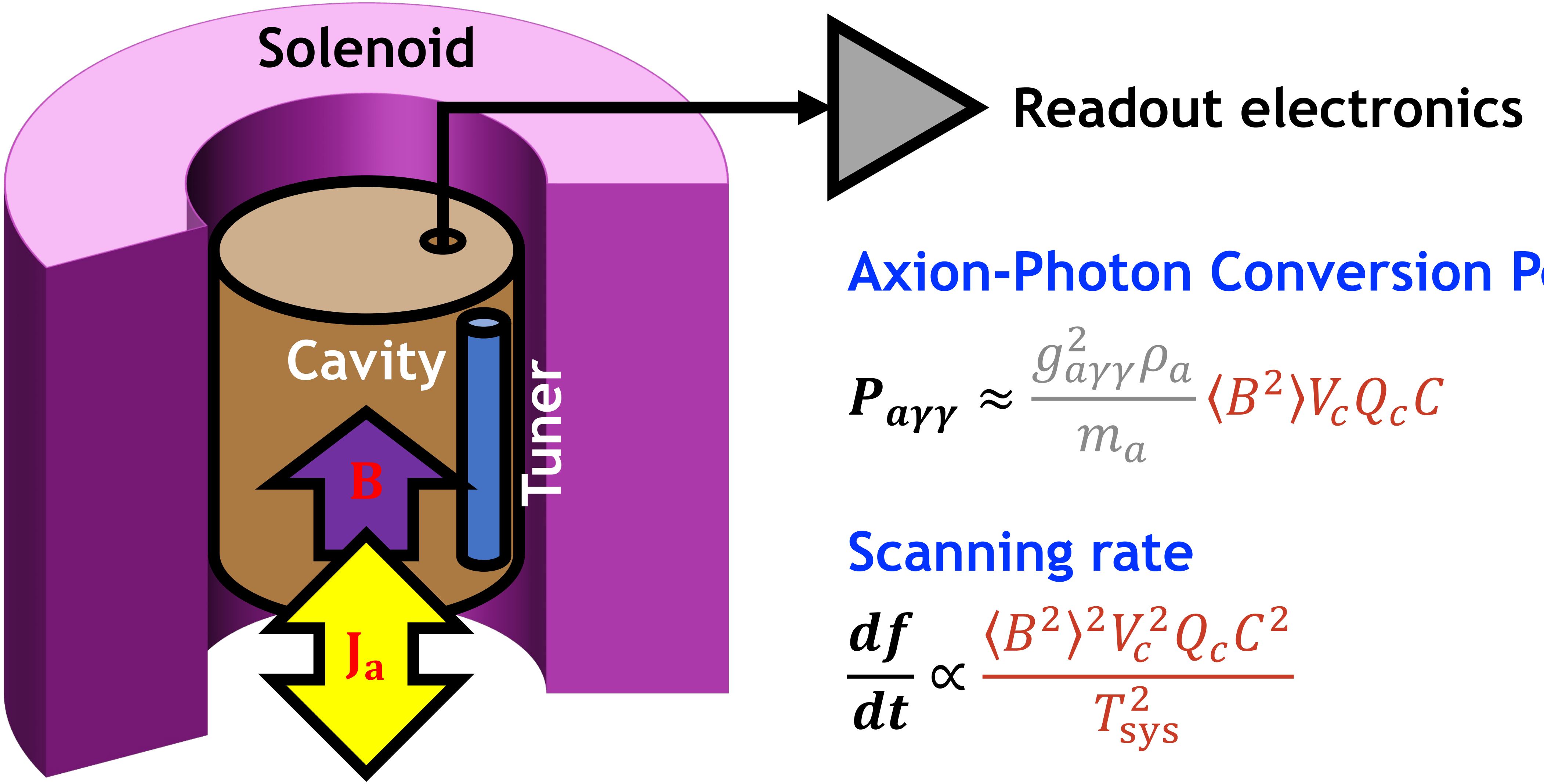


**Axion-Photon Conversion Power**

$$P_{a\gamma\gamma} \approx \frac{g_{a\gamma\gamma}^2 \rho_a}{m_a} \langle B^2 \rangle V_c Q_c C$$

**Scanning rate**

$$\frac{df}{dt} \propto \frac{\langle B^2 \rangle^2 V_c^2 Q_c C^2}{T_{sys}^2}$$

# Search for Dark Matter Axion

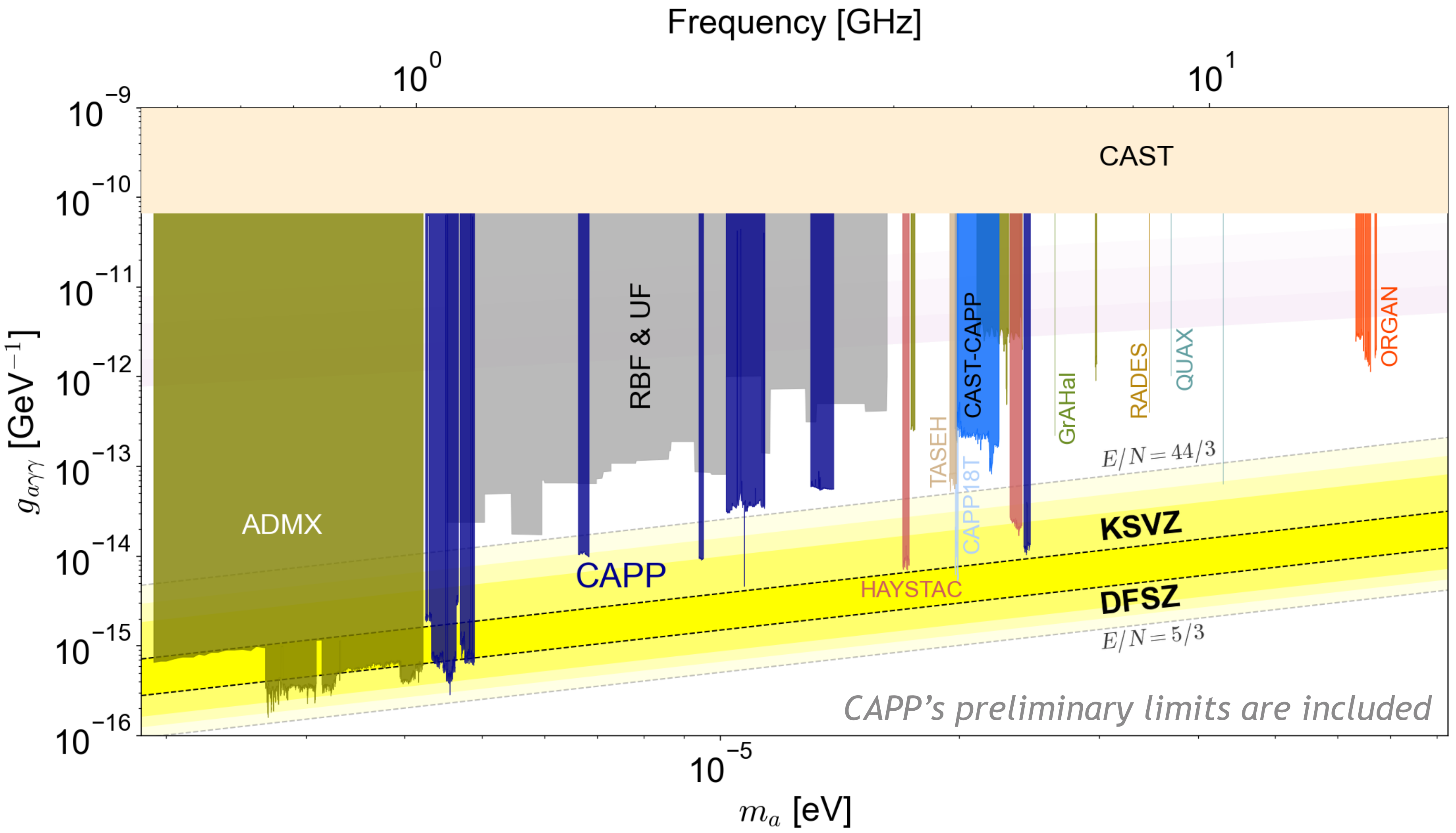

# CAPP's Dark Matter Axion Searches

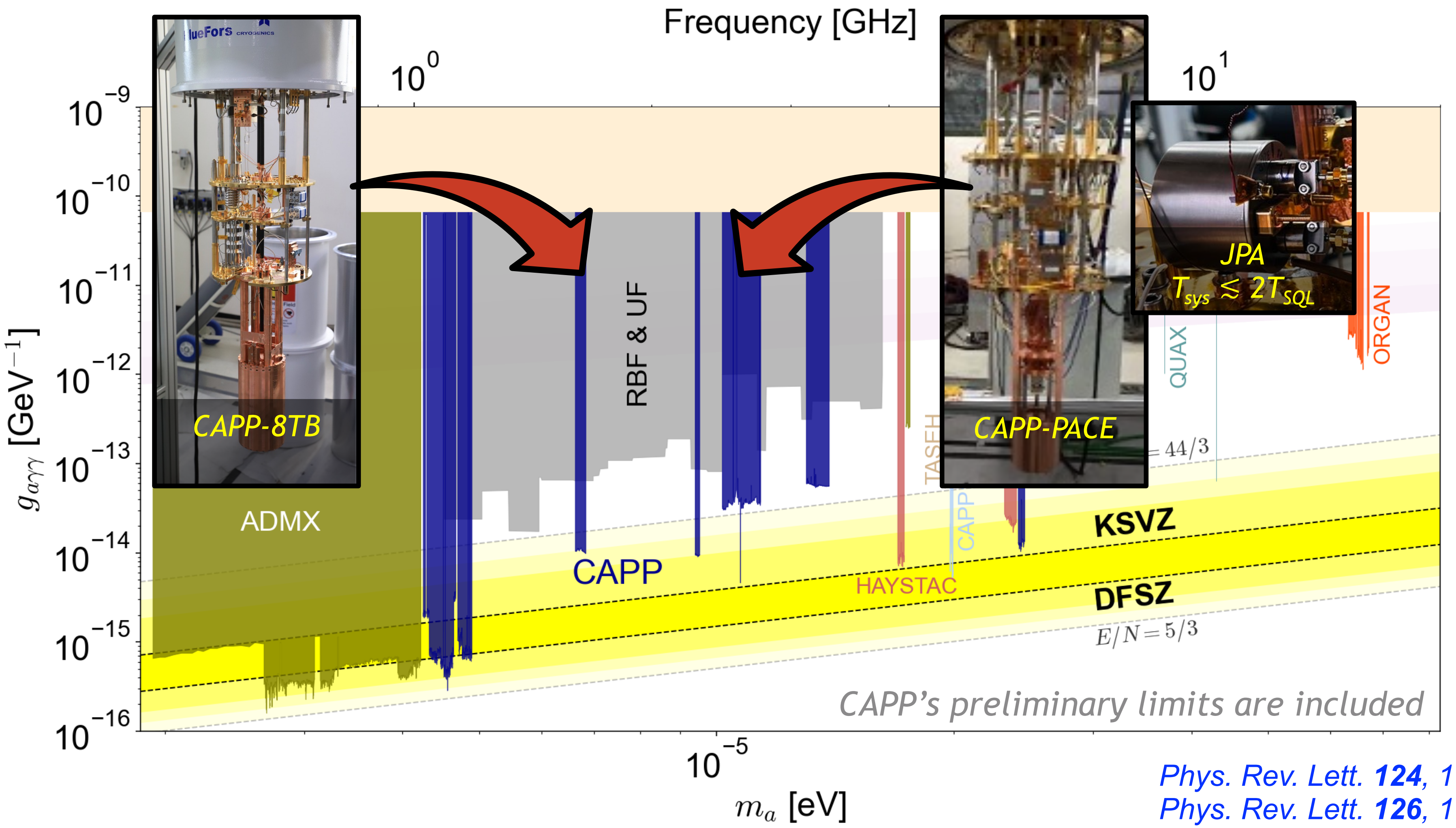


*Phys. Rev. Lett.* ***124***, *101802 (2020)*
*Phys. Rev. Lett.* ***126***, *191802 (2021)*
*Phys. Rev. Lett.* ***130***, *091602 (2023)*

# CAPP's Dark Matter Axion Searches

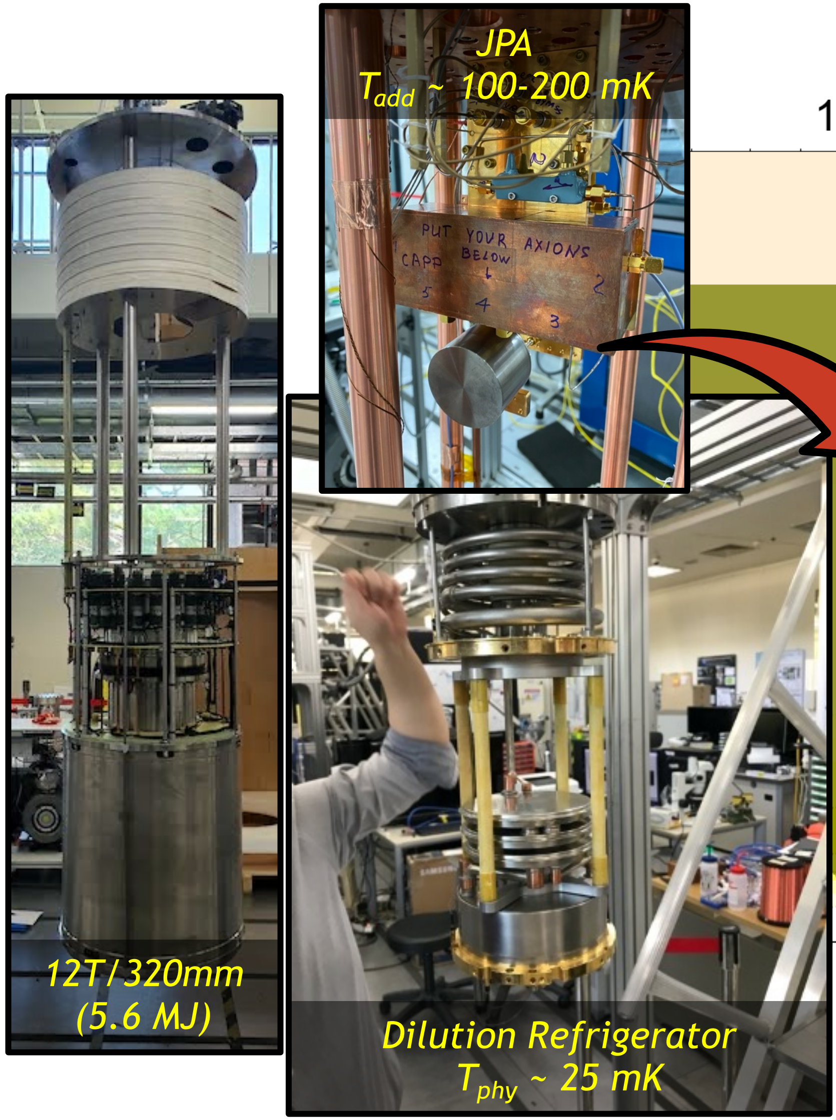


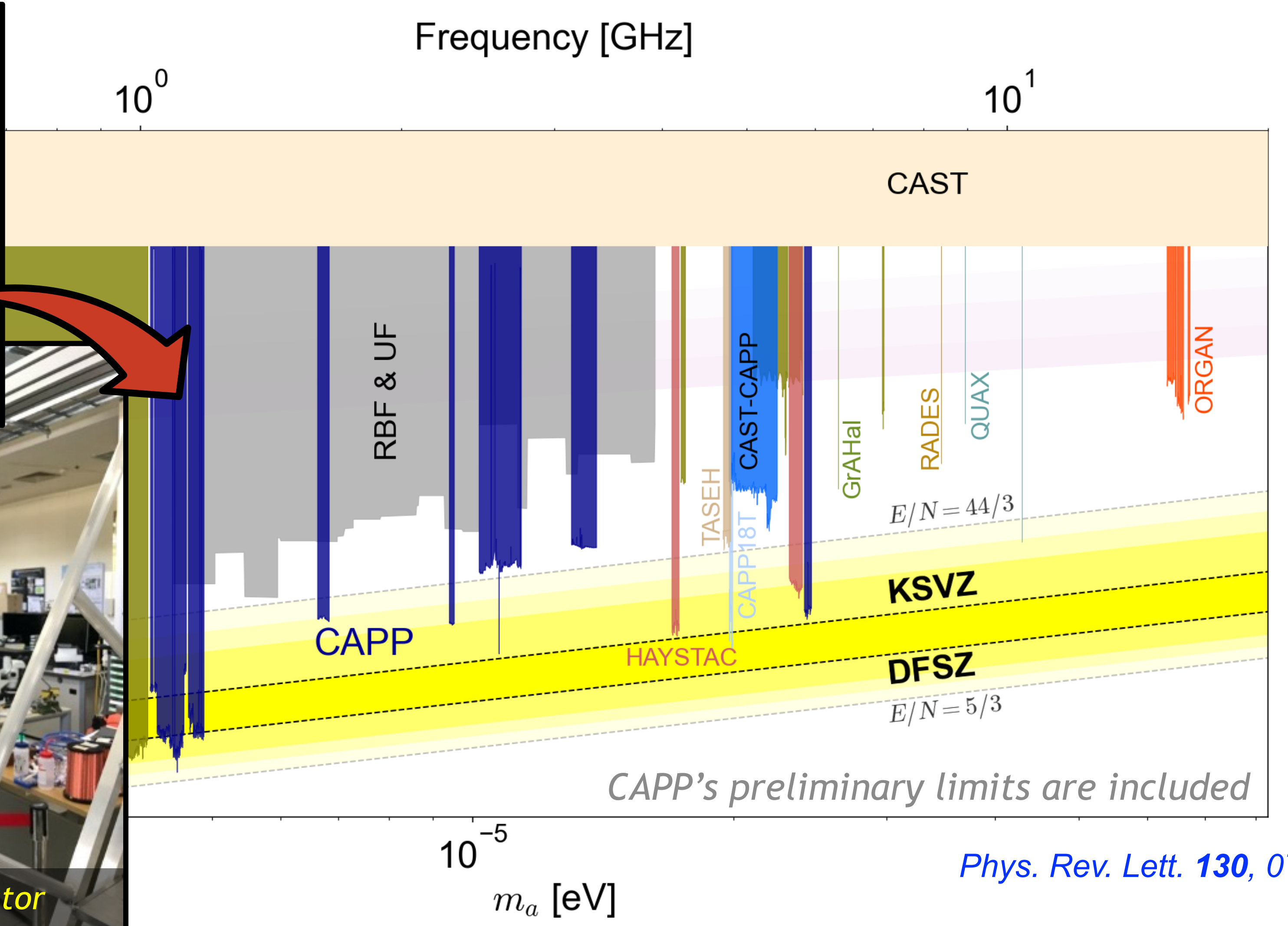


*Phys. Rev. Lett.* ***130***, *071002 (2023)*

# CAPP’s Dark Matter Axion Searches

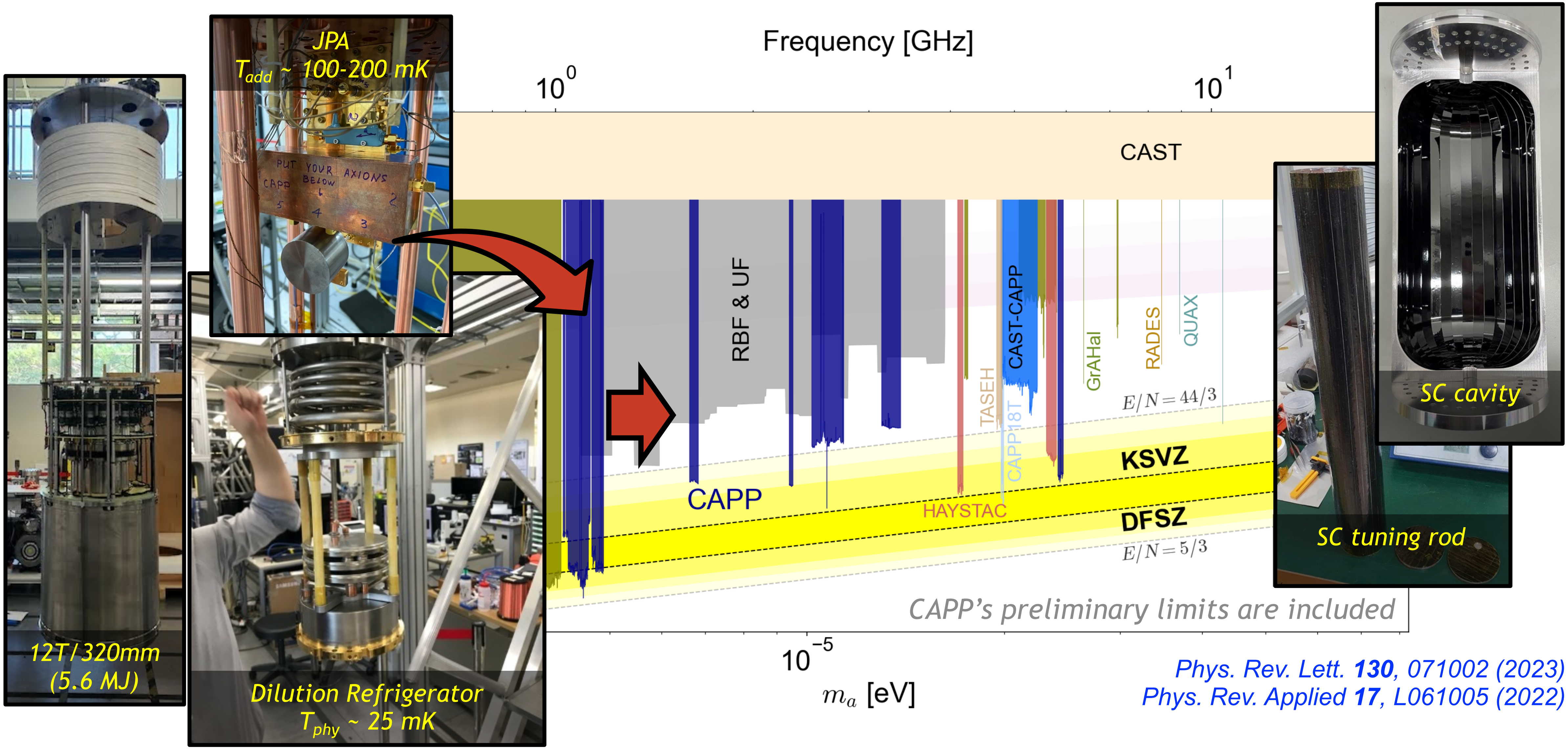


*Phys. Rev. Lett.* **130**, 071002 (2023)
*Phys. Rev. Applied* **17**, L061005 (2022)

# High Mass Axion Search

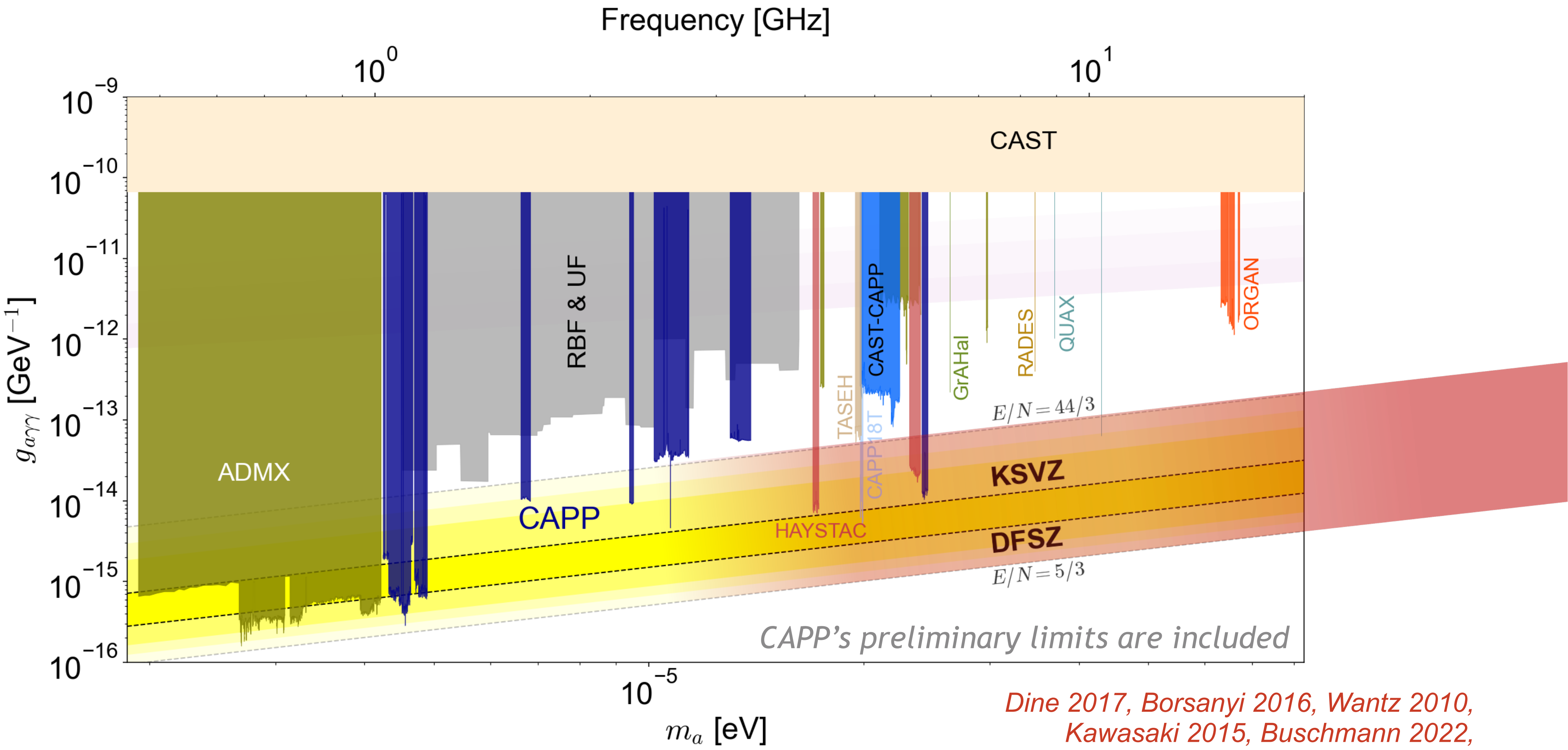


*Dine 2017, Borsanyi 2016, Wantz 2010,*
*Kawasaki 2015, Buschmann 2022,*
*Ballesteros 2017, Klaer 2017, …*

# CAPP's High Mass Axion Searches

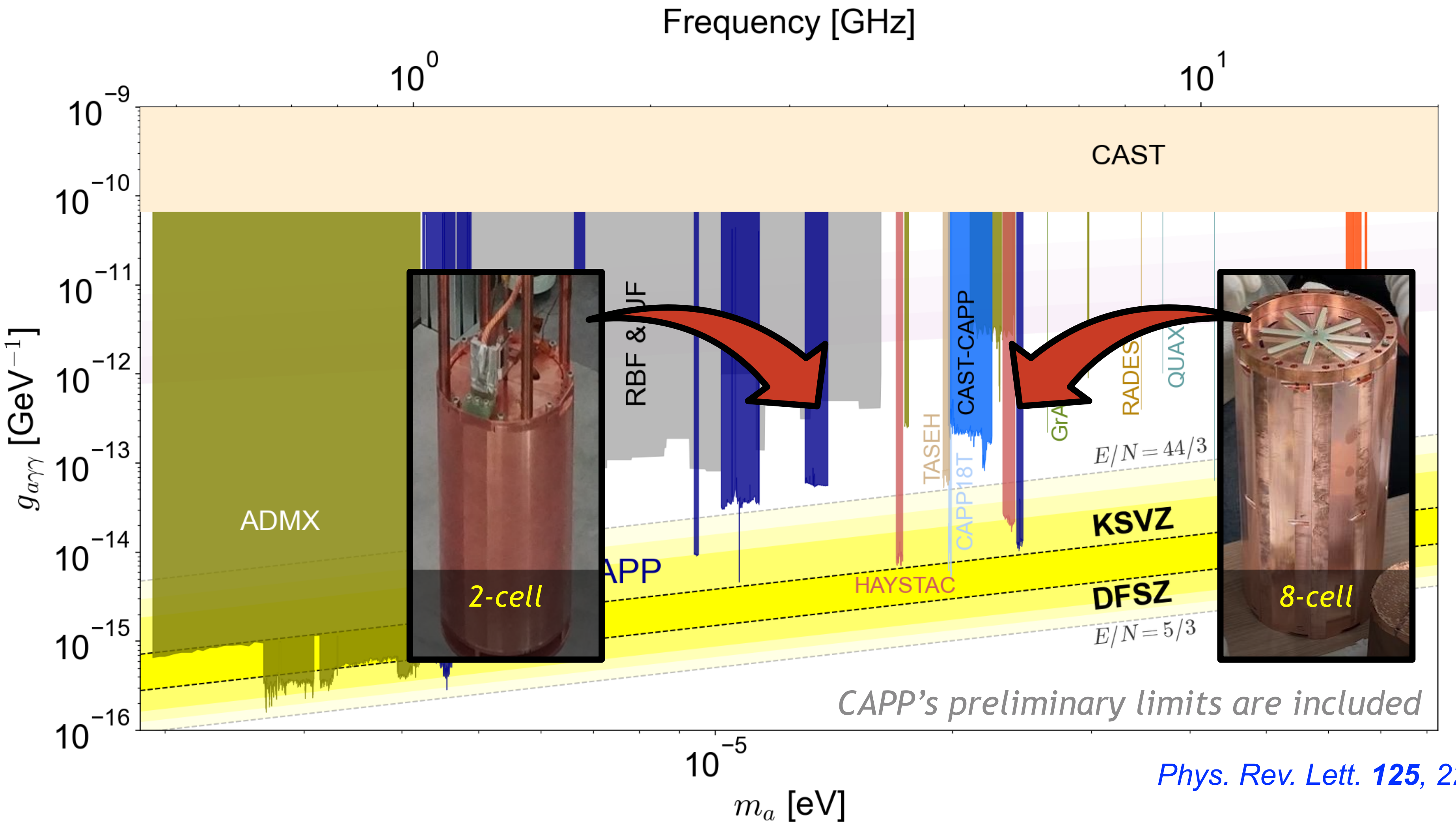


*Phys. Rev. Lett.* ***125***, *221302 (2020)*

# CAPP's High Mass Axion Searches

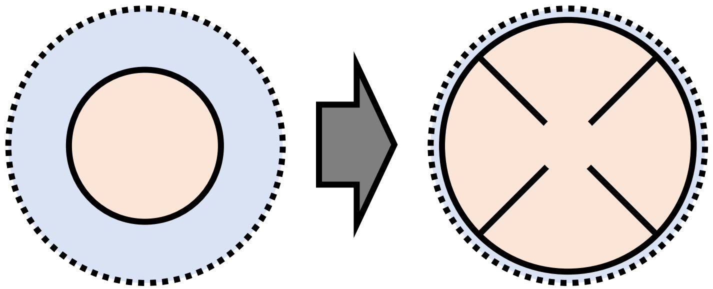

[Multiple-cell] Phys. Lett. B **777**, 412 (2018)

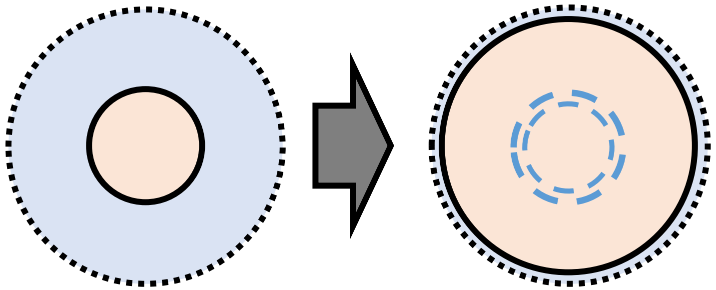

[Wheel] J. Phys. G **47**, 035203 (2020)

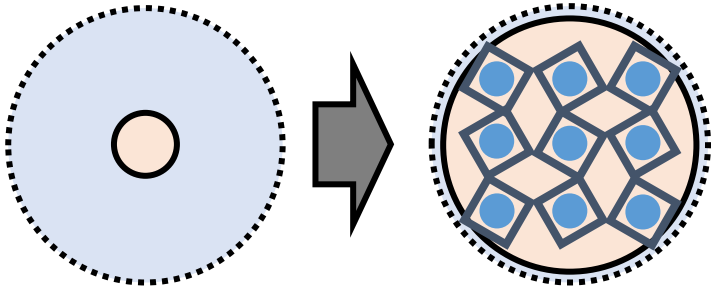

[PhC] Phys. Rev. D **107**, 015012 (2023)

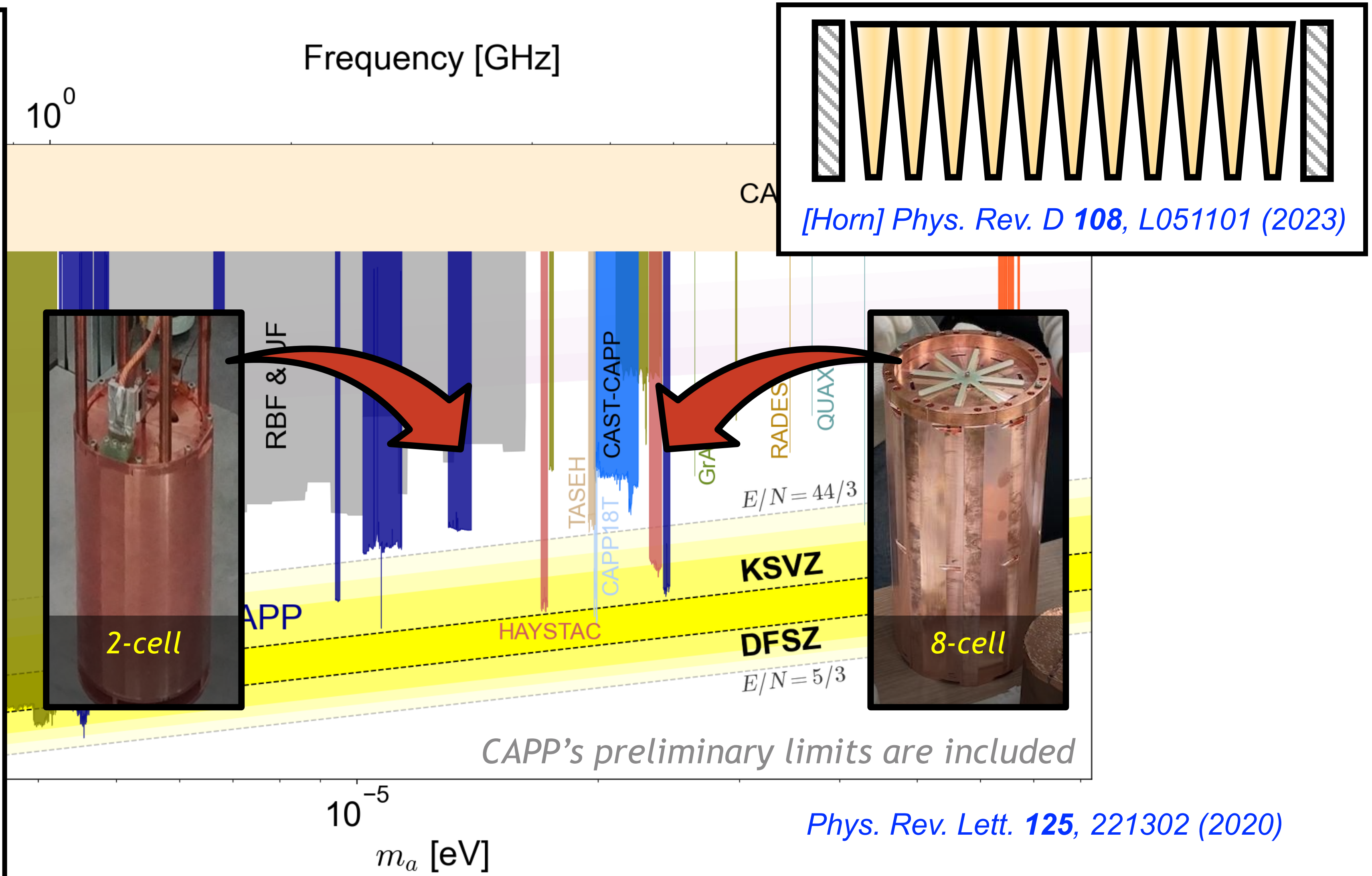


[Horn] Phys. Rev. D **108**, L051101 (2023)

Phys. Rev. Lett. **125**, 221302 (2020)

# Multiple-cell Cavity

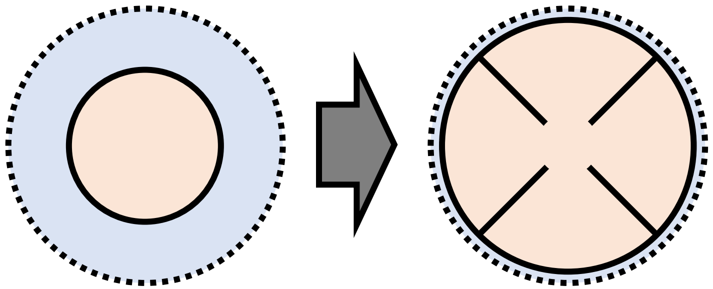

*J. Jeong et al., Phys. Lett. B **777**, 412 (2018)*

## x1.6 ~ 3.2 frequency increase

- Less volume loss
- Single antenna
- Robust against tolerance
- Frequency selectivity

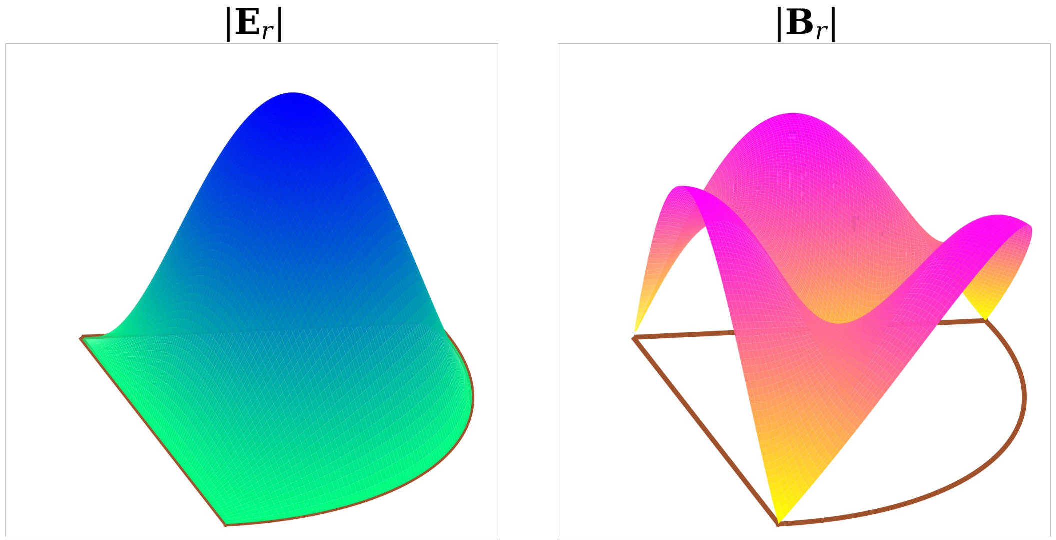

# Multiple-cell Cavity

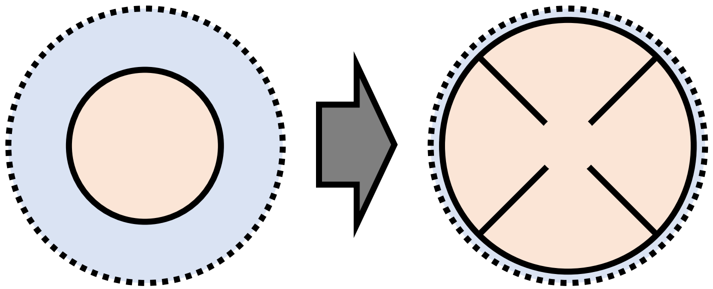

J. Jeong et al., Phys. Lett. B **777**, 412 (2018)

## x1.6 ~ 3.2 frequency increase

- Less volume loss
- Single antenna
- Robust against tolerance
- Frequency selectivity

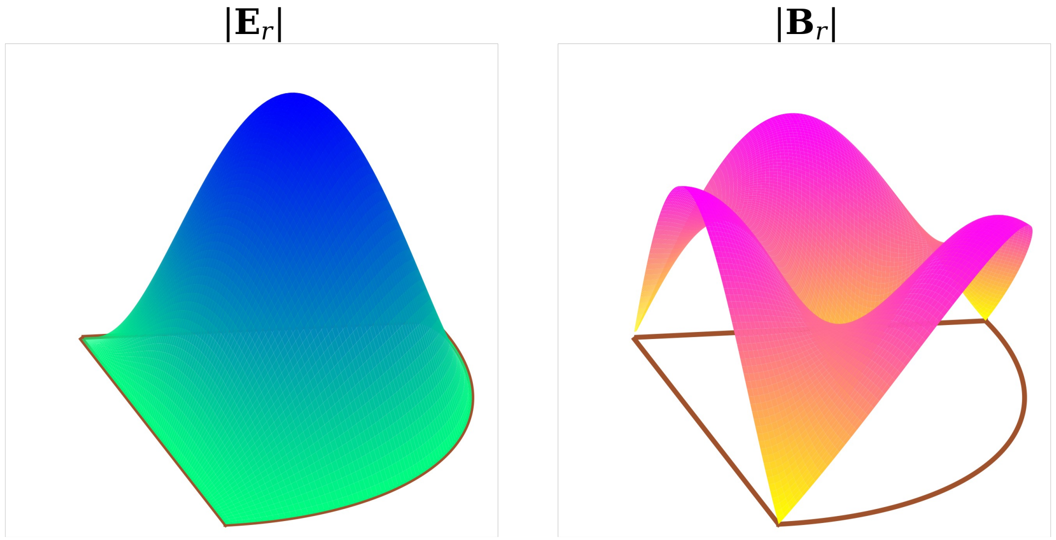


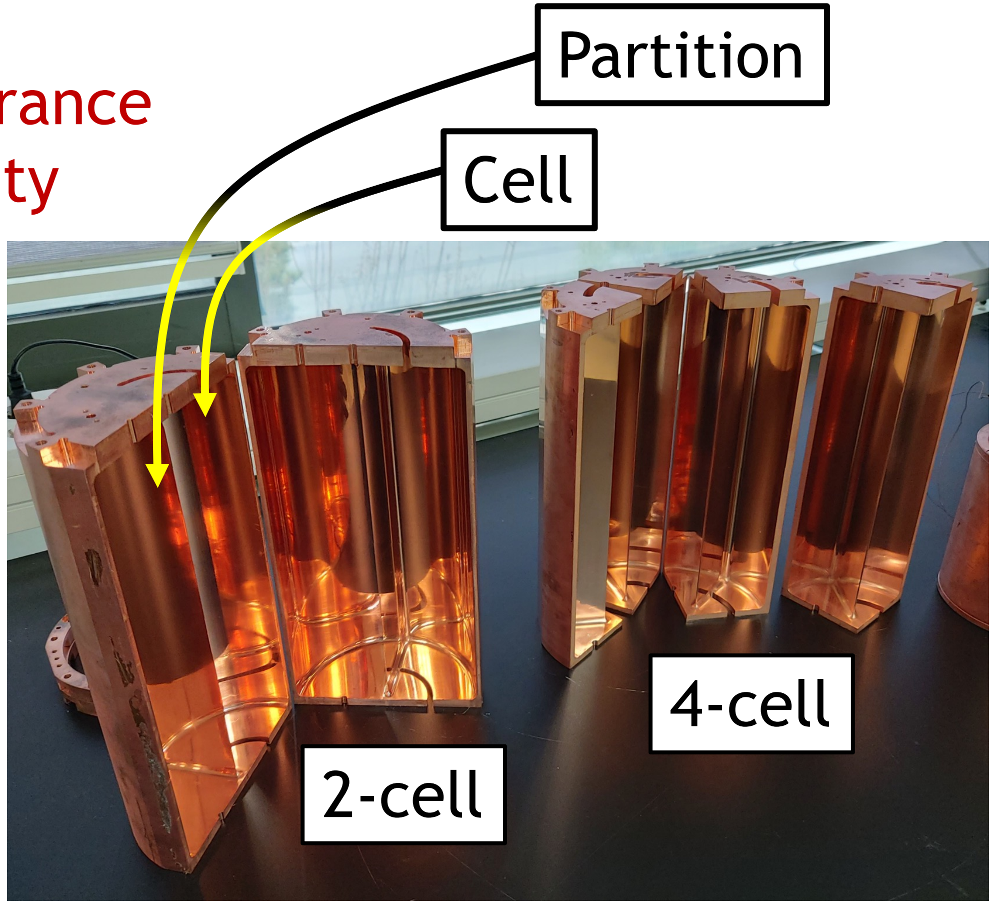

# CAPP-9T MC (Proof-of-concept Exp.)

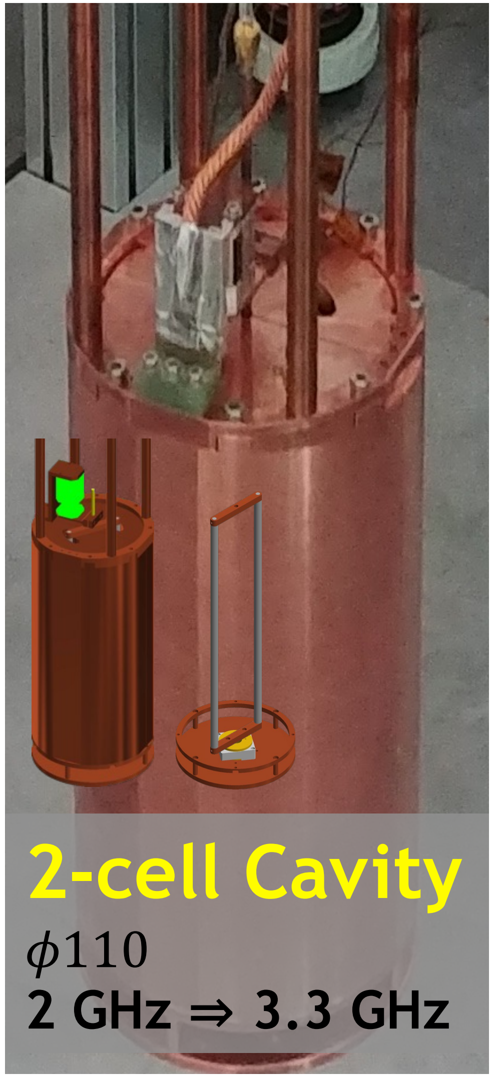

# CAPP-9T MC (Proof-of-concept Exp.)

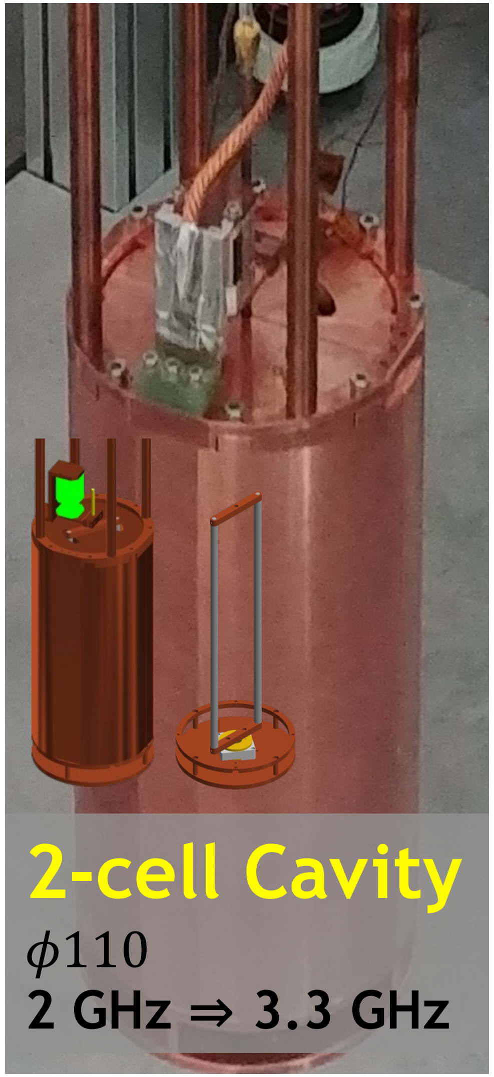

**2-cell Cavity**
$\phi 110$
2 GHz $\Rightarrow$ 3.3 GHz

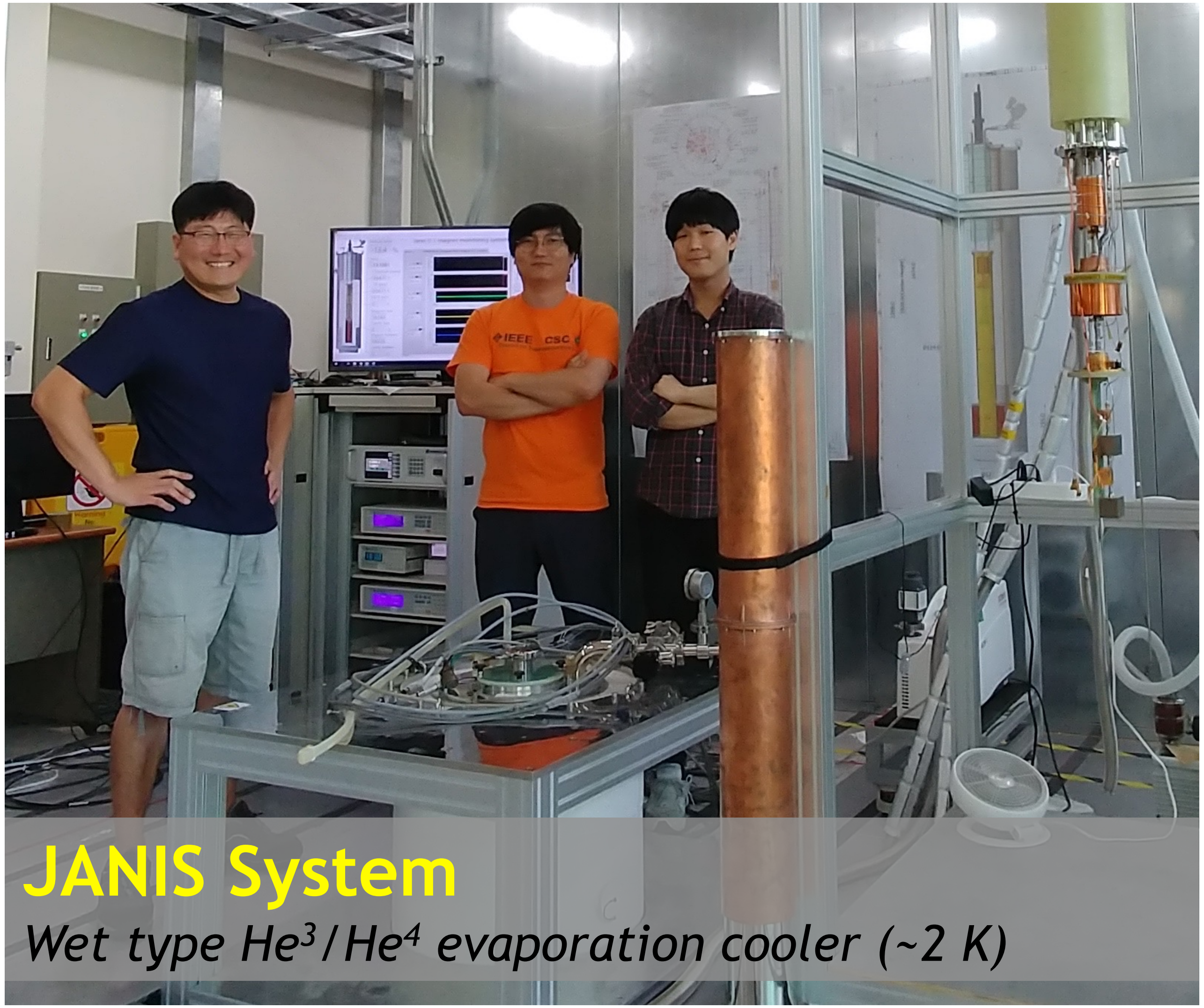

**JANIS System**
*Wet type $He^3$/$He^4$ evaporation cooler (~2 K)*

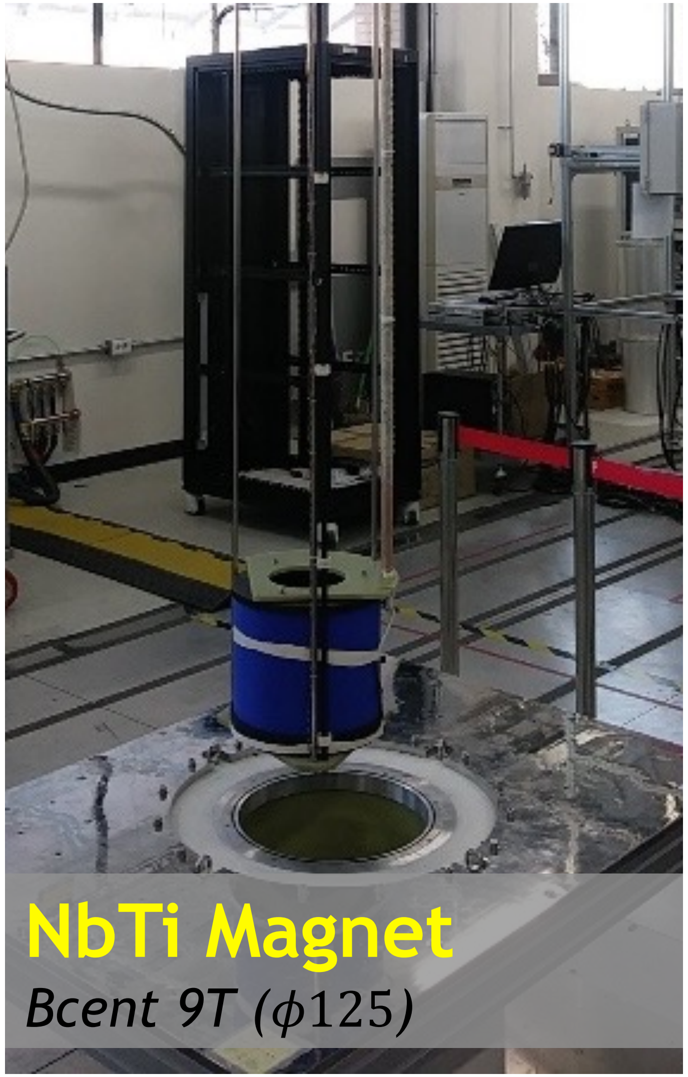

**NbTi Magnet**
*Bcent 9T ($\phi 125$)*

# CAPP-9T MC (Proof-of-concept Exp.)

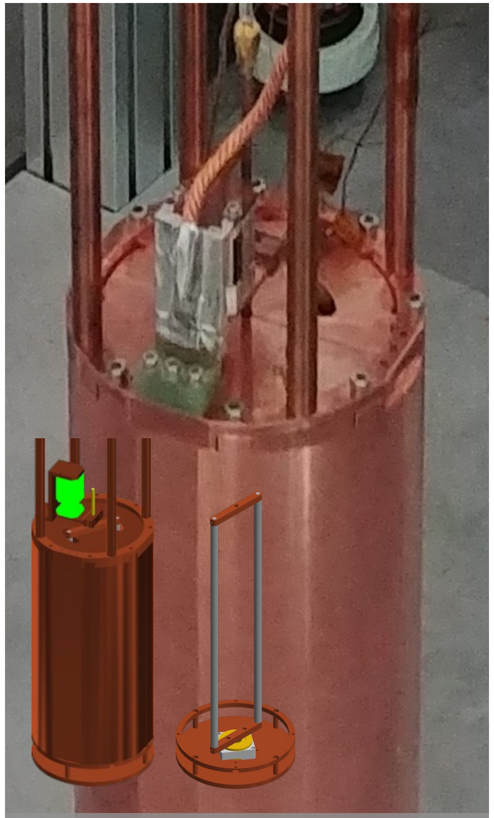

**2-cell Cavity**

$\phi 110$

2 GHz ⇒ 3.3 GHz

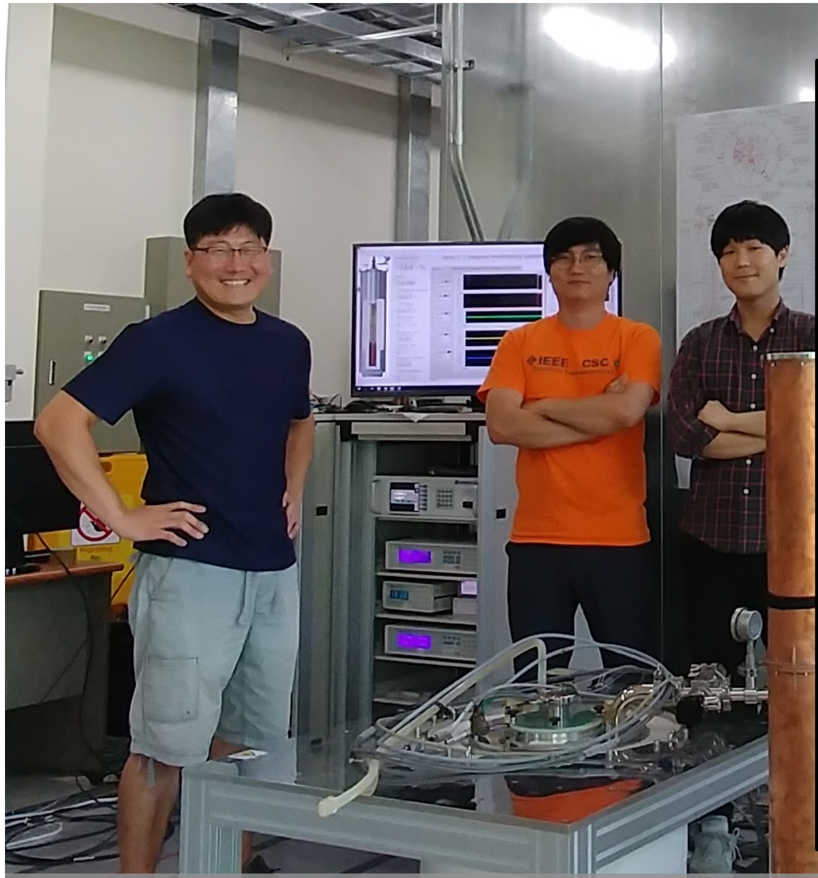

**JANIS System**

*Wet type $He^3/He^4$ evaporation cooler (~2 K)*

**NbTi Magnet**

*Bcent 9T ($\phi 125$)*

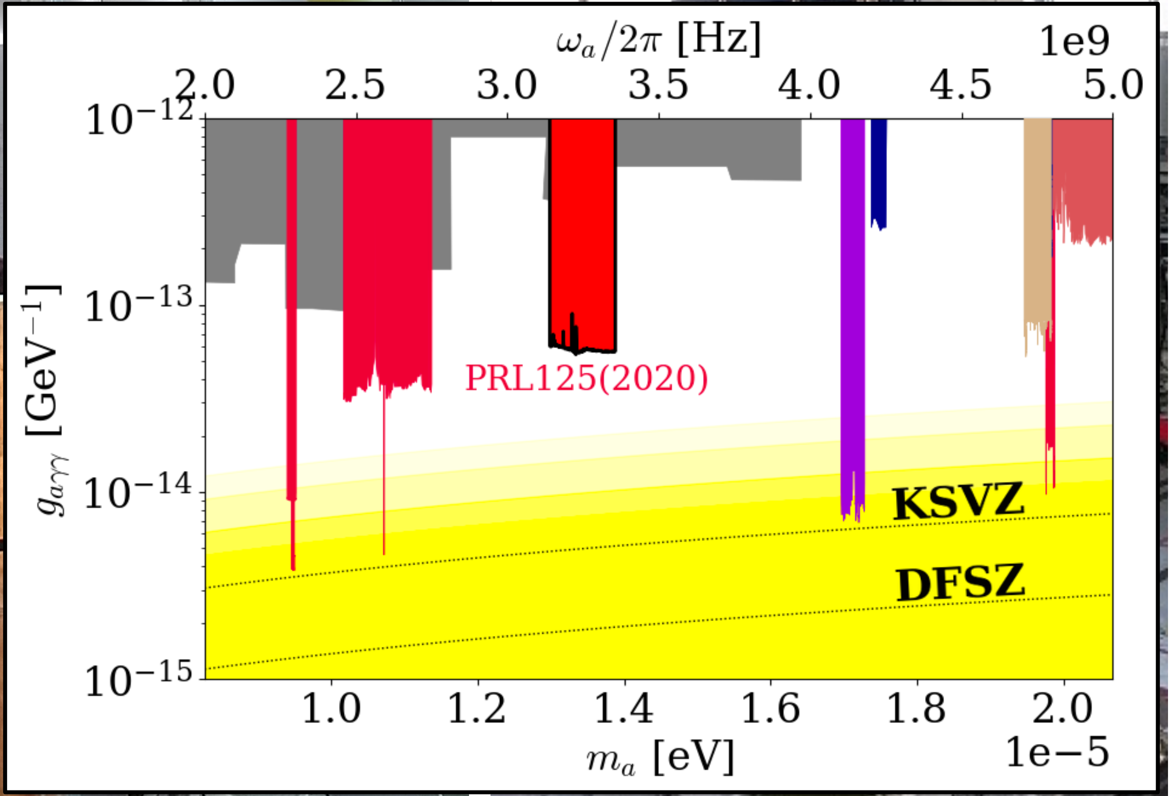

# CAPP-8TB 6G (8-cell)

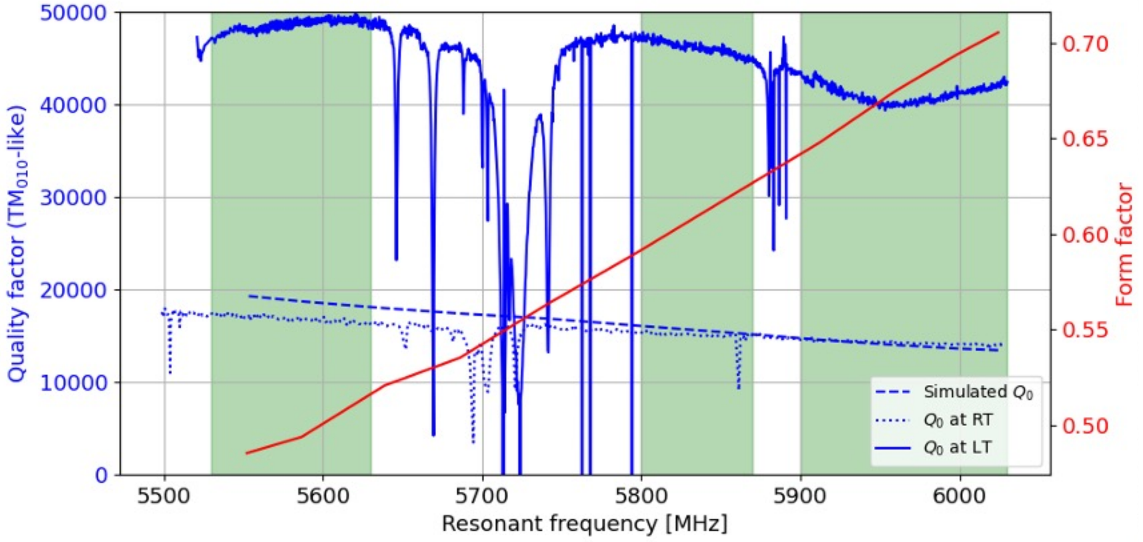


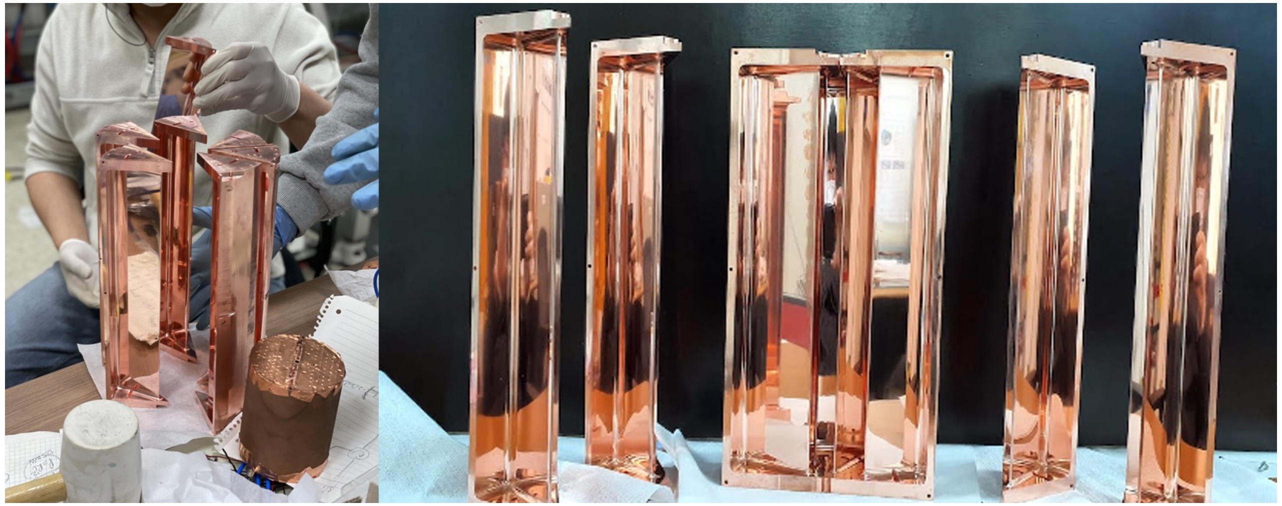

*[From S. Lee's talk, PATRAS 2023]*

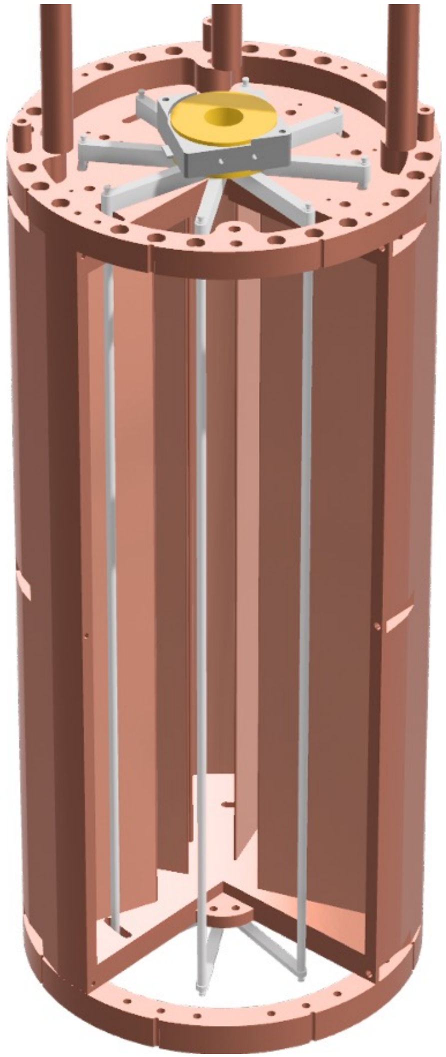

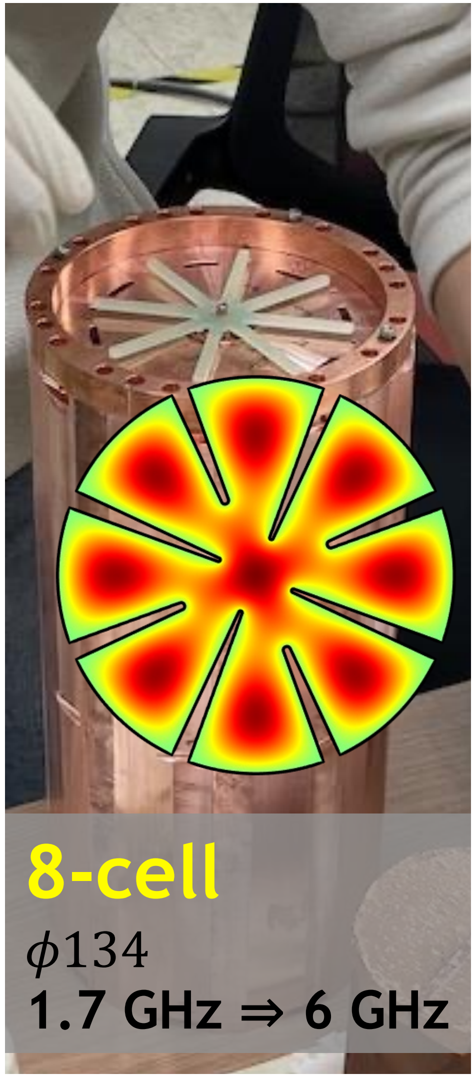

# CAPP-8TB 6G (8-cell)

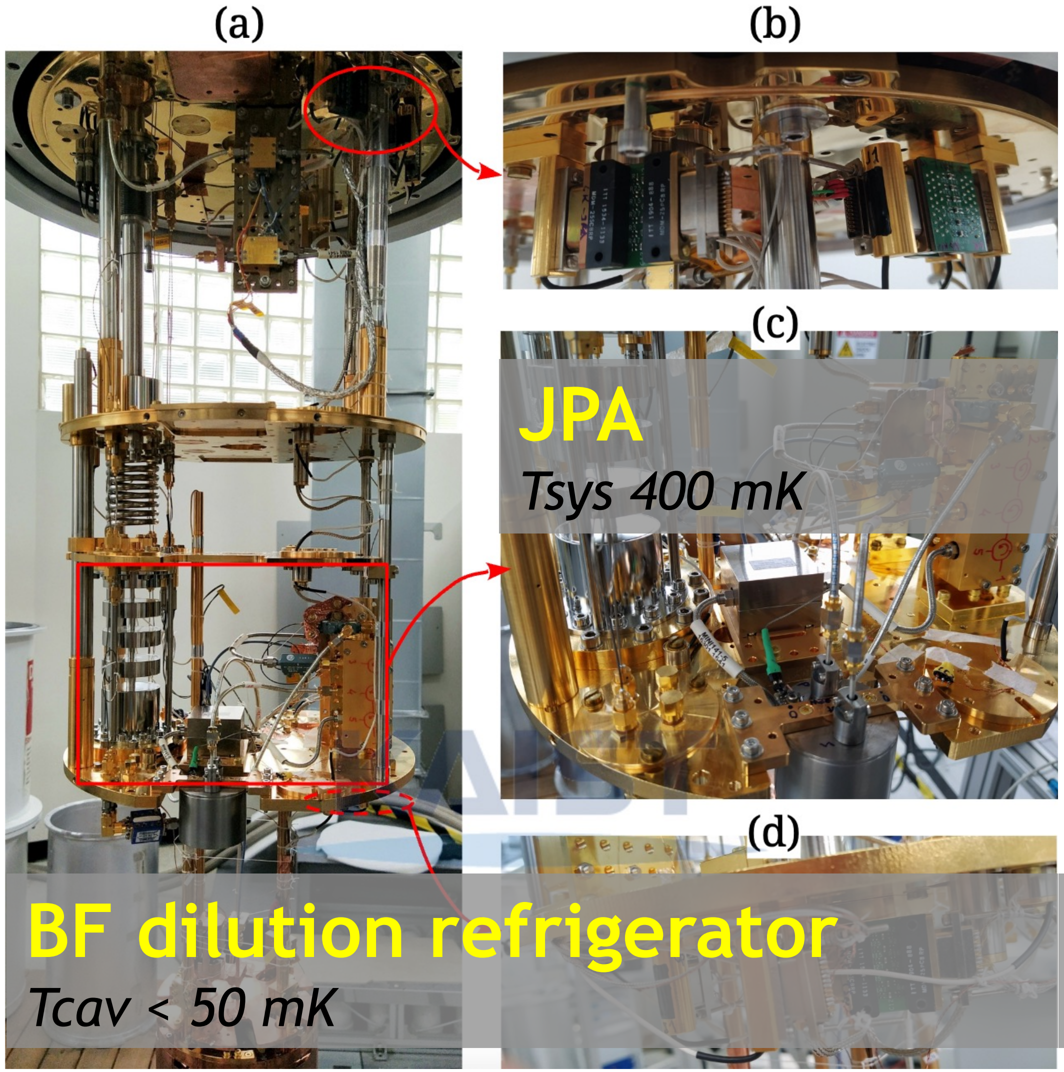


**JPA**
*Tsys 400 mK*

**BF dilution refrigerator**
*Tcav < 50 mK*

[From C. Kutlu's Thesis]

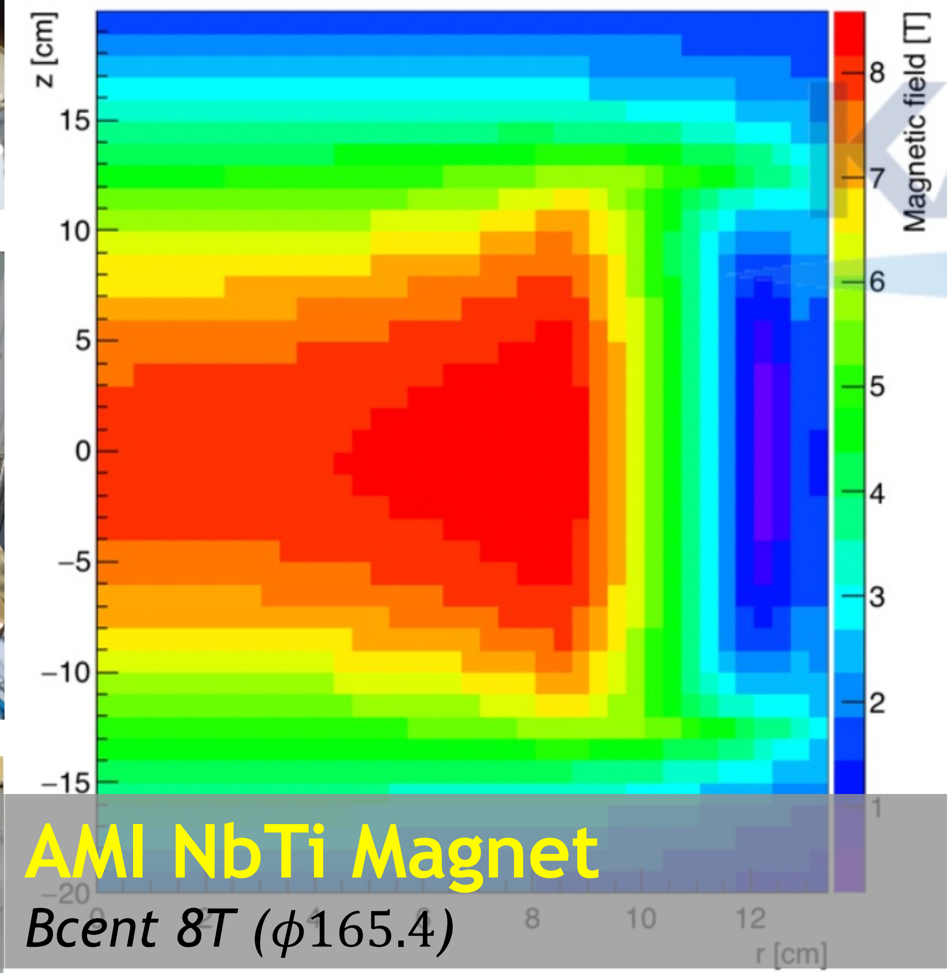


**AMI NbTi Magnet**
*Bcent 8T* ($\phi$165.4)

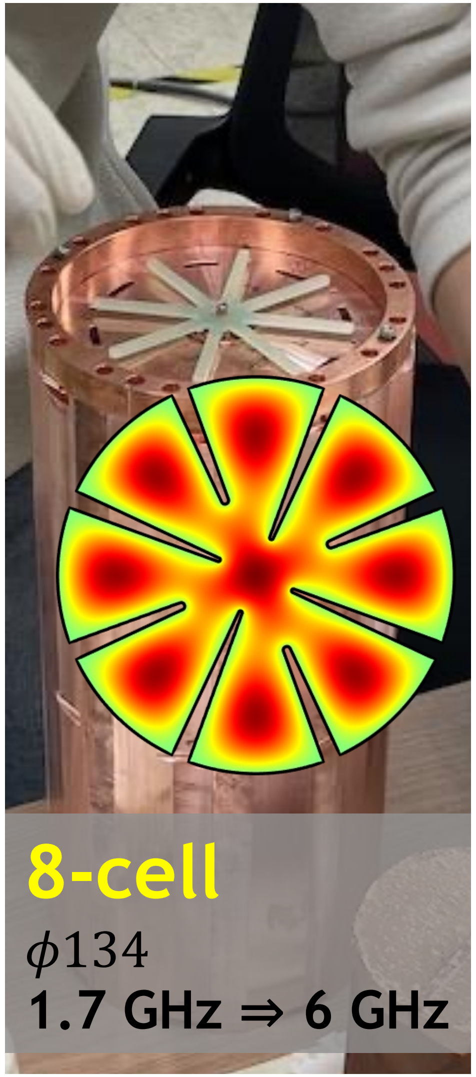

**8-cell**
$\phi$134
1.7 GHz ⇒ 6 GHz

# CAPP-8TB 6G (8-cell)

*[From C. Kutlu's Thesis]*

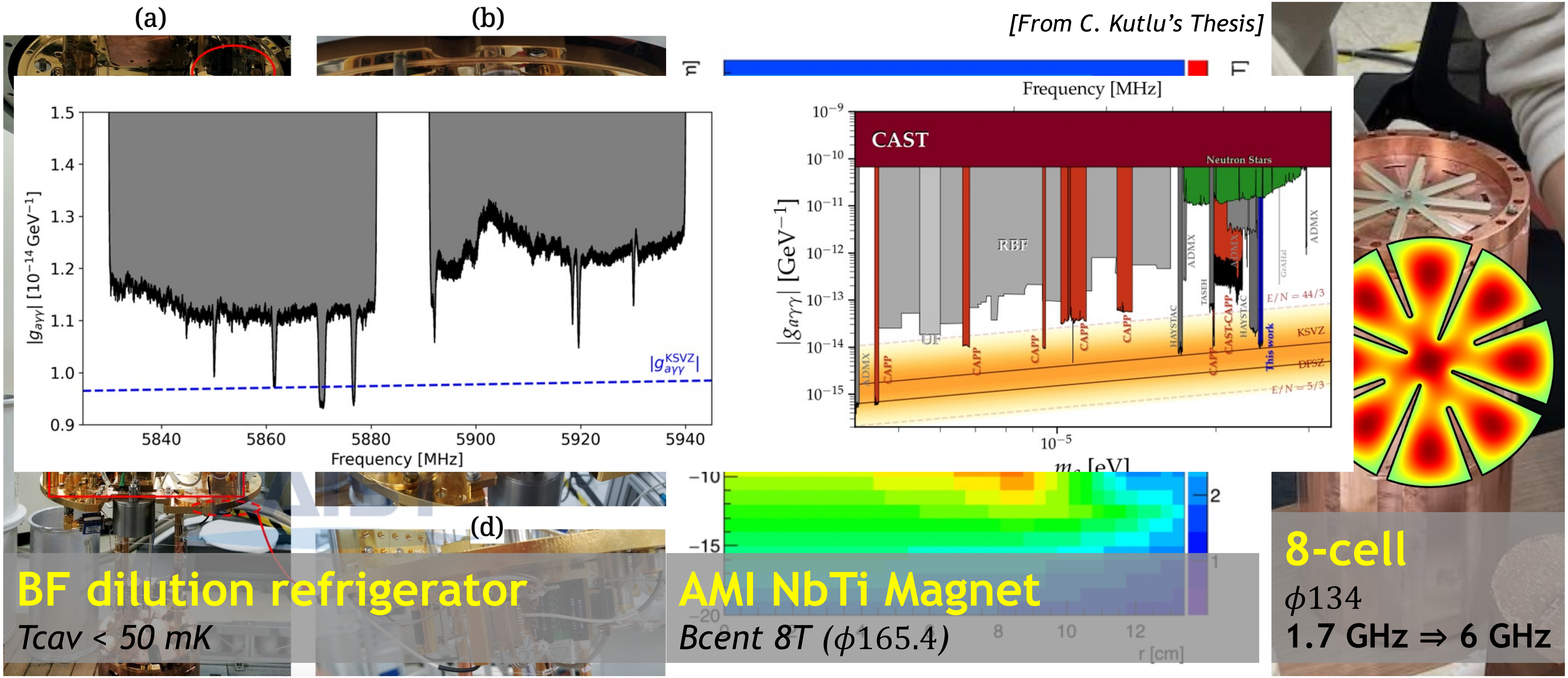


**BF dilution refrigerator**

*Tcav < 50 mK*

**AMI NbTi Magnet**

*Bcent 8T ($\phi$165.4)*

**8-cell**

$\phi$134

1.7 GHz ⇒ 6 GHz

# CAPP-12T (3-cell)

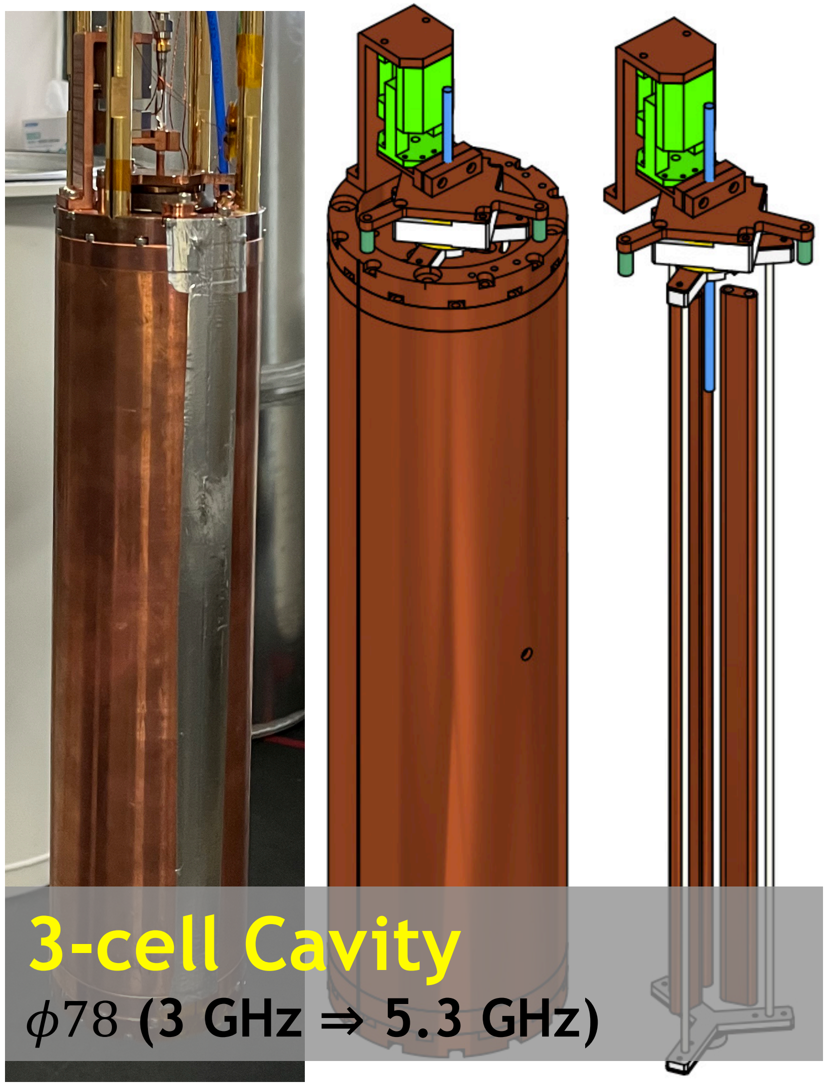


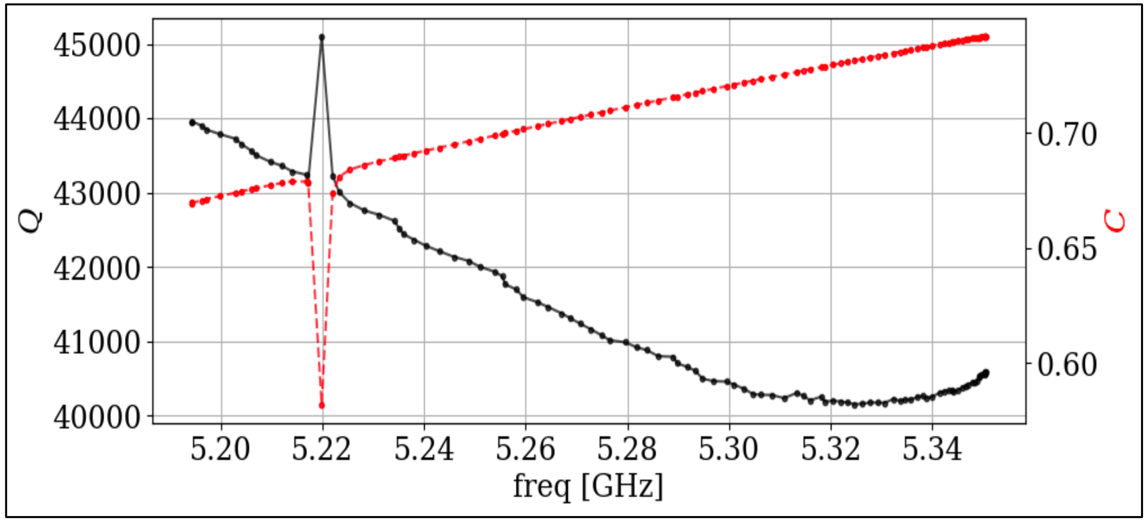


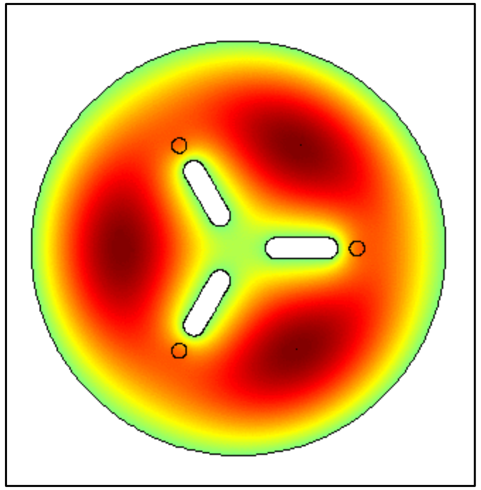

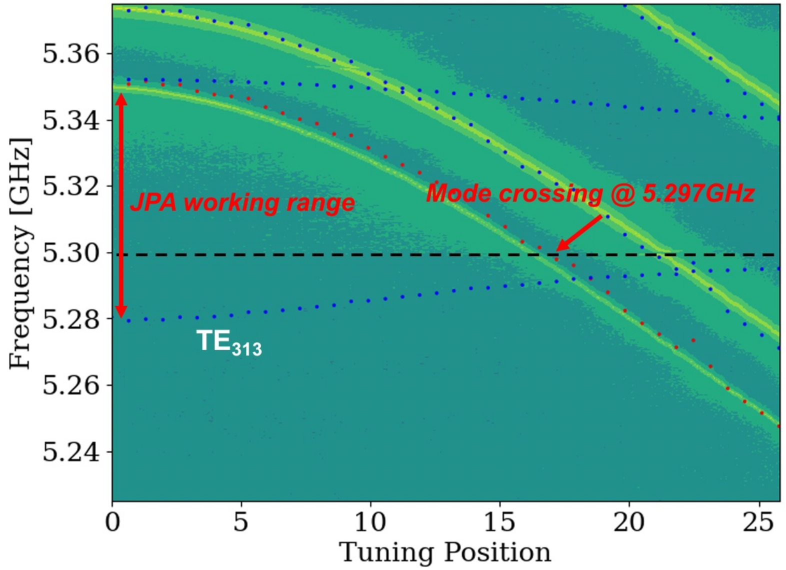

# CAPP-12T (3-cell)

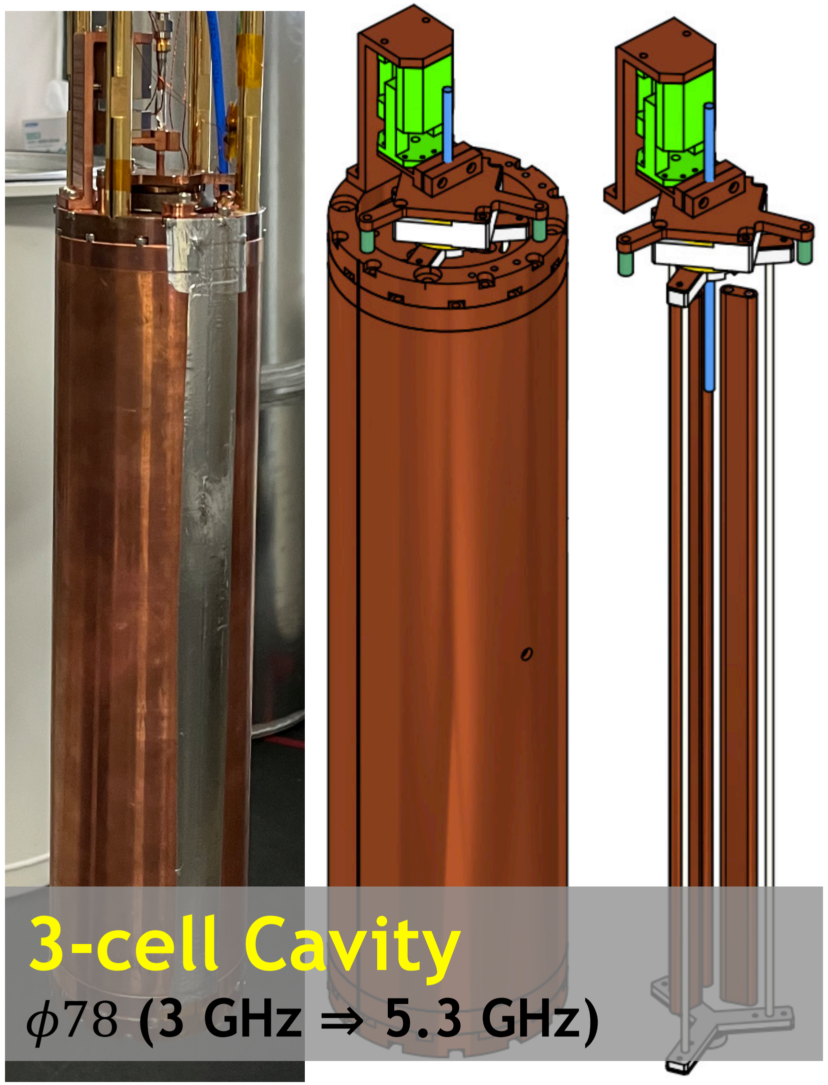


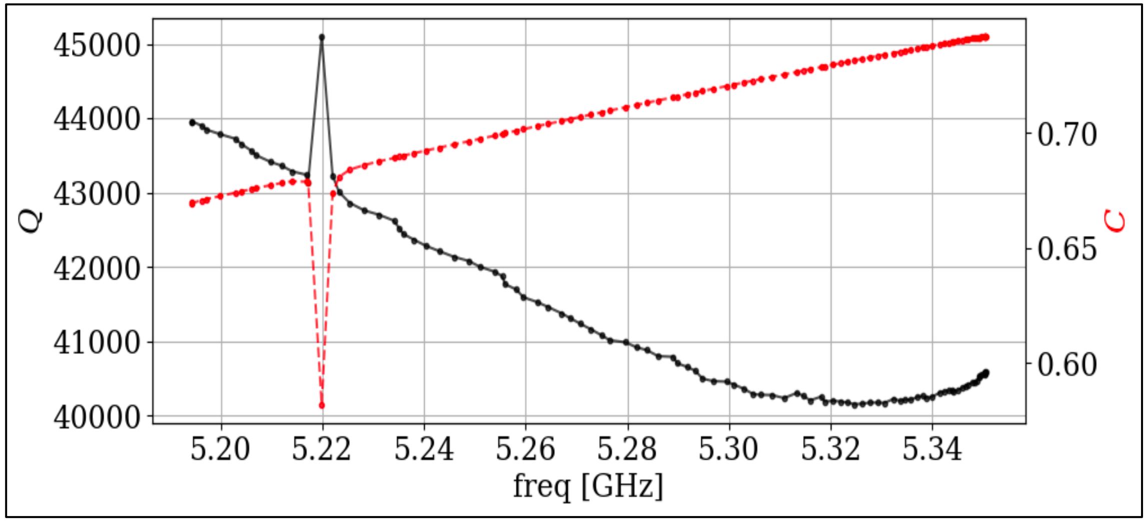


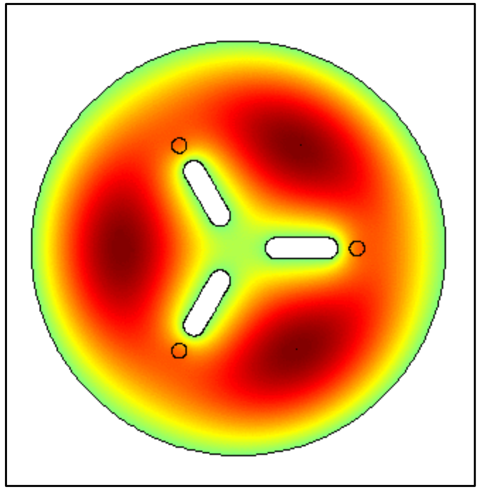

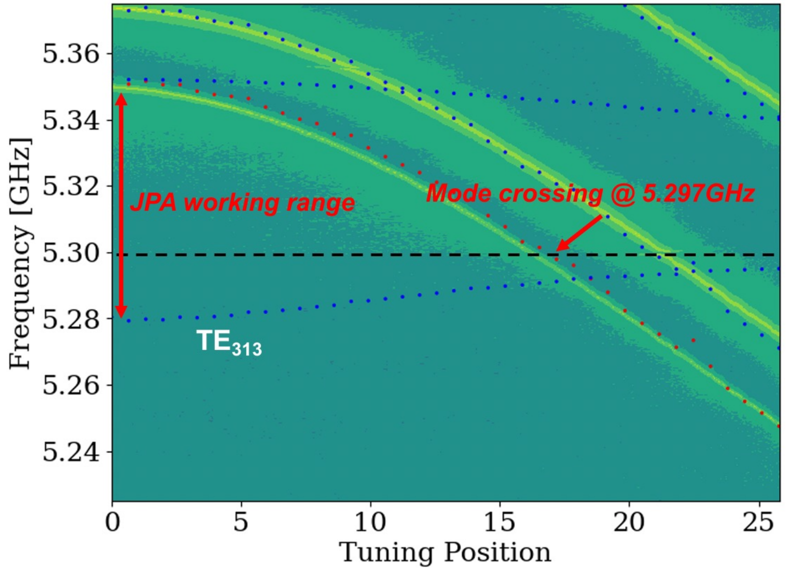


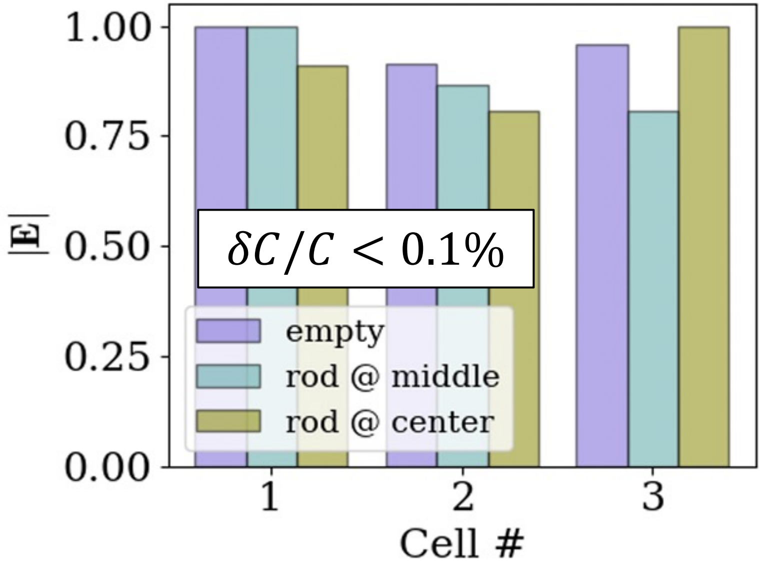

# CAPP-12T (3-cell)

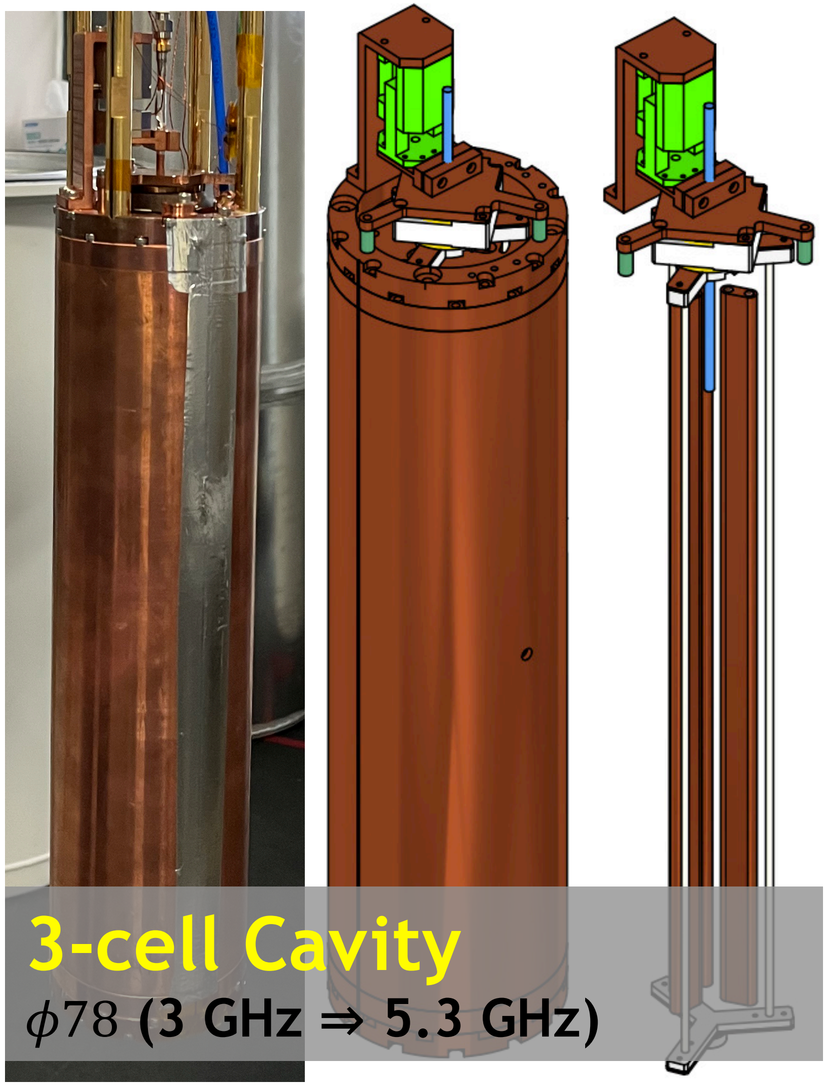


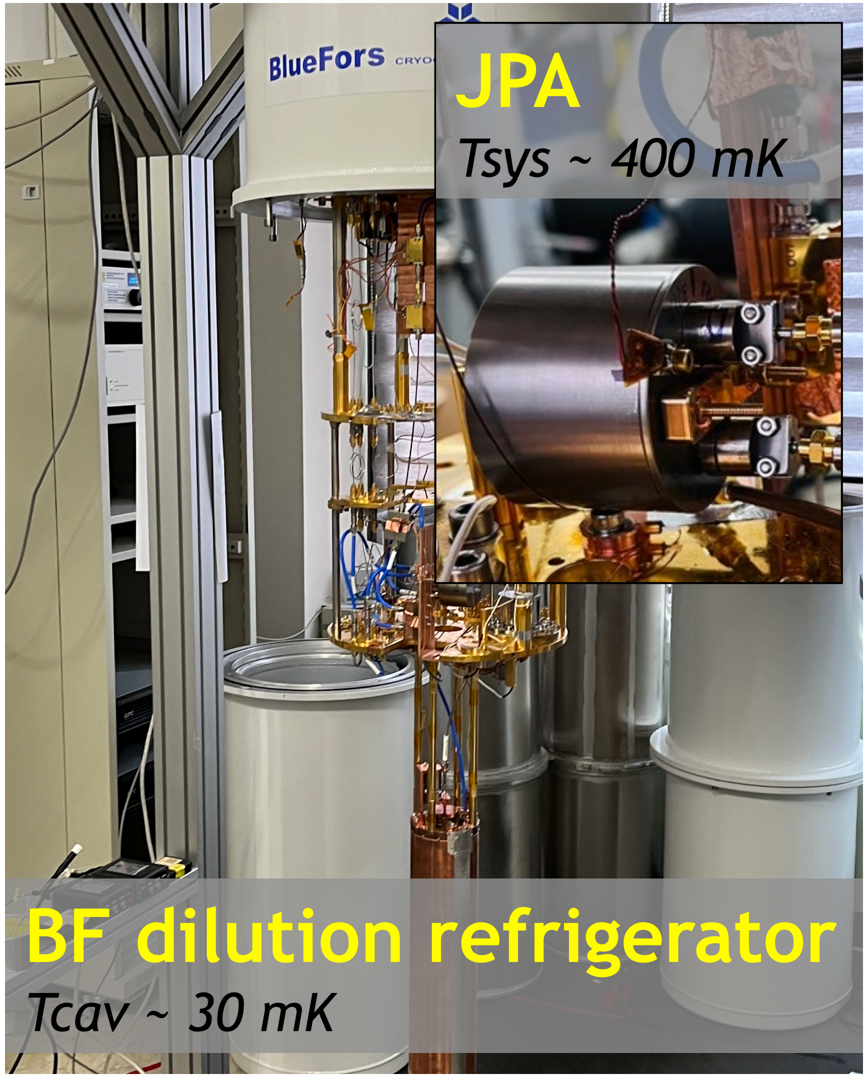


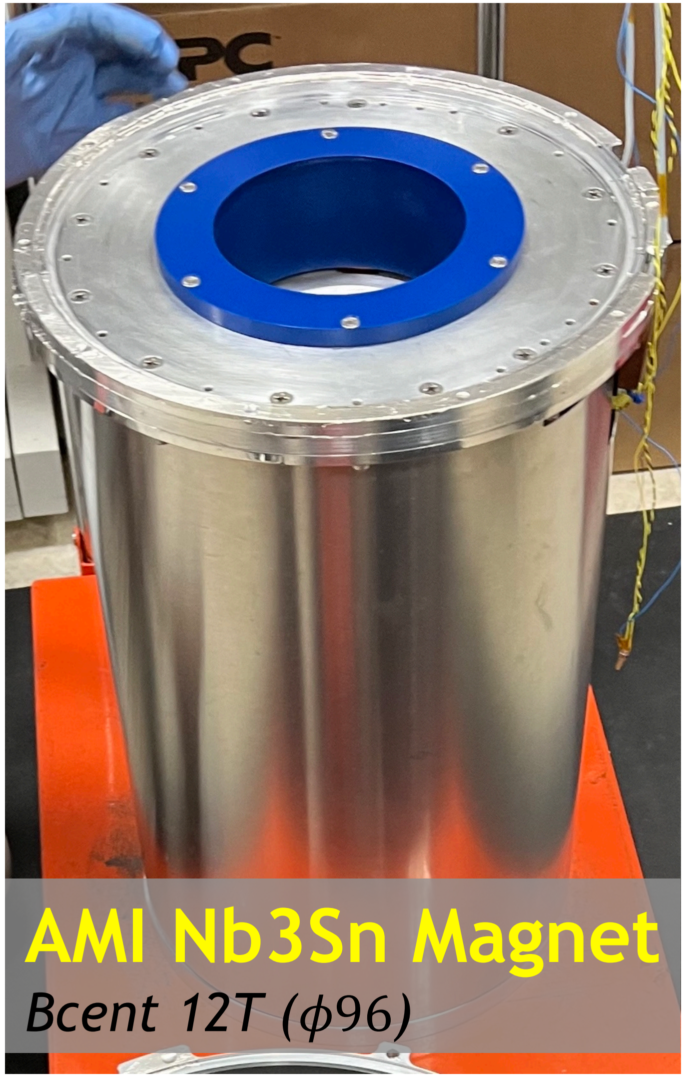

# CAPP-12T (3-cell)

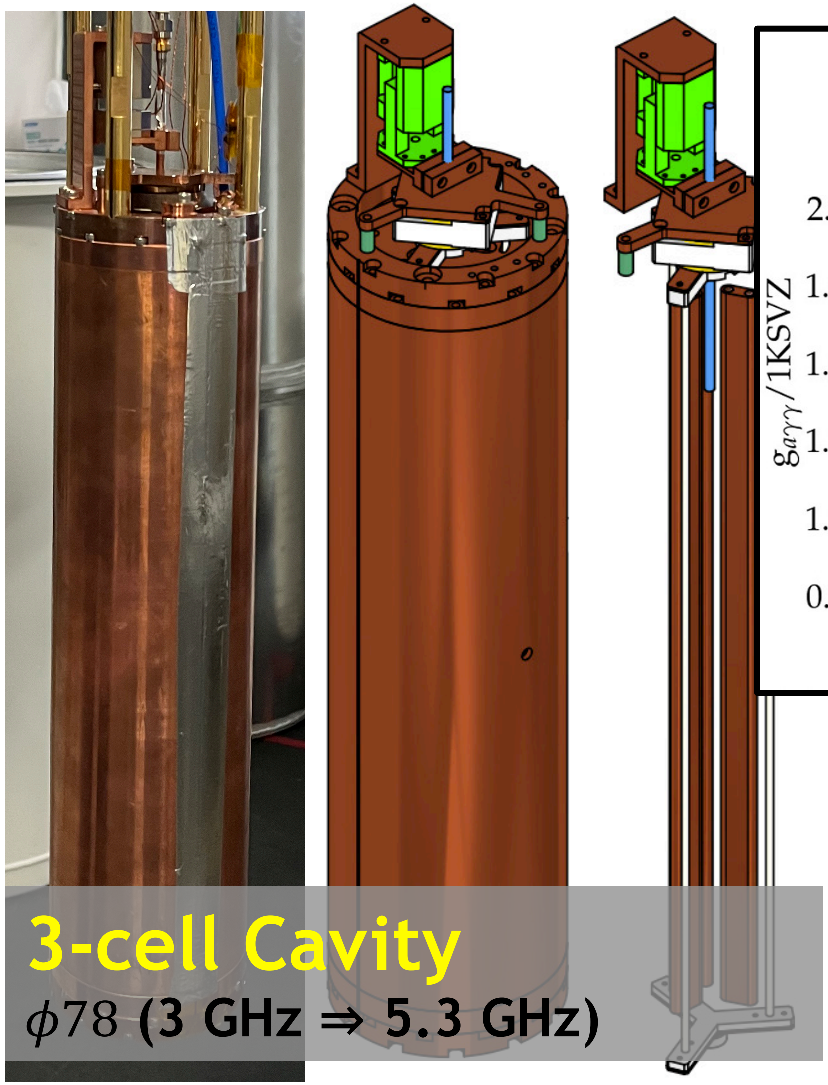

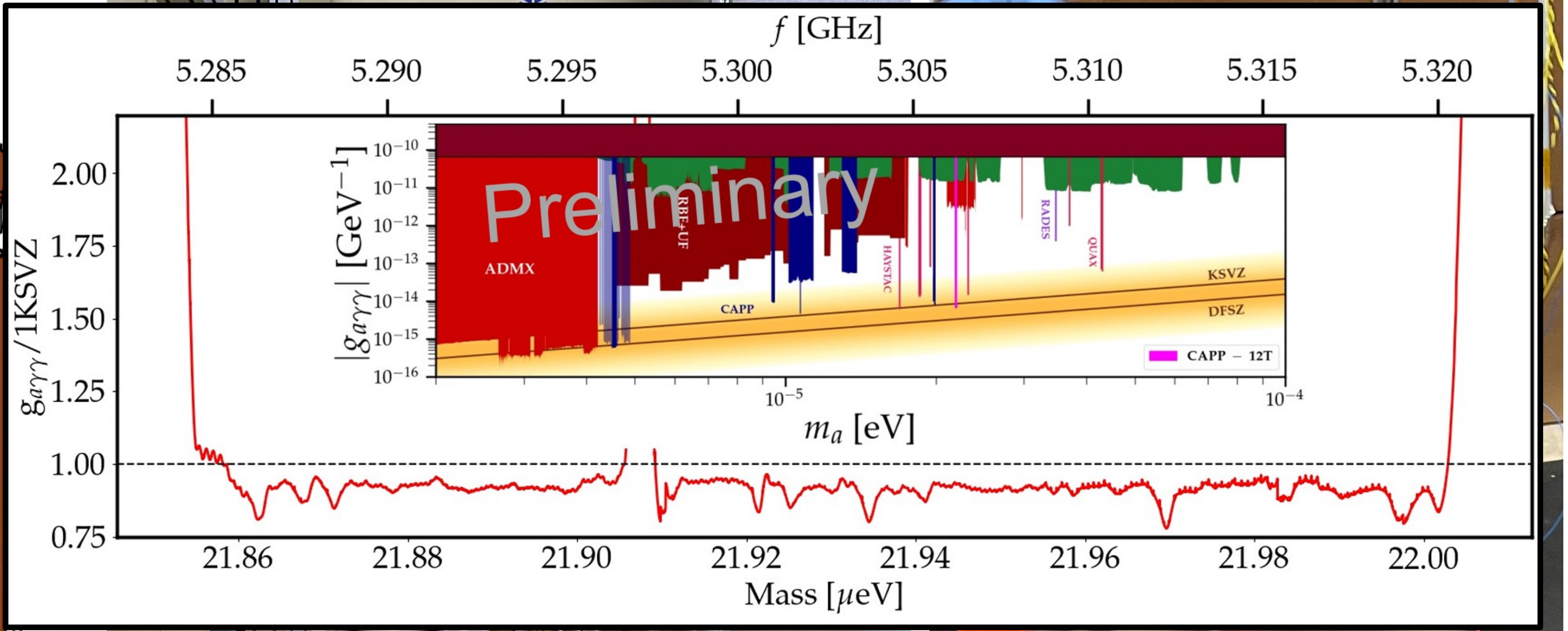


**3-cell Cavity**

$\phi$78 **(3 GHz ⇒ 5.3 GHz)**

**BF dilution refrigerator**

*Tcav ~ 30 mK*

**AMI Nb3Sn Magnet**

*Bcent 12T ($\phi$96)*

# Wheel Tuning Mechanism

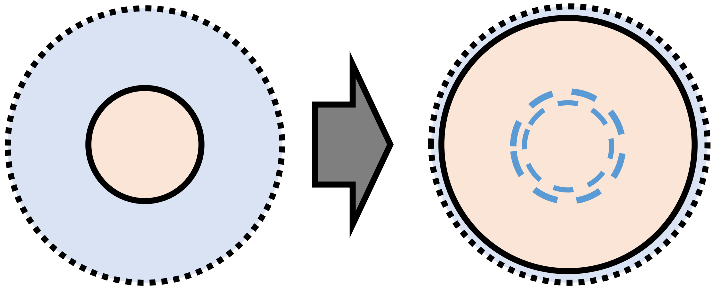

*J. Kim et al., J. Phys. G **47**, 035203 (2020)*

**x3 frequency increase**

- No volume loss
- Single antenna
- High Q-factor

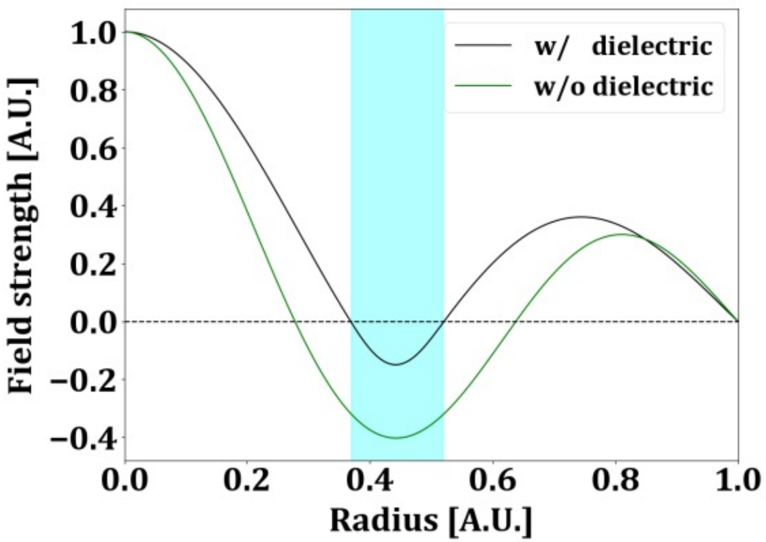


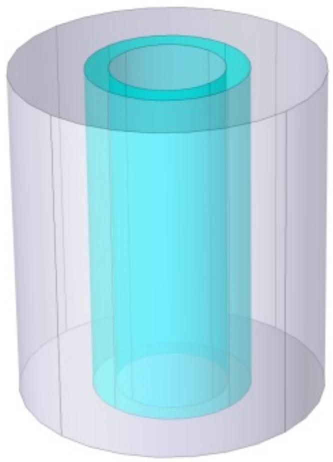

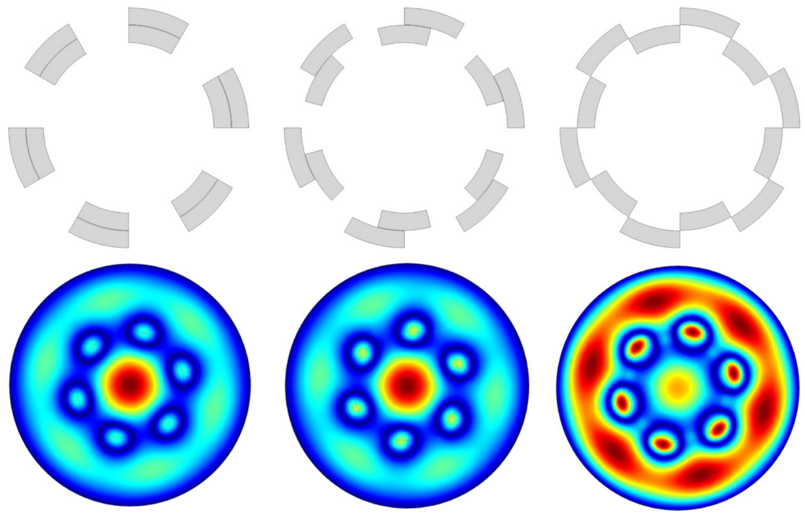

# Wheel Tuning Mechanism

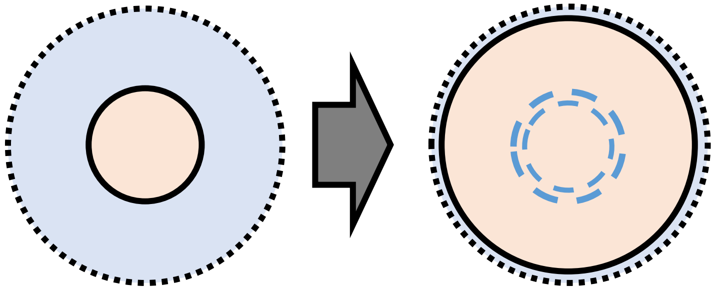

*J. Kim et al., J. Phys. G **47**, 035203 (2020)*

**x3 frequency increase**

- No volume loss
- Single antenna
- High Q-factor

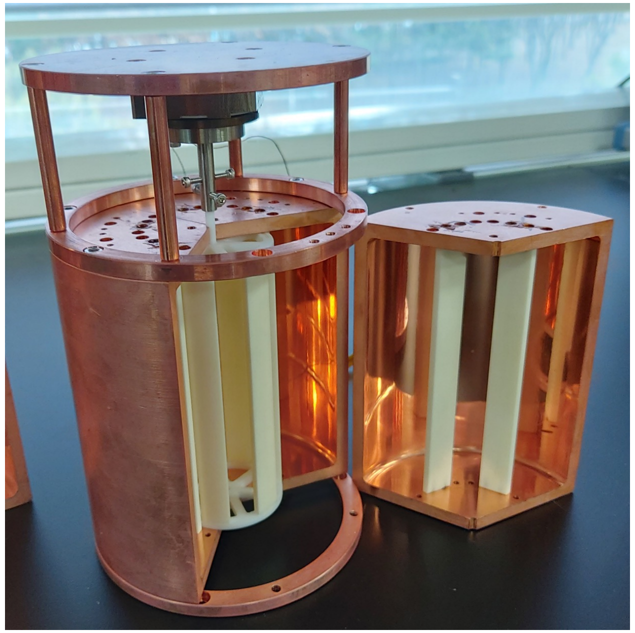

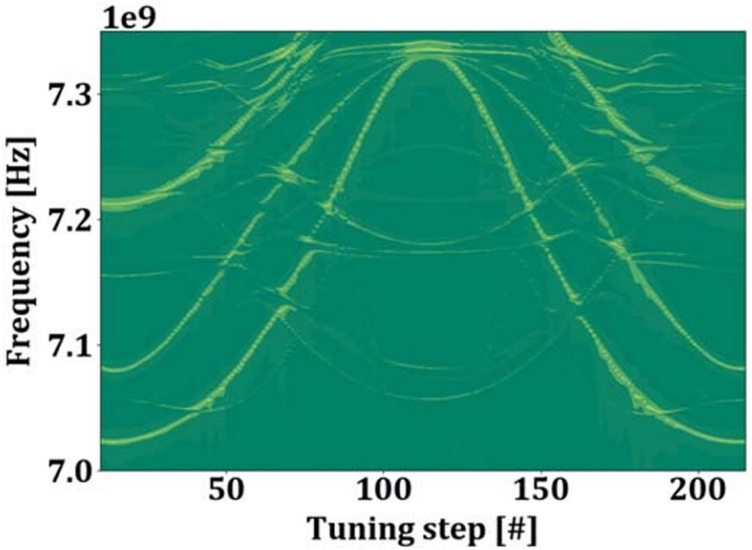


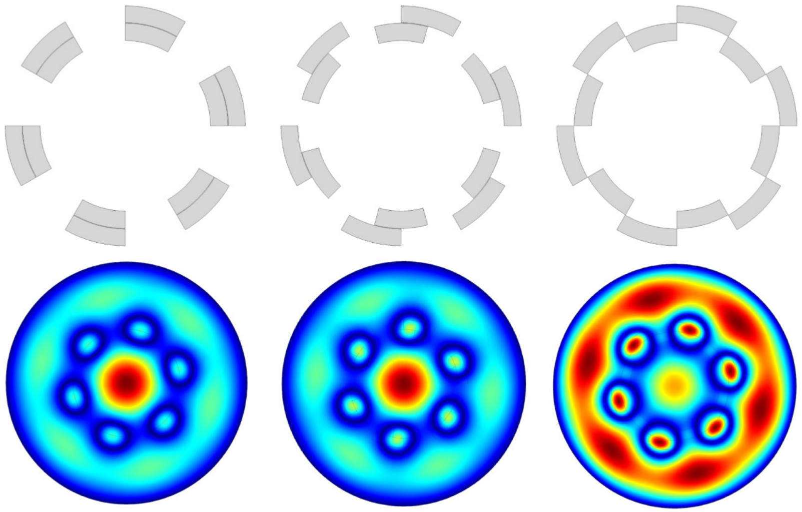

# Tunable Photonic Crystal Cavity

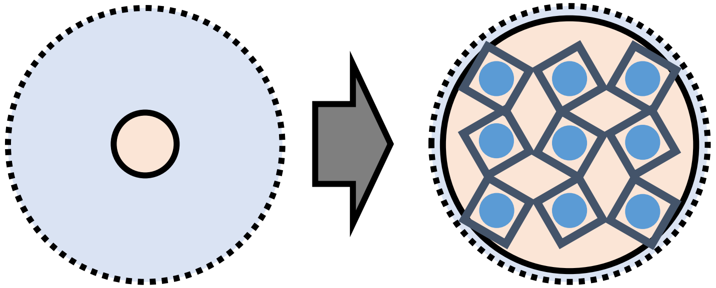

*S. Bae et al., Phys. Rev. D **107**, 015012 (2023)*

## x3 ~ 10 or more frequency increase

- No volume loss
- Single antenna
- High Q-factor
- Frequency selectivity

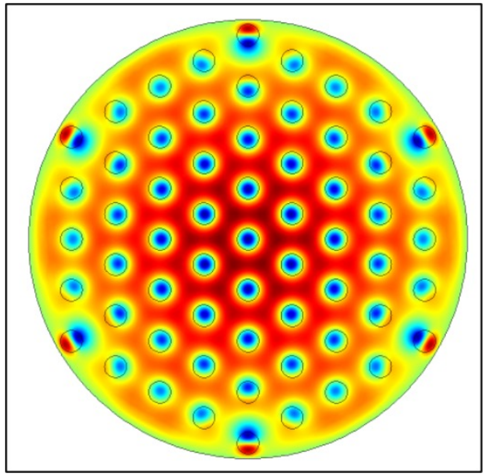

# Tunable Photonic Crystal Cavity

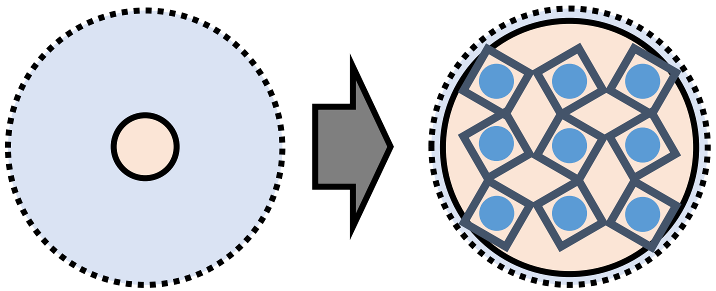

*S. Bae et al., Phys. Rev. D **107**, 015012 (2023)*

## x3 ~ 10 or more frequency increase

- No volume loss
- Single antenna
- High Q-factor
- Frequency selectivity

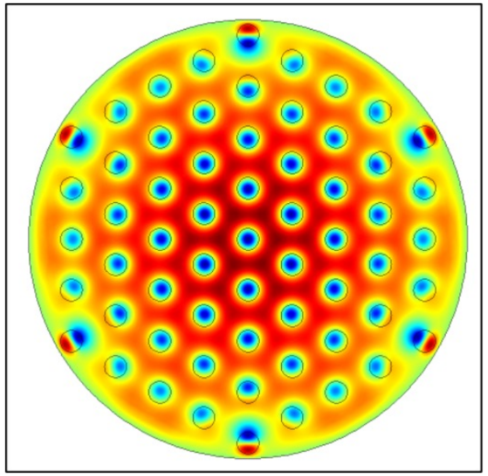

### Auxetic structure

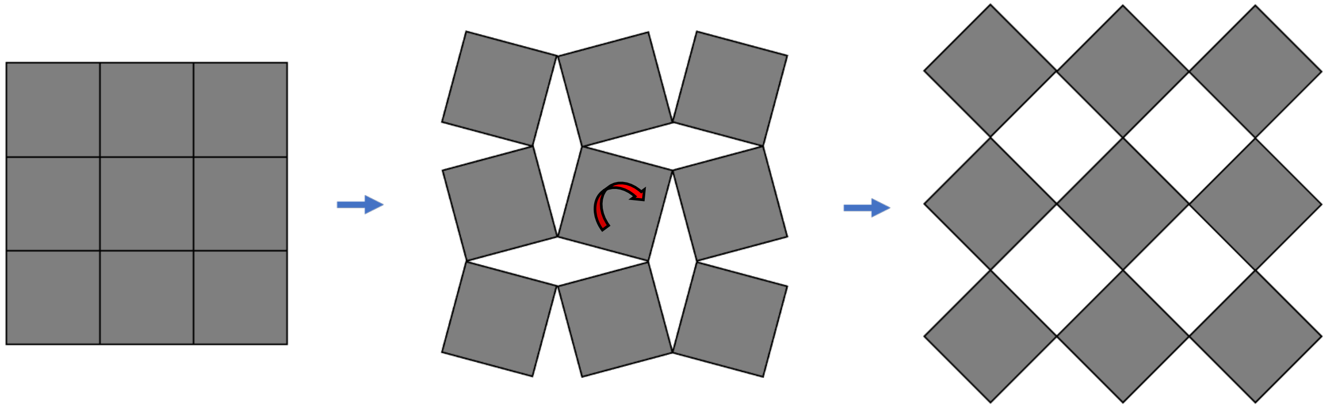

# Tunable Photonic Crystal Cavity

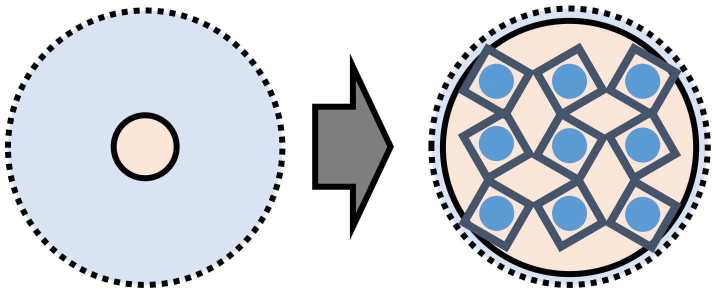

S. Bae et al., Phys. Rev. D **107**, 015012 (2023)

## x3 ~ 10 or more frequency increase

- No volume loss
- Single antenna
- High Q-factor
- Frequency selectivity

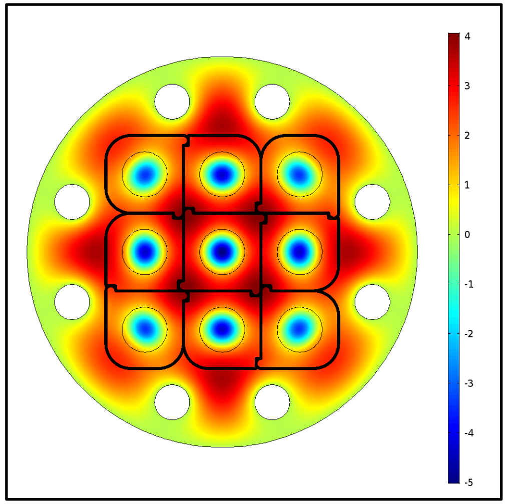

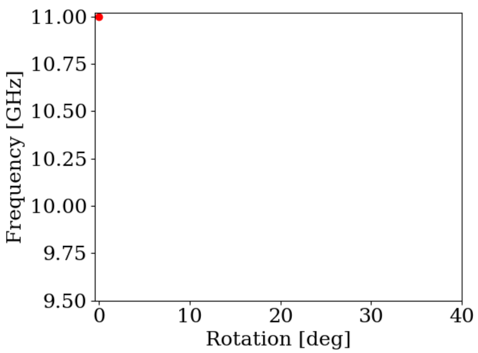


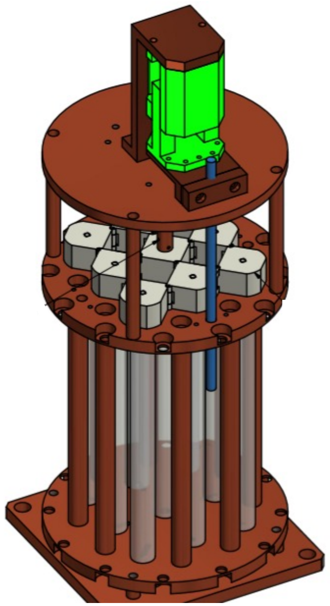

# Tunable Photonic Crystal Cavity

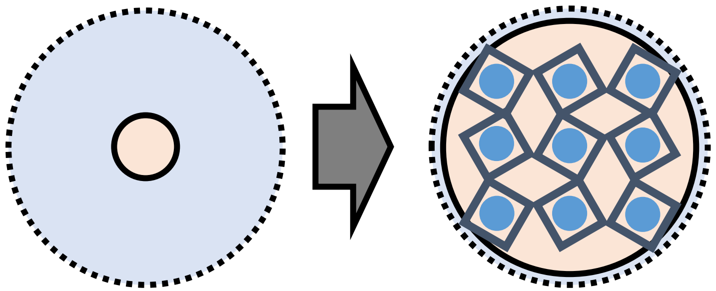

*S. Bae et al., Phys. Rev. D **107**, 015012 (2023)*

## x3 ~ 10 or more frequency increase

- No volume loss
- Single antenna
- High Q-factor
- Frequency selectivity

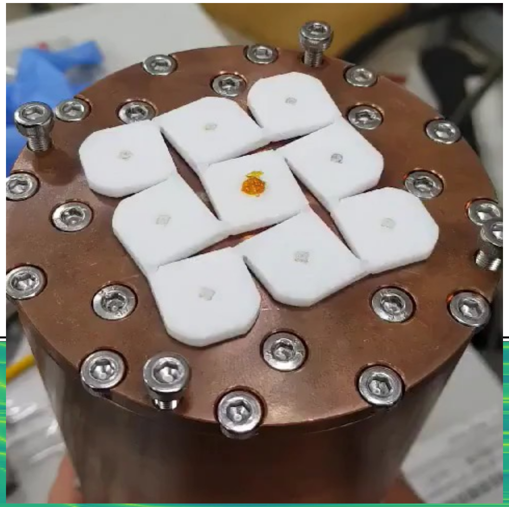

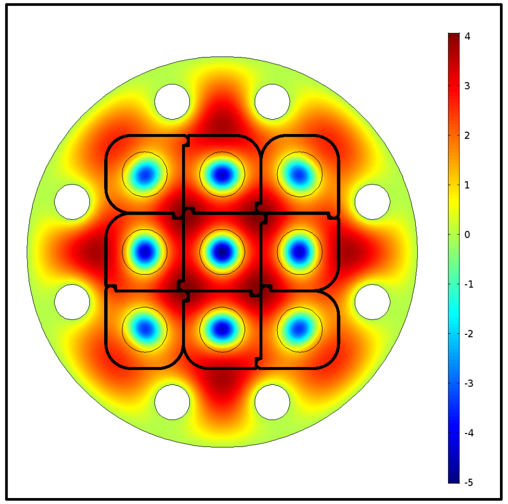


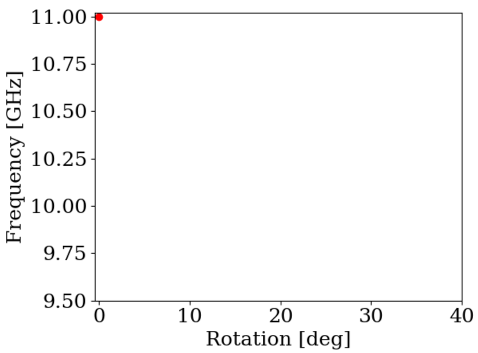


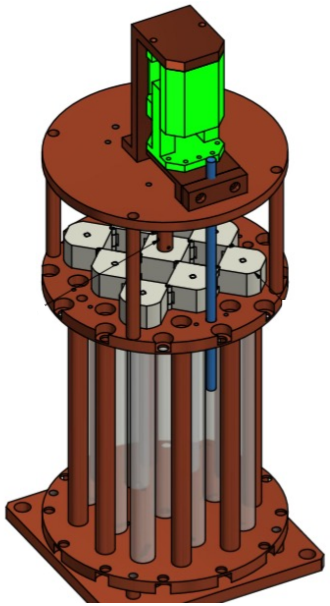

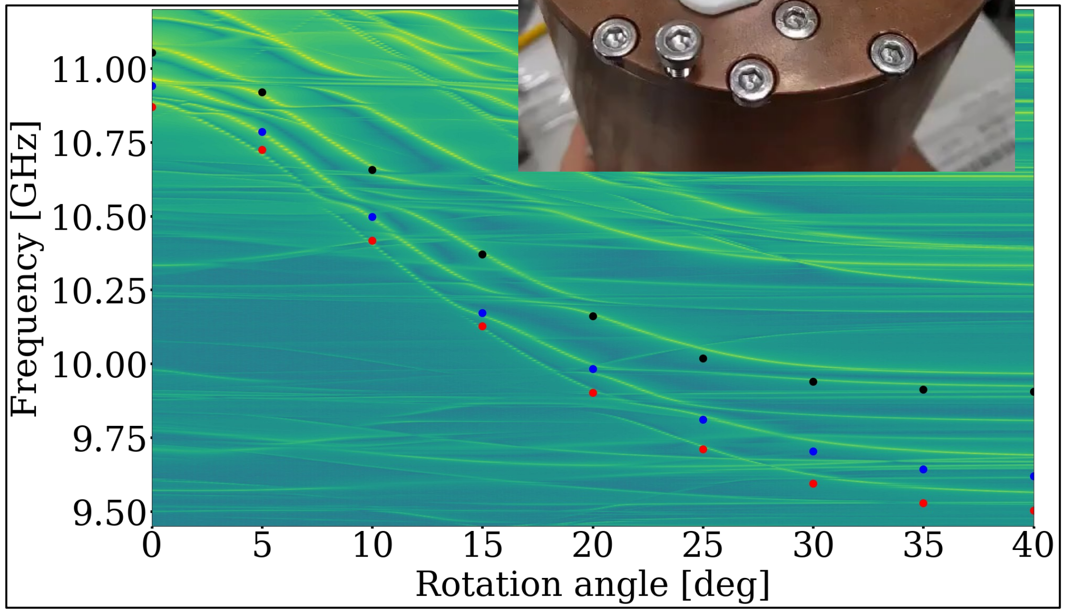

# Proof-of-Concept Experiment (5x5)

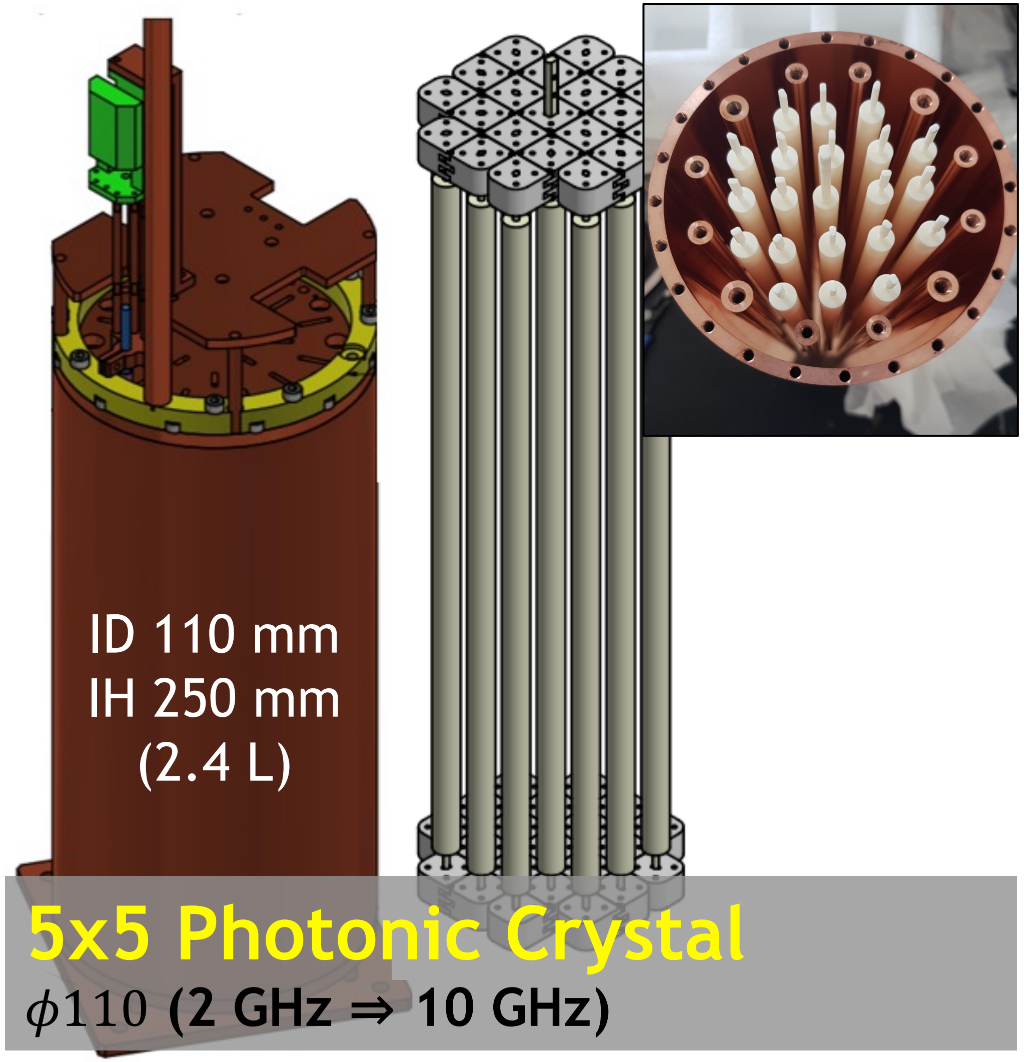


**5x5 Photonic Crystal**

$\phi 110$ (2 GHz ⇒ 10 GHz)

# Proof-of-Concept Experiment (5x5)

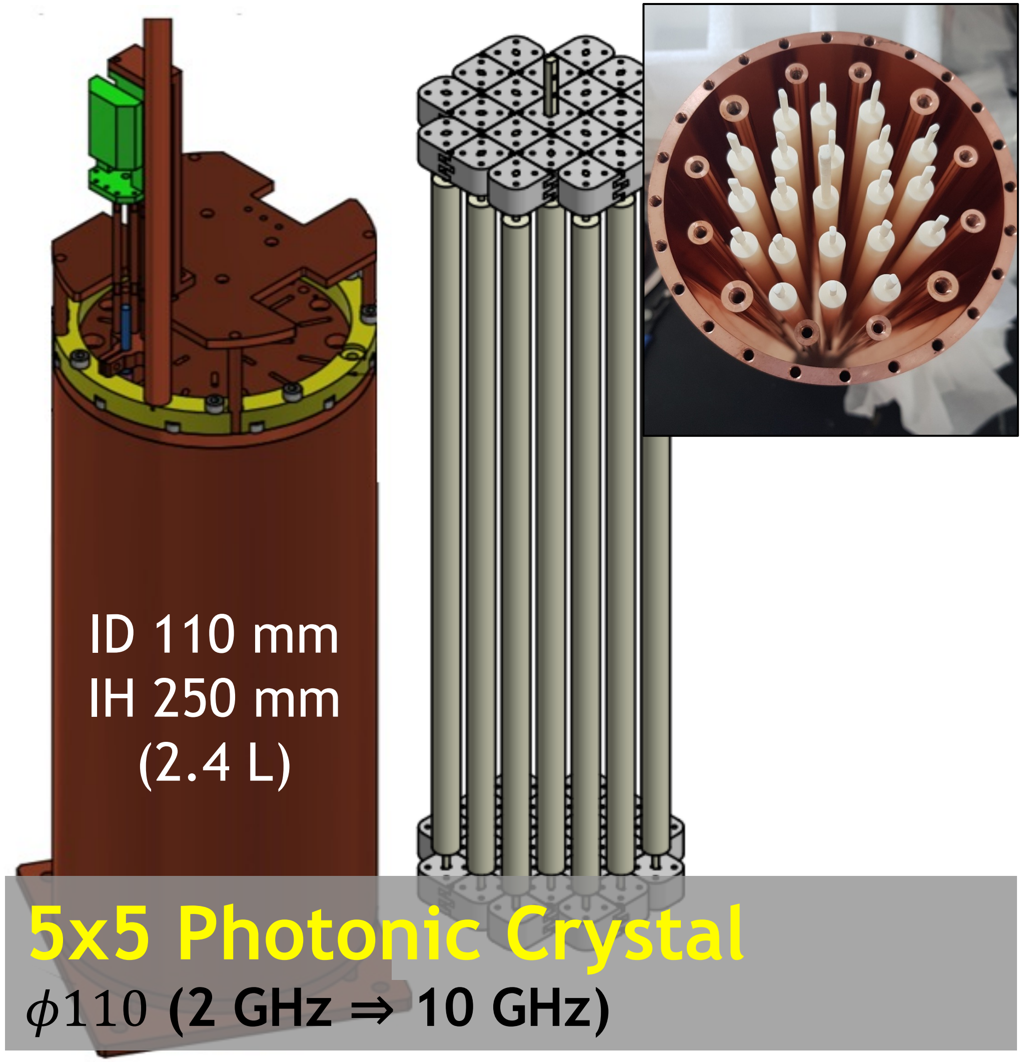


**5x5 Photonic Crystal**
$\phi 110$ **(2 GHz ⇒ 10 GHz)**

**JANIS System**
*Evaporation cooler (~2 K)*

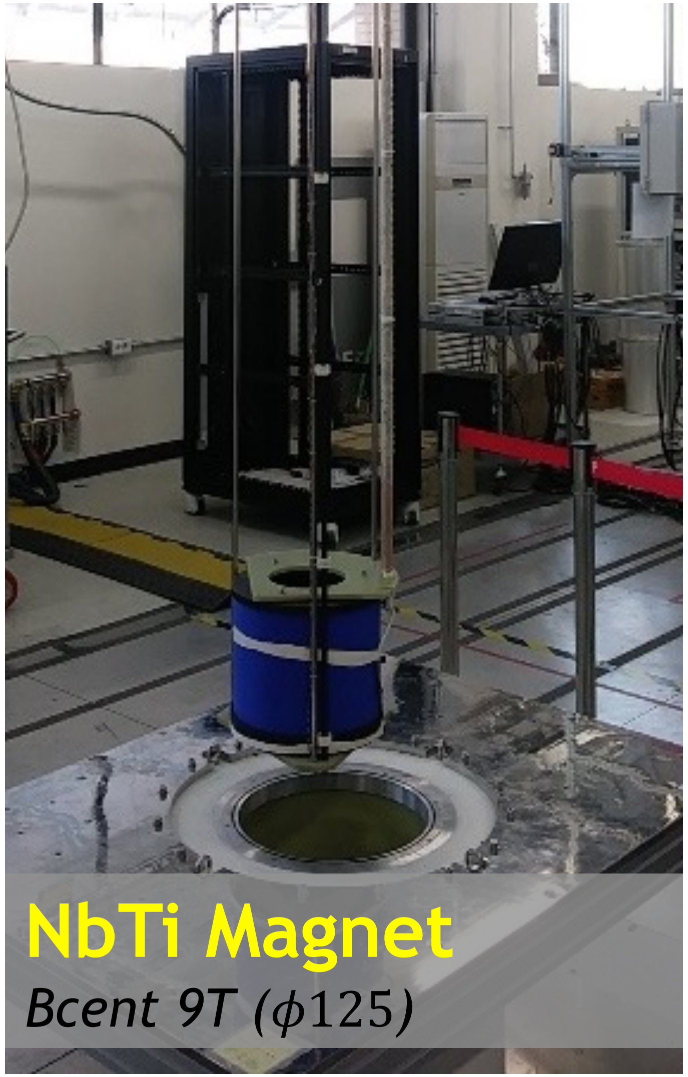

**NbTi Magnet**
*Bcent 9T ($\phi 125$)*

# Proof-of-Concept Experiment (5x5)

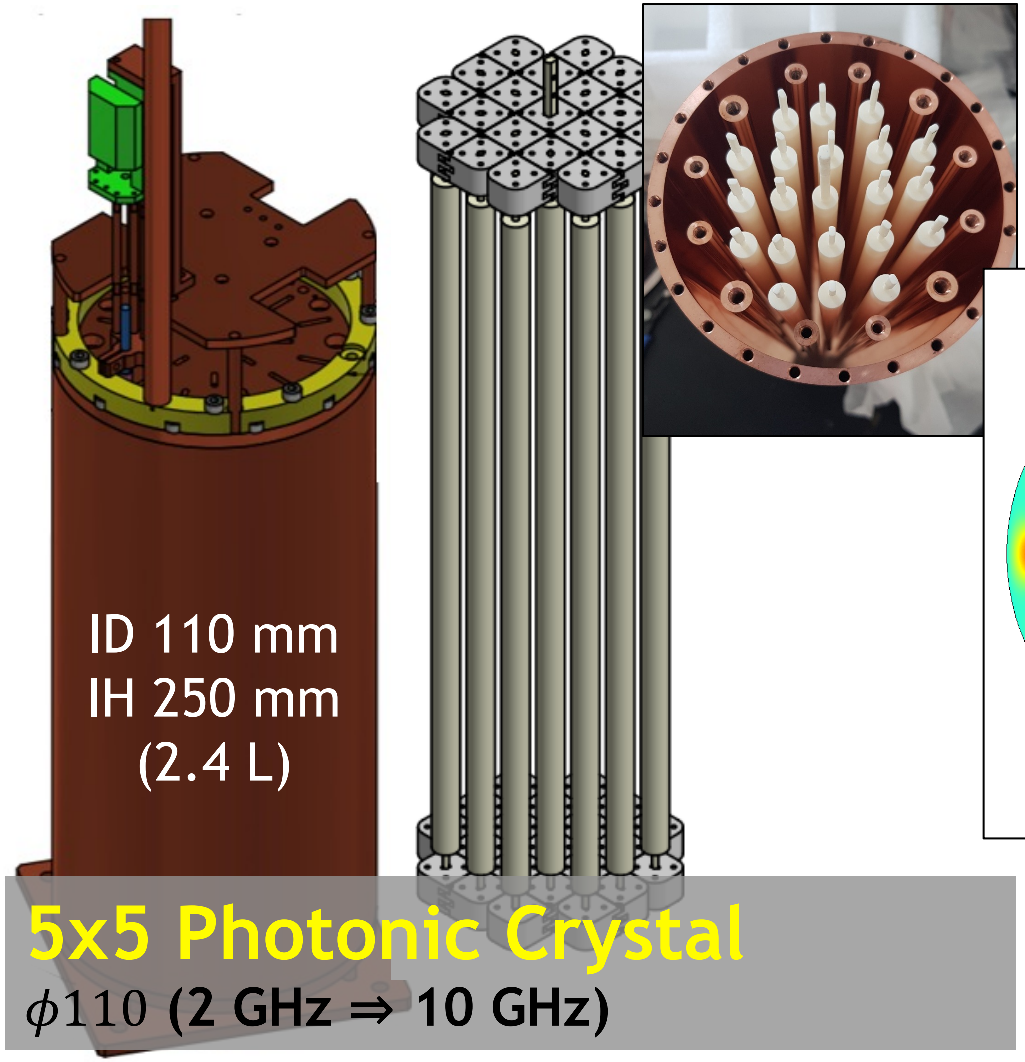


**5x5 Photonic Crystal**

$\phi$110 **(2 GHz ⇒ 10 GHz)**

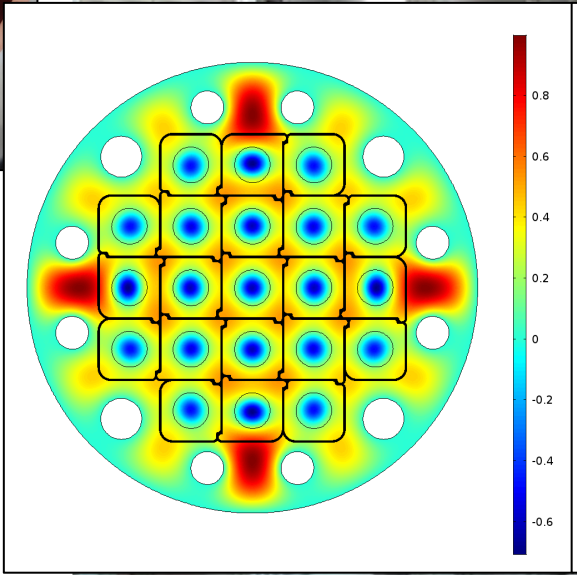


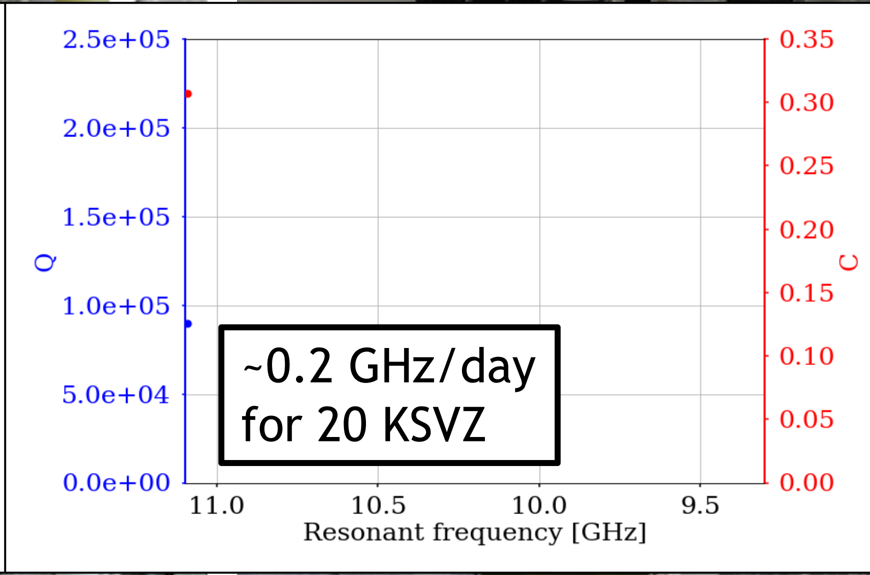


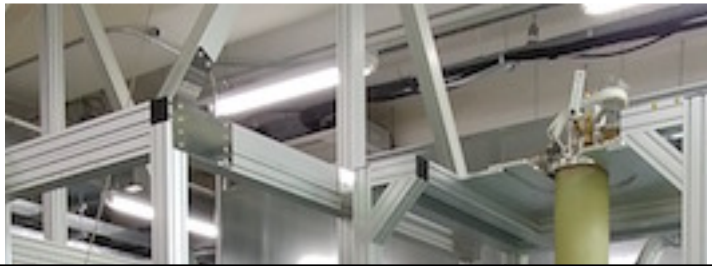

**JANIS System**

*Evaporation cooler (~2 K)*

**NbTi Magnet**

*Bcent 9T ($\phi$125)*

# CAPP’s Novel Cavity Designs

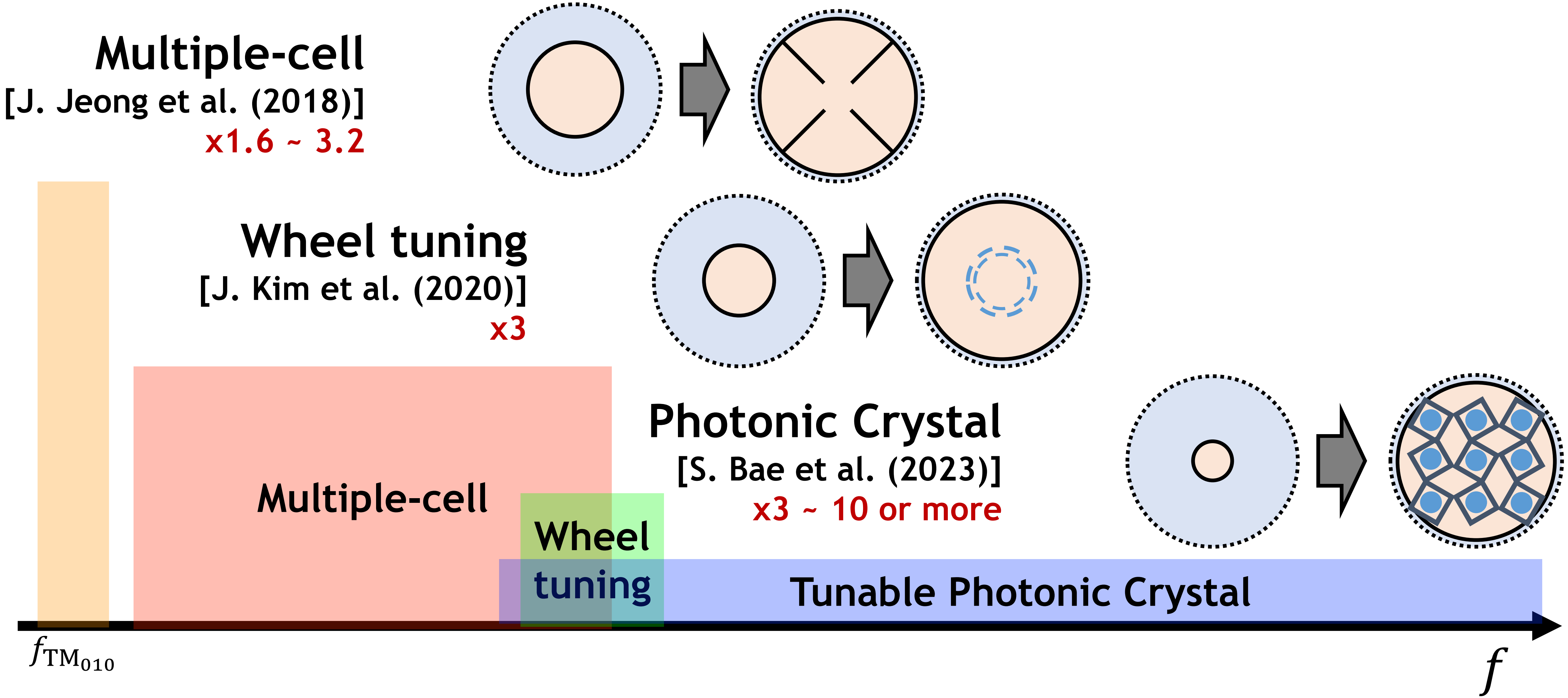

# Dish Antenna Haloscope

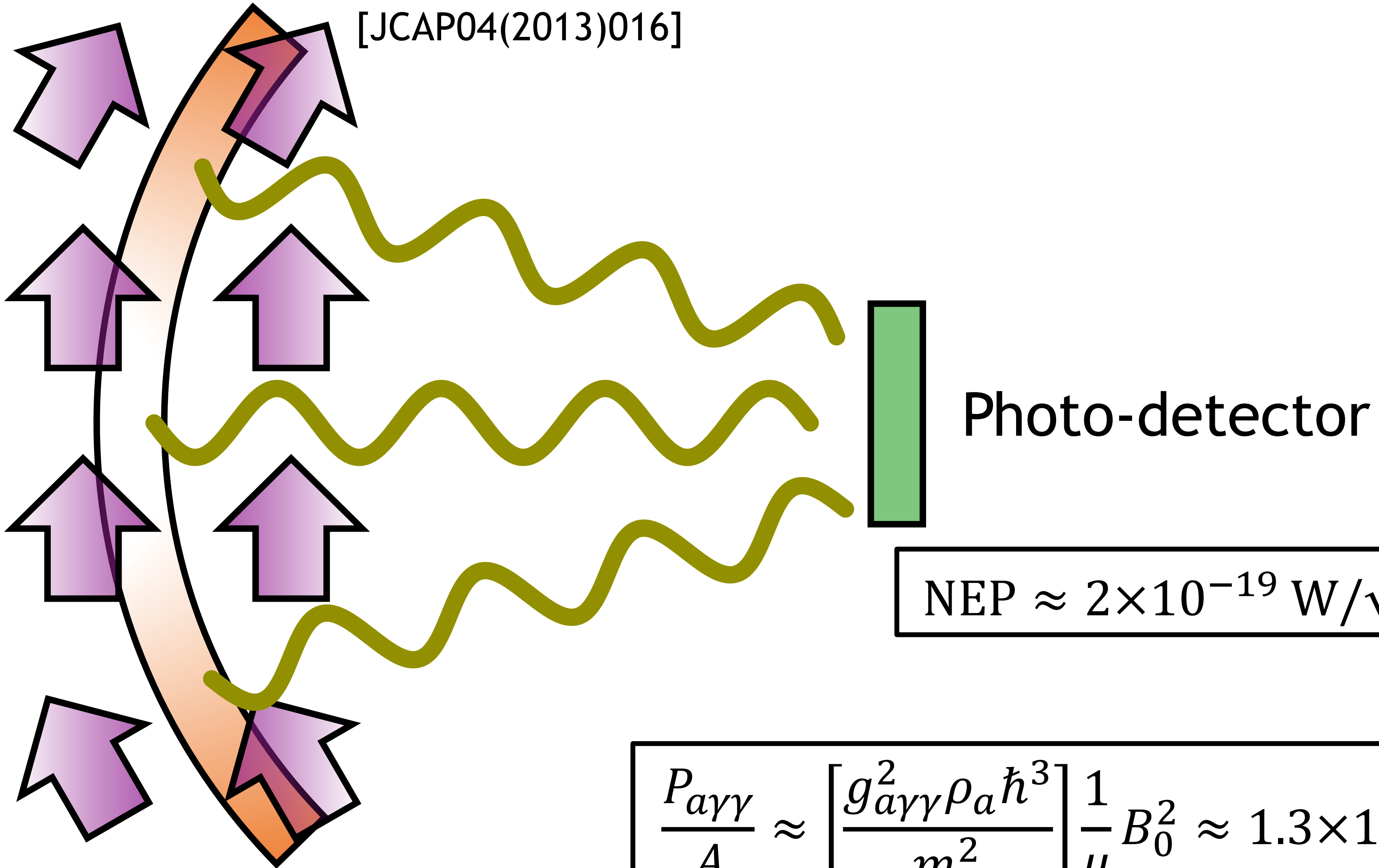


$$\mathrm{NEP} \approx 2\times10^{-19}\ \mathrm{W}/\sqrt{\mathrm{Hz}}$$

$$\frac{P_{a\gamma\gamma}}{A} \approx \left[\frac{g_{a\gamma\gamma}^2 \rho_a \hbar^3}{m_a^2}\right]\frac{1}{\mu} B_0^2 \approx 1.3\times10^{-26}\mathrm{W/m^2}\left(\frac{B_0}{10\ \mathrm{T}}\right)^2\left(\frac{g_\gamma}{0.97}\right)^2$$

# Dish Antenna Haloscope

[JCAP04(2013)016]

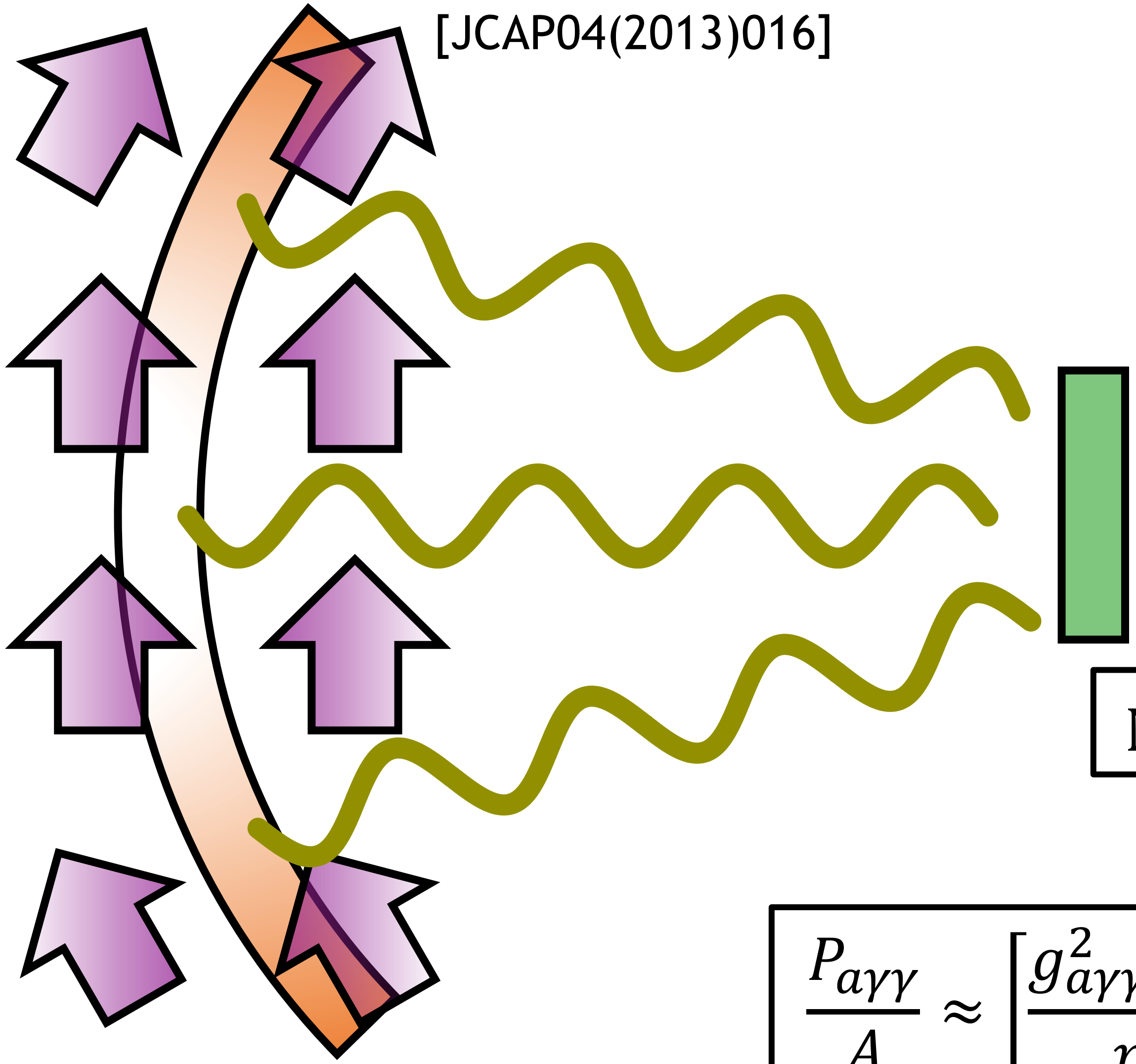

Photo-detector

$$\Delta t \approx \left(\frac{\mathrm{SNR}\times\mathrm{NEP}}{P_{a\gamma\gamma}}\right)^2 = 2\ \mathrm{years}\left(\frac{\mathrm{SNR}}{5}\right)^2\left(\frac{10\ \mathrm{T}}{B_0}\right)^4\left(\frac{30}{g_\gamma}\right)^4\left(\frac{10\ \mathrm{m}^2}{A}\right)^2$$

$$\mathrm{NEP} \approx 2\times10^{-19}\ \mathrm{W}/\sqrt{\mathrm{Hz}}$$

$$\frac{P_{a\gamma\gamma}}{A} \approx \left[\frac{g_{a\gamma\gamma}^2\rho_a\hbar^3}{m_a^2}\right]\frac{1}{\mu}B_0^2 \approx 1.3\times10^{-26}\mathrm{W/m^2}\left(\frac{B_0}{10\ \mathrm{T}}\right)^2\left(\frac{g_\gamma}{0.97}\right)^2$$

# BREAD

[Phys. Rev. Lett. **128**, 131801 (2022)]

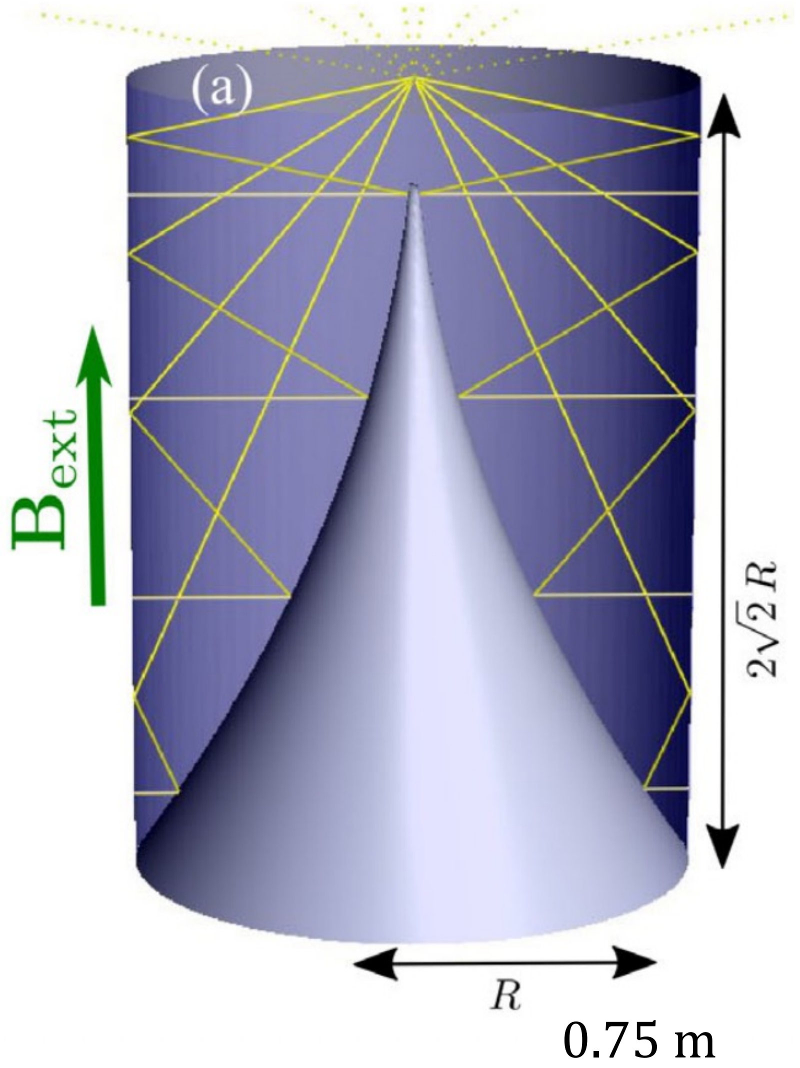


Effectively focus DAH photons on the lateral surface by an innovative parabolic mirror in solenoid geometry

$$P_{\mathrm{BREAD}} \approx 1.3\times10^{-25}\,\mathrm{W}\left(\frac{B_0}{10\ \mathrm{T}}\right)^2\left(\frac{g_\gamma}{0.97}\right)^2\left(\frac{A}{10\ \mathrm{m}^2}\right)$$

$$\Delta t \approx 2\ \mathrm{years}\left(\frac{\mathrm{SNR}}{5}\right)^2\left(\frac{10\ \mathrm{T}}{B_0}\right)^4\left(\frac{30}{g_\gamma}\right)^4\left(\frac{10\ \mathrm{m}^2}{A}\right)^2$$

# BREAD

[Phys. Rev. Lett. **128**, 131801 (2022)]

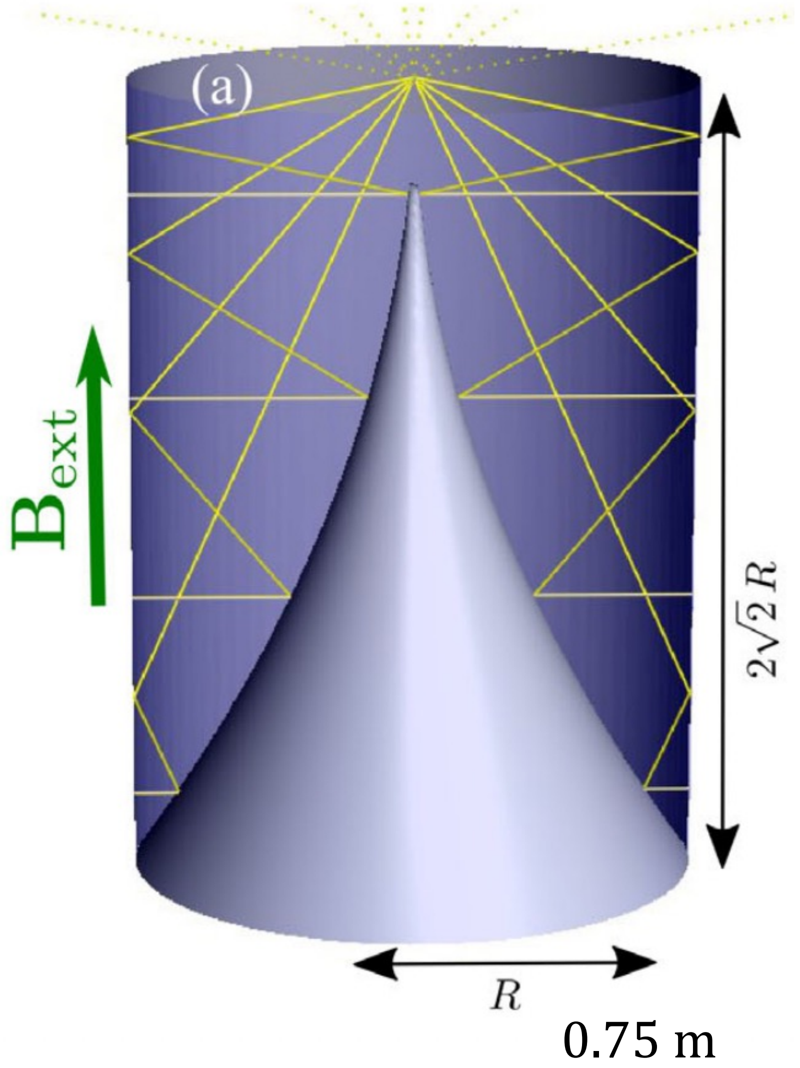


Effectively focus DAH photons on the lateral surface by an innovative parabolic mirror in solenoid geometry

$$P_{\rm BREAD} \approx 1.3\times10^{-25}\ {\rm W}\left(\frac{B_0}{10\ {\rm T}}\right)^2\left(\frac{g_\gamma}{0.97}\right)^2\left(\frac{A}{10\ {\rm m}^2}\right)$$

$$\Delta t \approx 2\ {\rm years}\left(\frac{\rm SNR}{5}\right)^2\left(\frac{10\ {\rm T}}{B_0}\right)^4\left(\frac{30}{g_\gamma}\right)^4\left(\frac{10\ {\rm m}^2}{A}\right)^2$$

Still some available space inside the bore where the m agnetic field is applied

# Volume-Efficient Way?

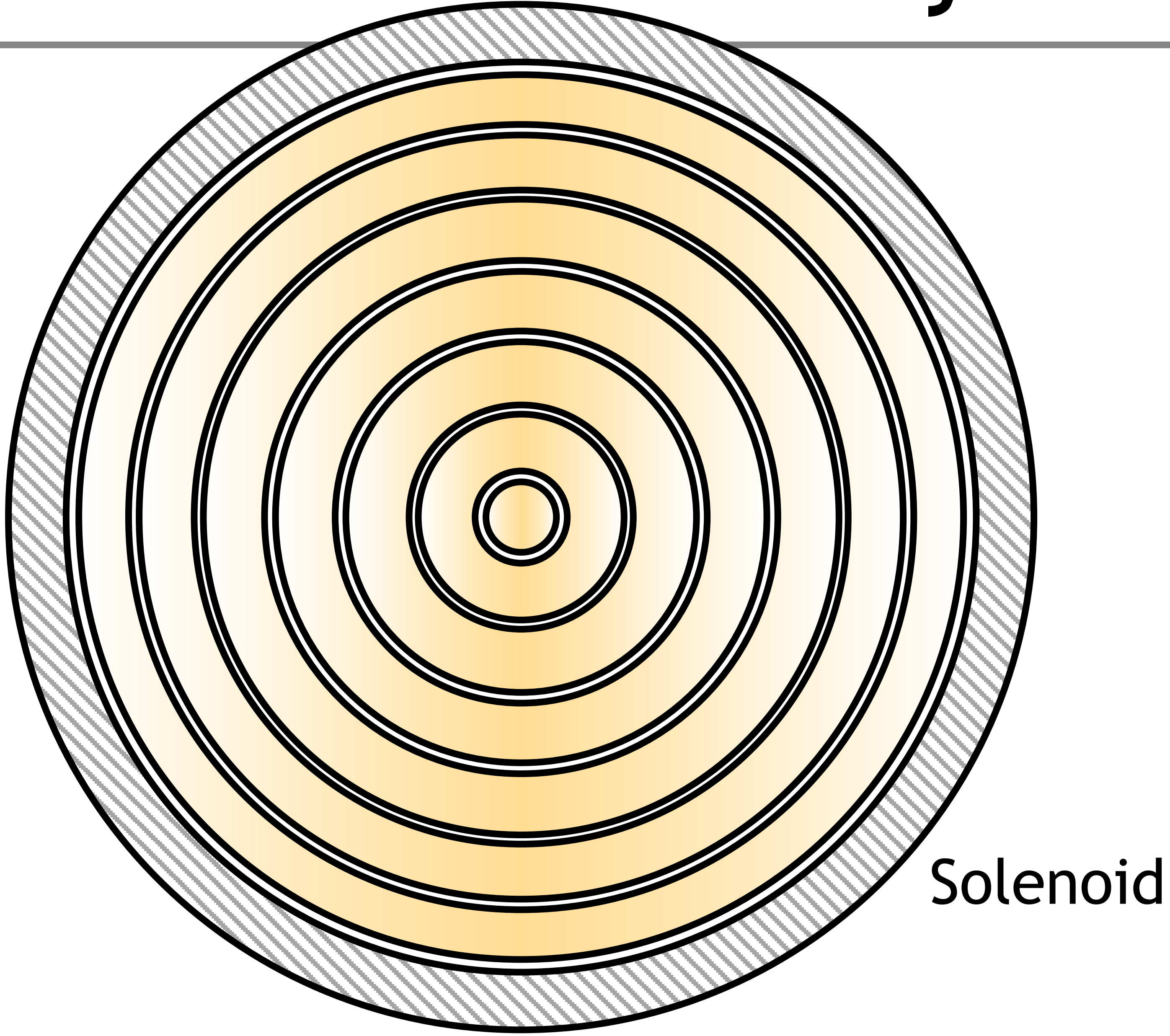

# Volume-Efficient Way?

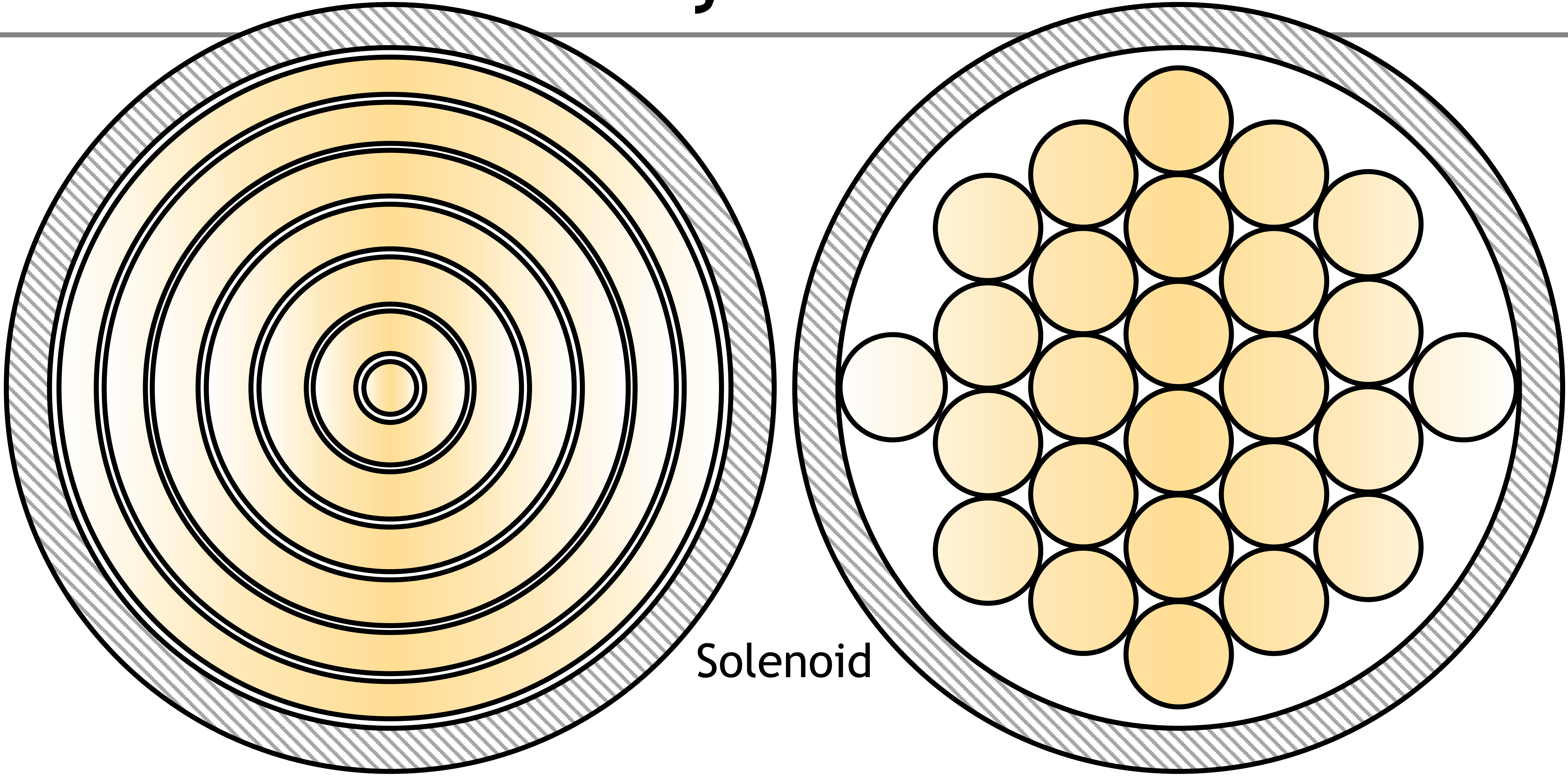

# Horn Array Haloscope

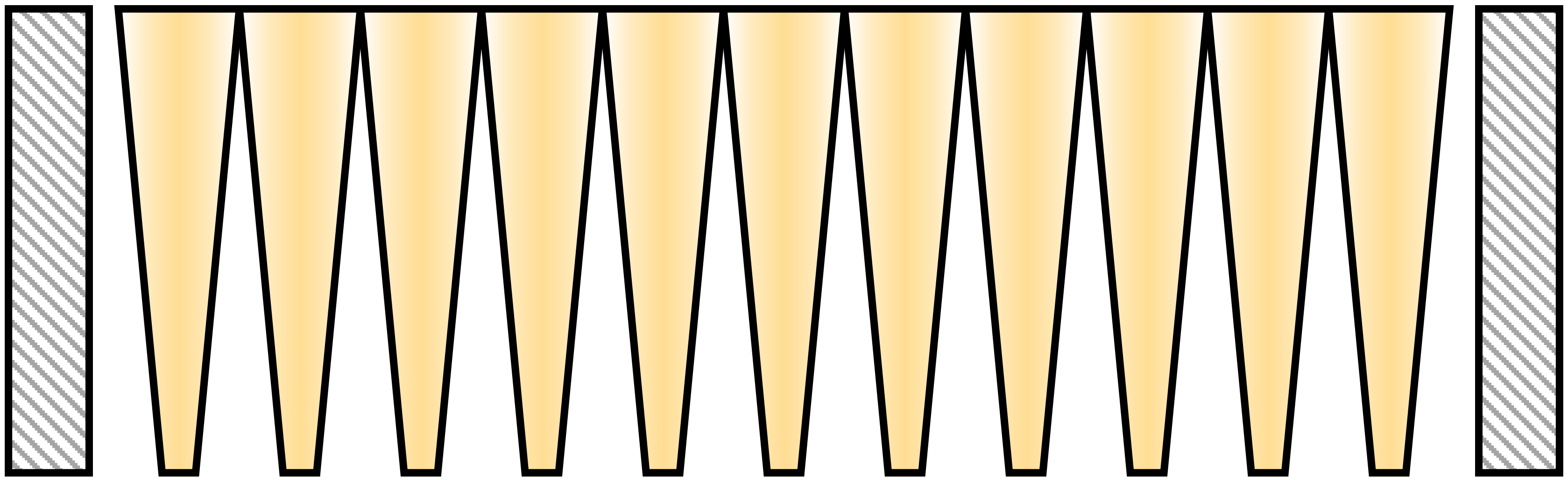

# Horn Array Haloscope

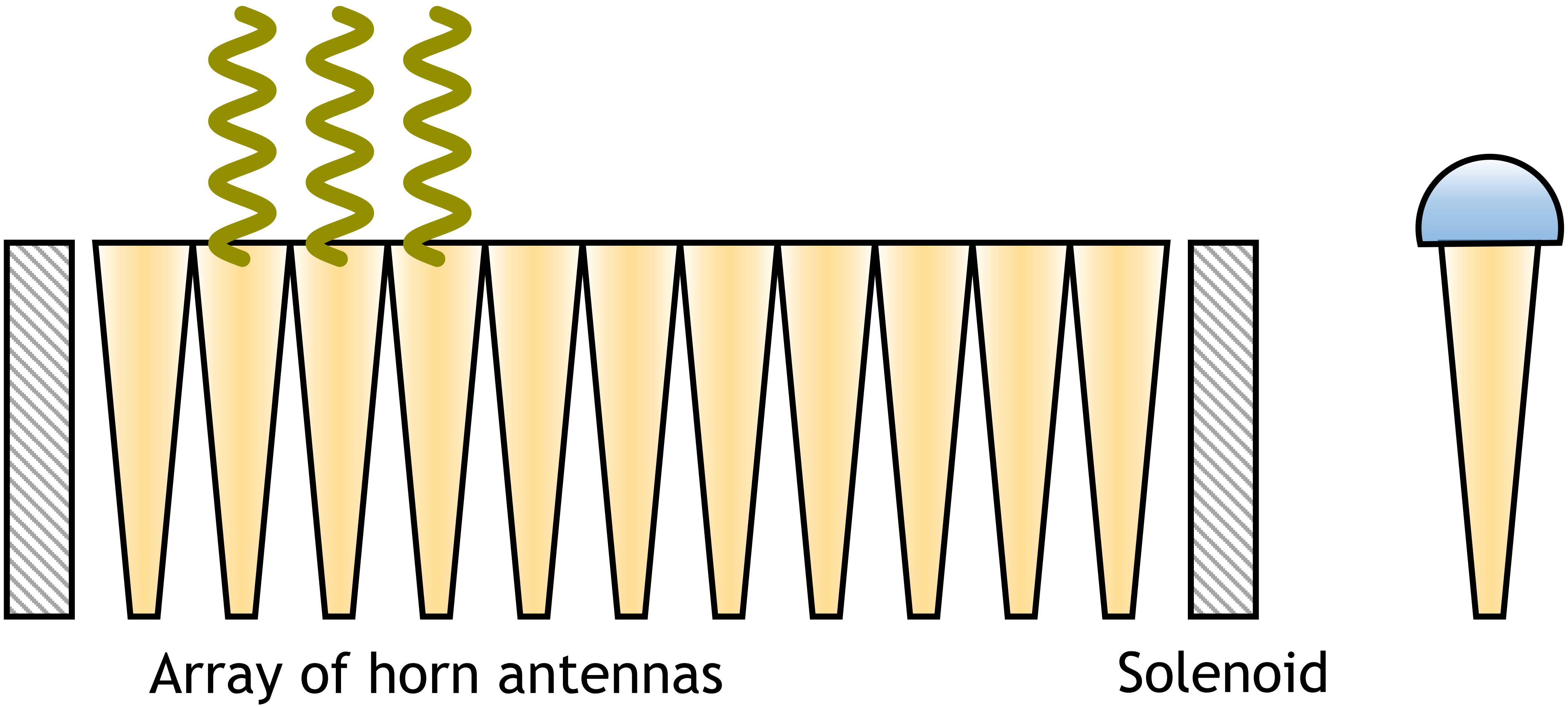

# Horn Array Haloscope

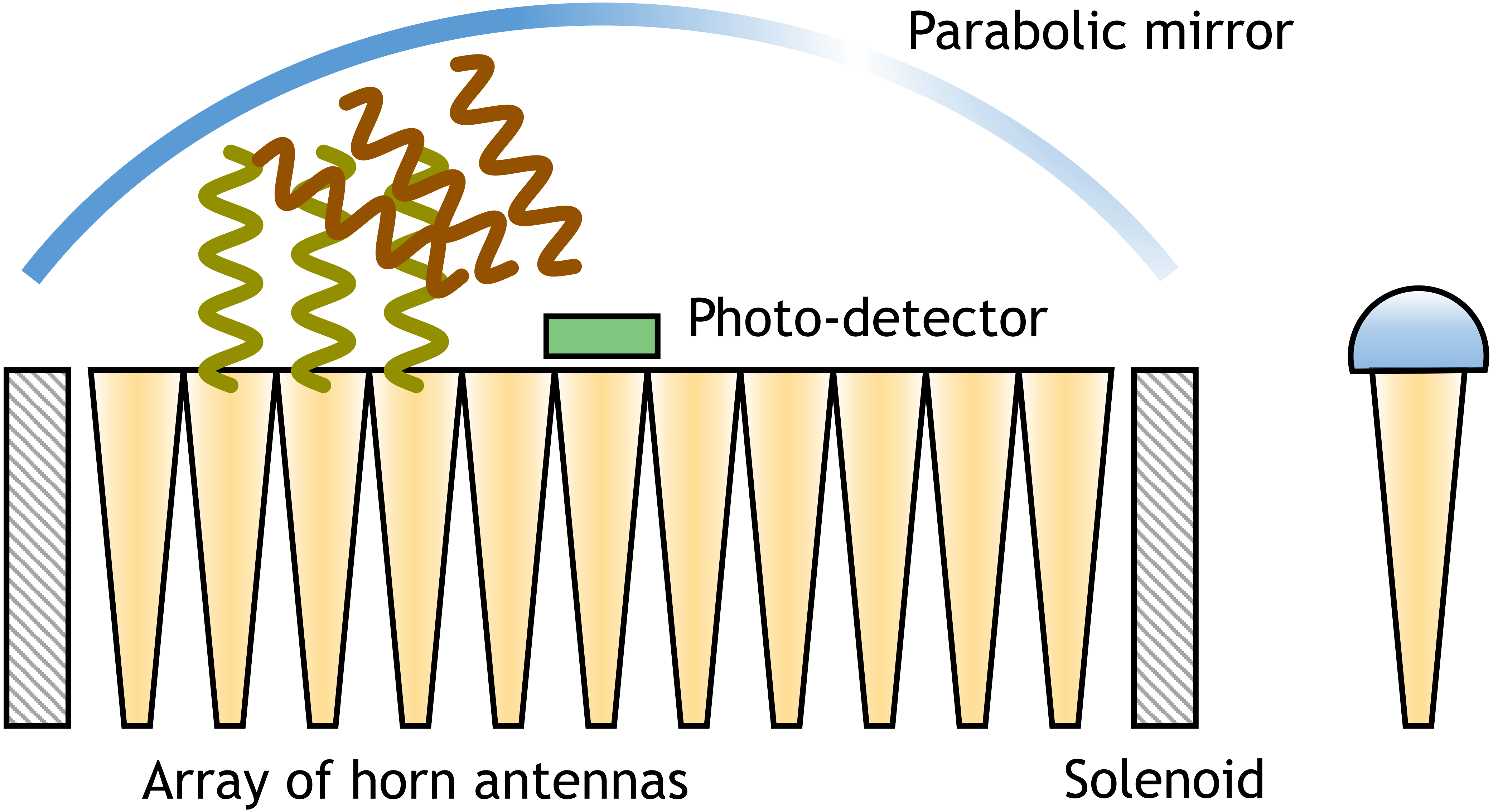

# Single Horn Antenna

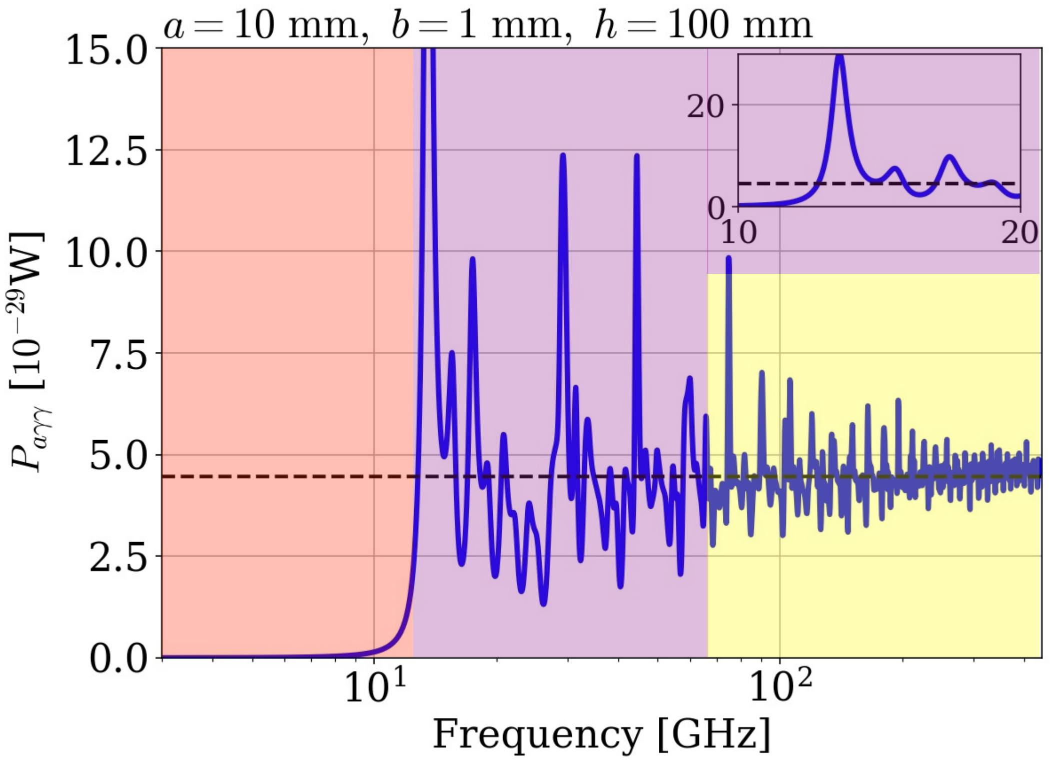


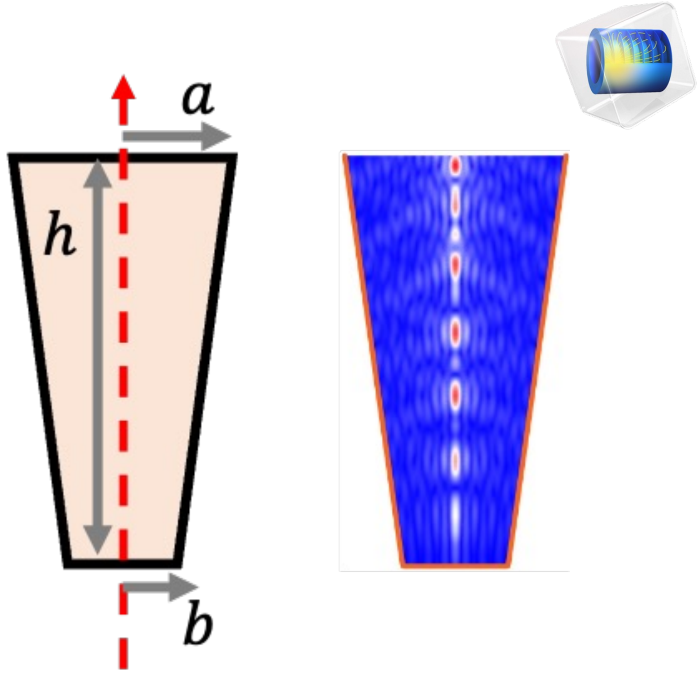


$a = 10$ mm, $b = 1$ mm, $h = 100$ mm

$$P_{\text{horn}} \approx 4.5\times10^{-29}\,\text{W}\left(\frac{B_0}{10\text{ T}}\right)^2\left(\frac{g_\gamma}{0.97}\right)^2\left(\frac{A}{3440\text{ mm}^2}\right)$$

- Low frequency: no converion
- Intermediate frequency: resonance peaks
- High frequency: dish antenna haloscope

# Projected Sensitivity

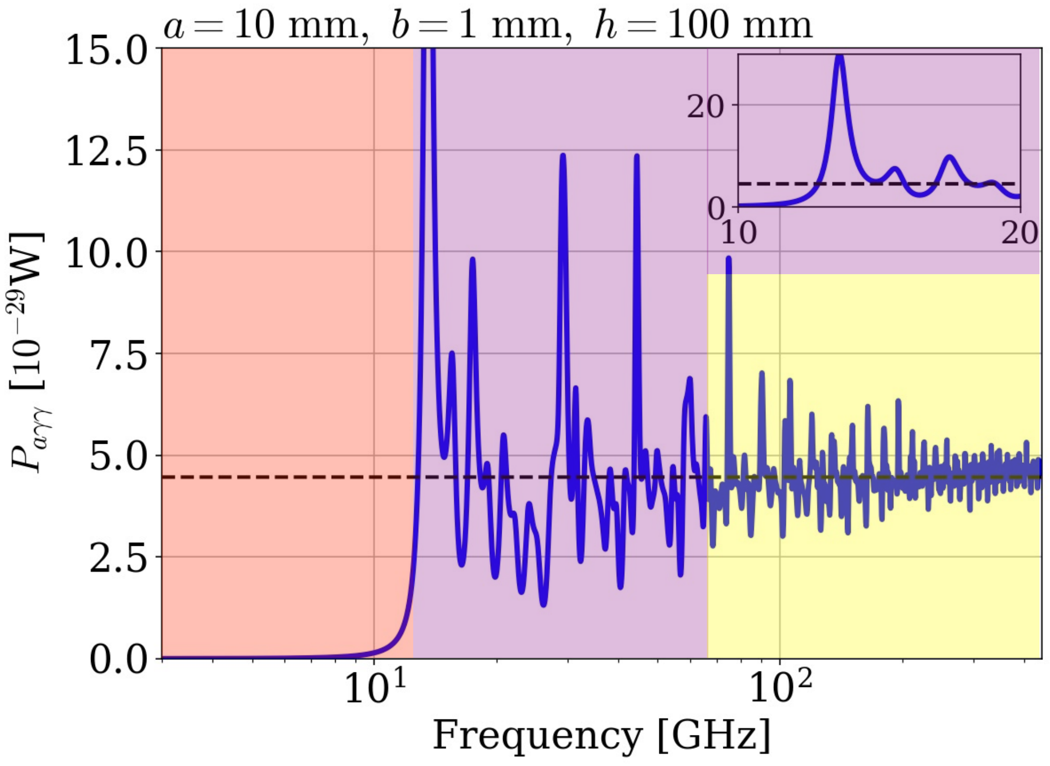


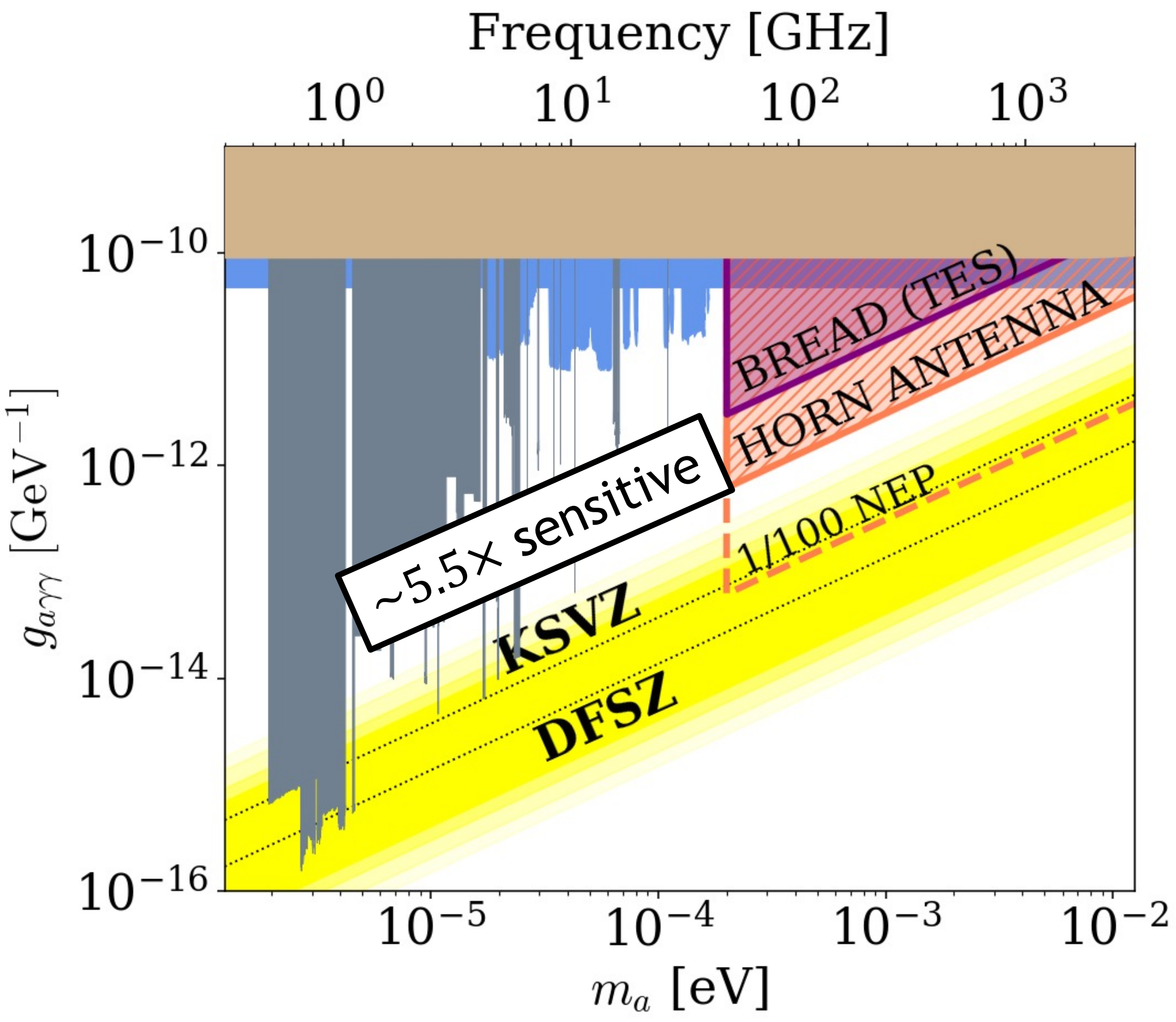


* NEP $\approx 2\times10^{-19}$ W/$\sqrt{\mathrm{Hz}}$, $R = 0.75$ m, $h = 2.1$ m, 3 years of DAQ

# Power Detection

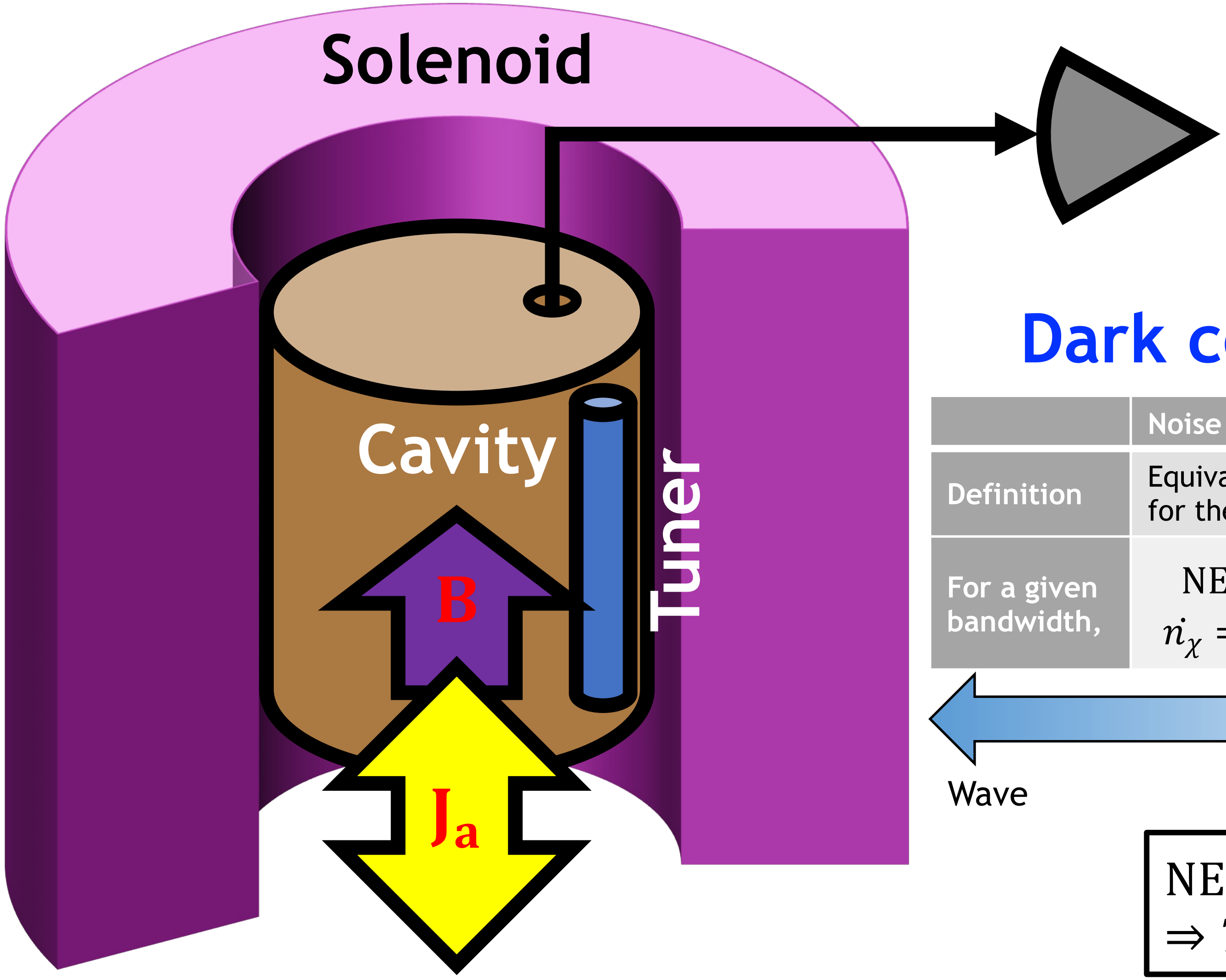


**Photo-detector (bolometer)**

## Dark count rate ≫ Noise of amplifier

| | Noise temperature | Noise equivalent power | Dark count rate |
|---|---|---|---|
| Definition | Equivalent temperature for the noise baseline | Minimum detectable power with 1 sec acq. | False positive count rate |
| For a given bandwidth, | $\mathrm{NEP} = k_B T_n \sqrt{\Delta f}$ <br> $\dot{n}_\chi = k_B T_n \Delta f / (hf)$ | $T_n = \mathrm{NEP} / \left(k_B \sqrt{\Delta f}\right)$ <br> $\dot{n}_\chi = \mathrm{NEP} \sqrt{\Delta f} / (hf)$ | $T_n = hf \dot{n}_\chi / (k_B \Delta f)$ <br> $\mathrm{NEP} = hf \dot{n}_\chi / \sqrt{\Delta f}$ |

Wave ⟷ Particle

$$\mathrm{NEP} \approx 2\times10^{-19}\ \mathrm{W}/\sqrt{\mathrm{Hz}},\ \Delta f = 10\ \mathrm{kHz}$$
$$\Rightarrow T_n \approx 150\ \mathrm{K}$$

# Optical Heterodyne Interferrometer

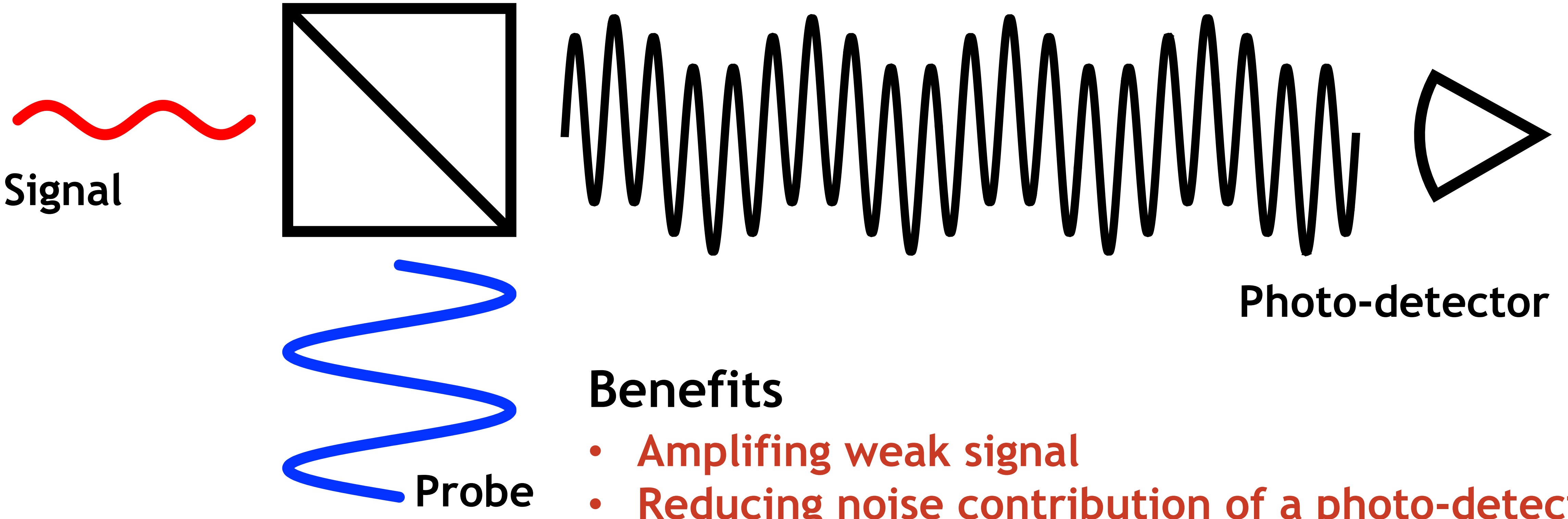


**Benefits**

- Amplifing weak signal
- Reducing noise contribution of a photo-detector
- Detecting a phase change in a signal
- Shifting the frequency (up/down conversion)

# Optical Heterodyne Interferrometer

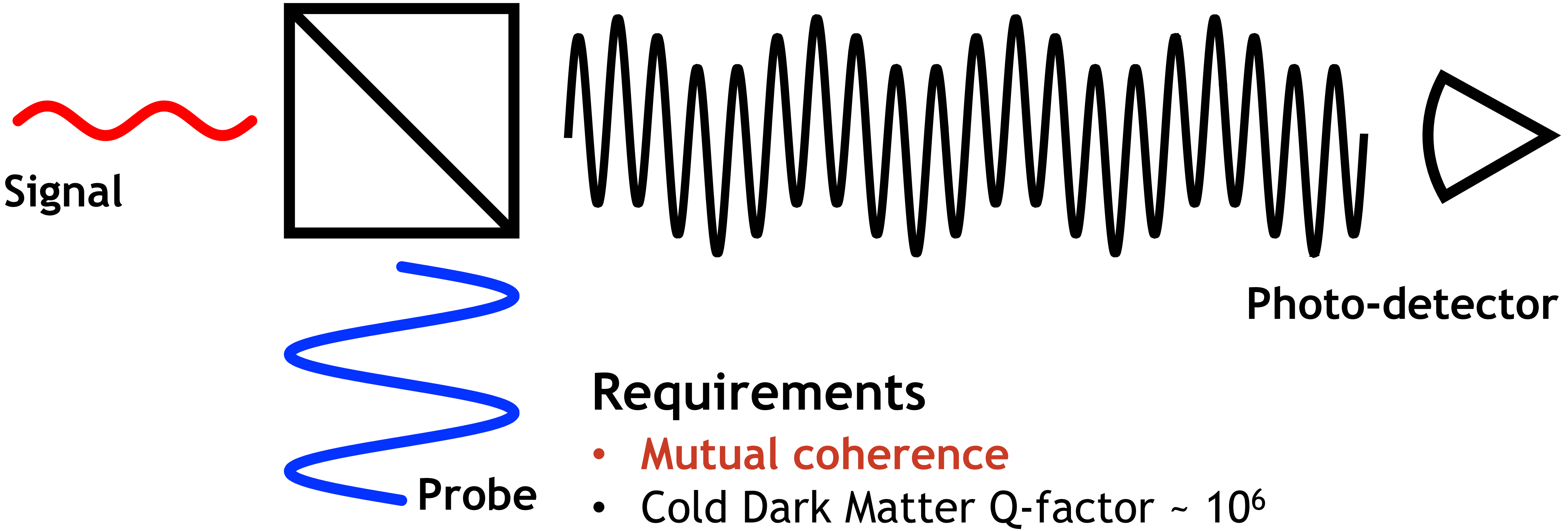


**Requirements**

- Mutual coherence
- Cold Dark Matter Q-factor ~ $10^6$
- Average for long time ⇒ No interference effect

# Optical Heterodyne Interferrometer

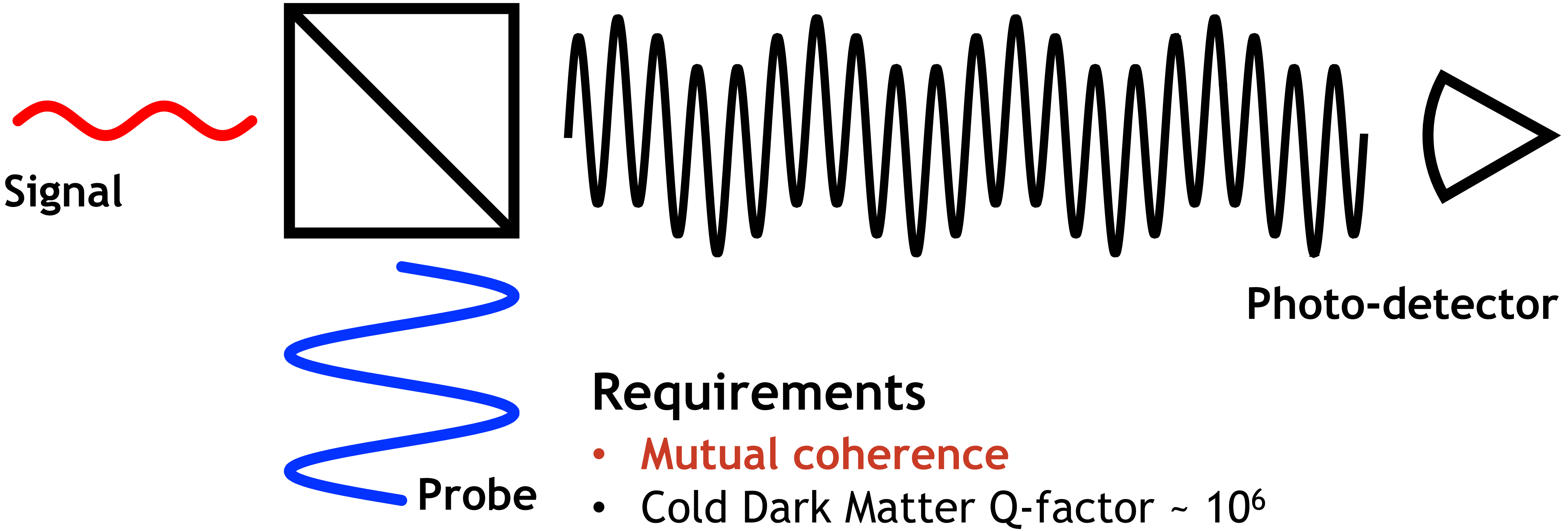


**Requirements**

- Mutual coherence
- Cold Dark Matter Q-factor ~ $10^6$
- Average for long time ⇒ No interference effect

**Variance?**

# Heterodyne-Based Variance Method

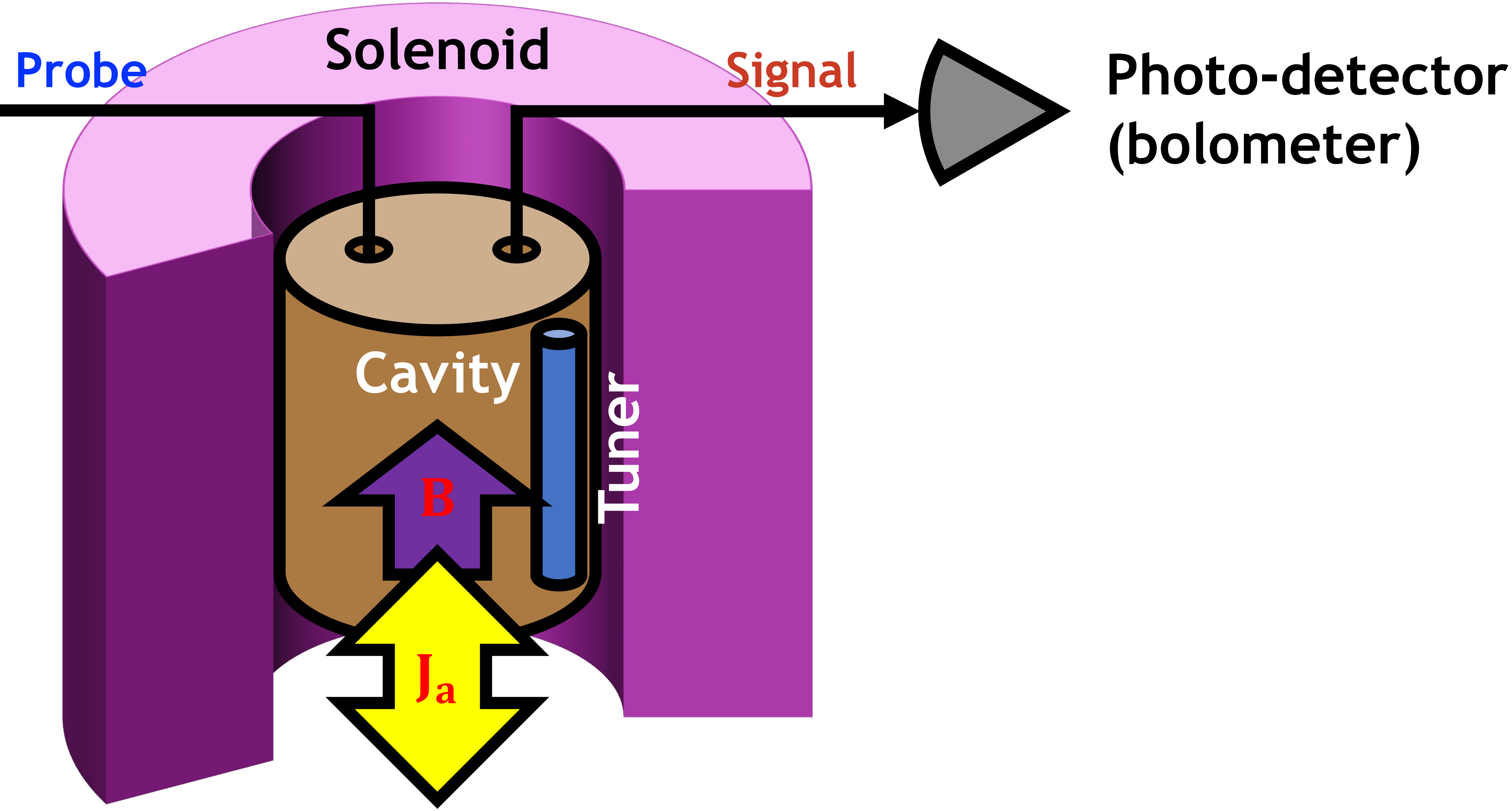

# Heterodyne-Based Variance Method

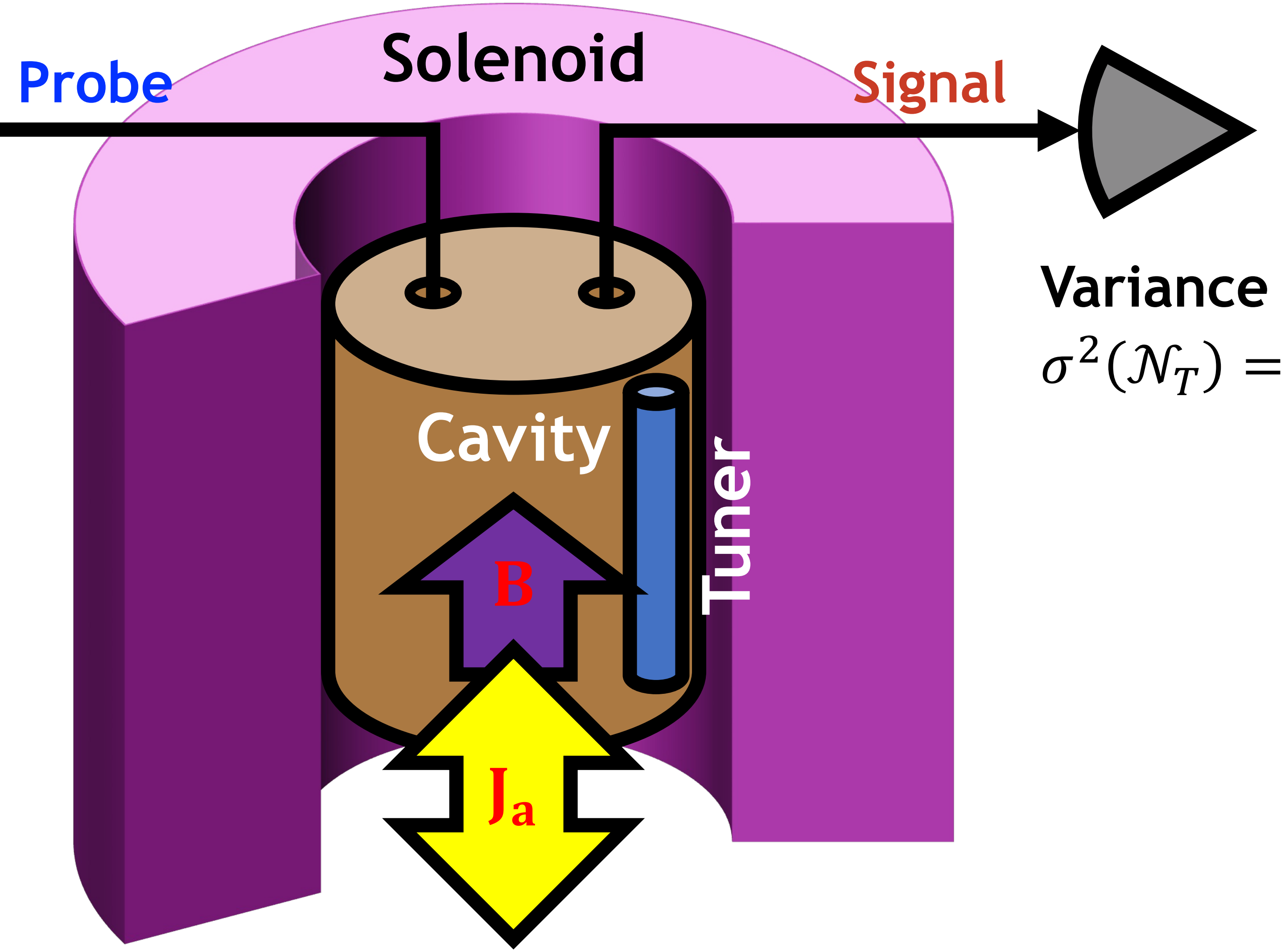


Variance for every signal coherence time

$$\sigma^2(\mathcal{N}_T) = \underbrace{N_{\text{th.}} + N_D + N_s + N_p}_{\text{Shot noise}} + \underbrace{N_p N_s + N_p N_{\text{th.}}}_{\text{Interference}}$$

# Heterodyne-Based Variance Method

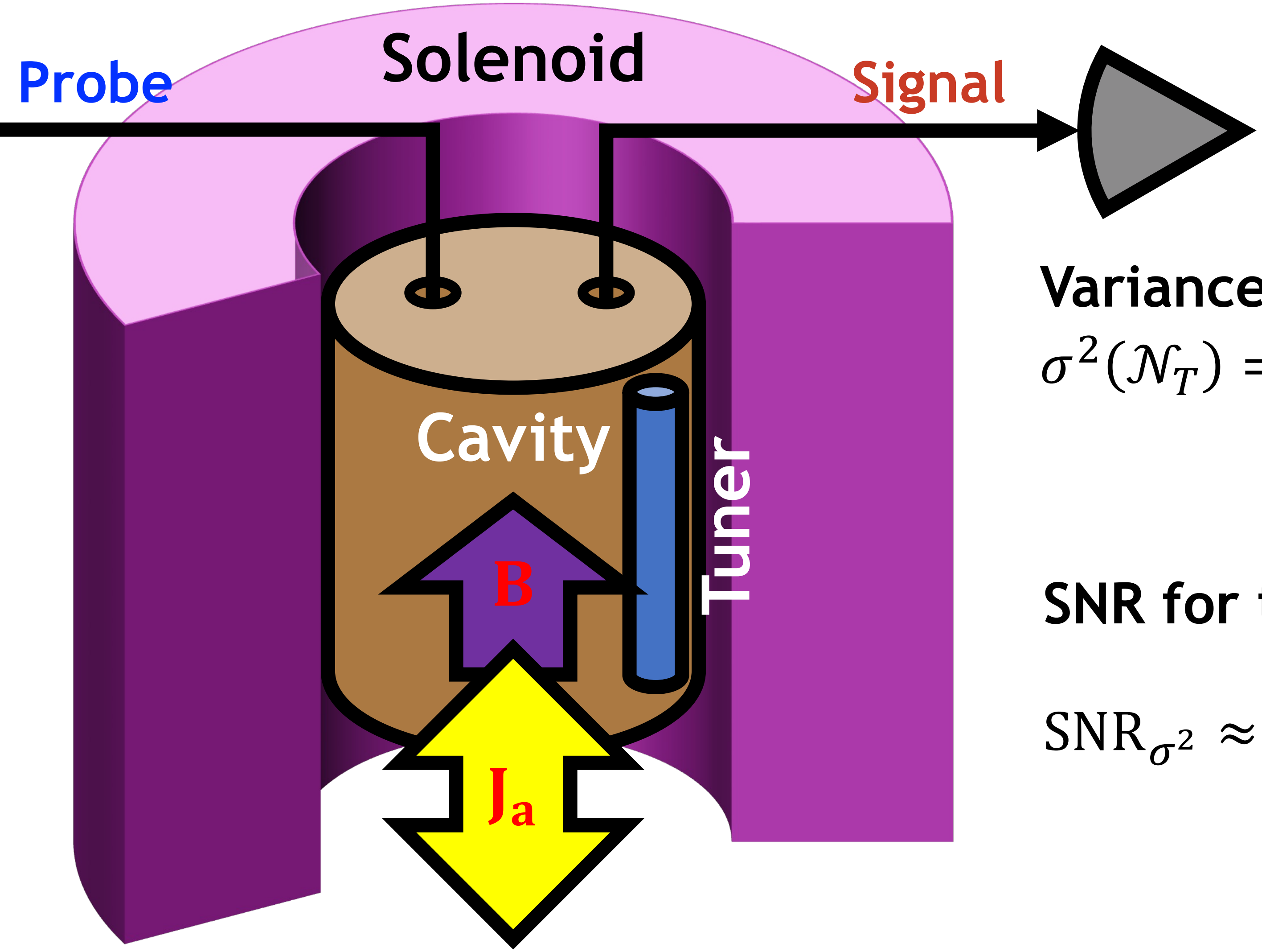


Photo-detector (bolometer)

**Variance for every signal coherence time**

$$\sigma^2(\mathcal{N}_T) = \underbrace{N_{\text{th.}} + N_D + N_s + N_p}_{\text{Shot noise}} + \underbrace{N_p N_s + N_p N_{\text{th.}}}_{\text{Interference}}$$

**SNR for the $\sigma^2$ estimator ($N_{\text{th.}} \ll 1$)**

$$\text{SNR}_{\sigma^2} \approx \frac{\left(N_s + N_s N_p\right)}{\left(N_D + N_p\right)\sqrt{2 + 1/\left(N_D + N_p\right)}}\sqrt{n}$$

# Signal-to-Noise Retio

**In terms of photon rate,**

Photon rate ($\dot{N}$) = Number of Photon ($N$) $\times$ Sampling rate ($f_s$)

$$\mathrm{SNR}_{\sigma^2} \approx \frac{\dot{N}_s\left(1+\dot{N}_p/f_s\right)\sqrt{f_s\Delta t}}{\left(\dot{N}_D+\dot{N}_p\right)\sqrt{2+f_s/\left(\dot{N}_D+\dot{N}_p\right)}}$$

# Signal-to-Noise Retio

## In terms of photon rate,

Photon rate ($\dot{N}$) = Number of Photon ($N$) $\times$ Sampling rate ($f_s$)

$$\mathrm{SNR}_{\sigma^2} \approx \frac{\dot{N}_s\left(1+\dot{N}_p/f_s\right)\sqrt{f_s\Delta t}}{\left(\dot{N}_D+\dot{N}_p\right)\sqrt{2+f_s/\left(\dot{N}_D+\dot{N}_p\right)}}$$

$f_a = 10^9$ Hz, $f_s = 10^3$ Hz

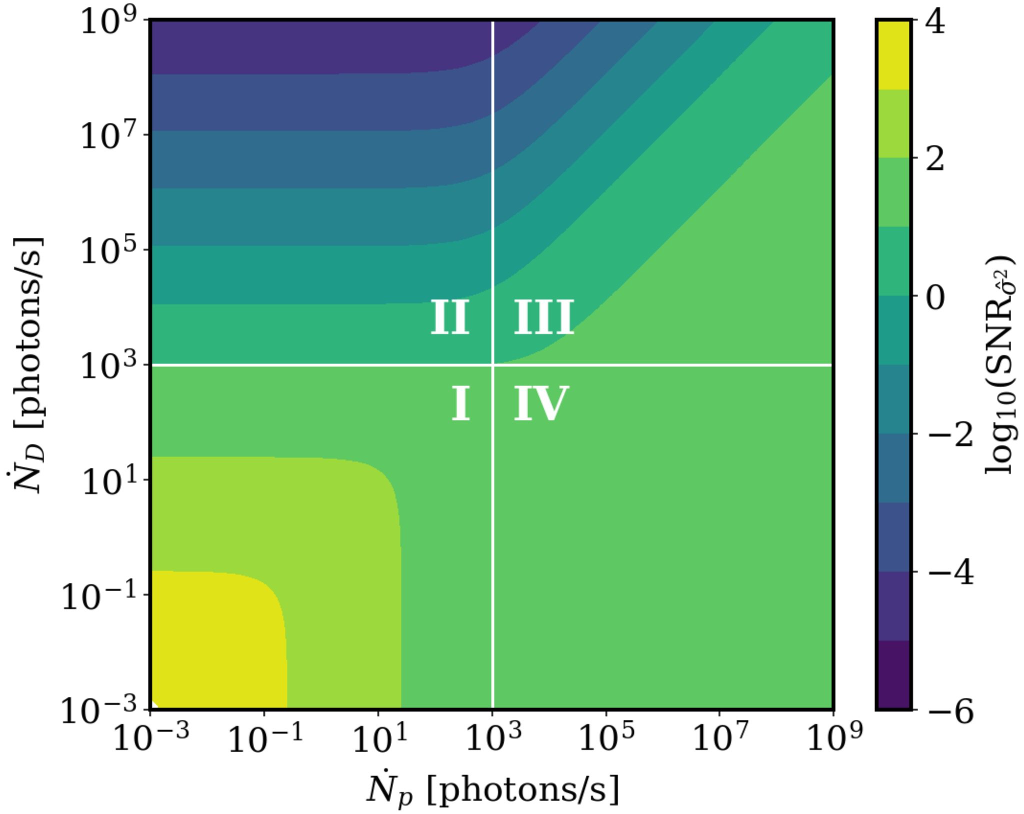

# Signal-to-Noise Retio

## In terms of photon rate,

Photon rate ($\dot{N}$) = Number of Photon ($N$) $\times$ Sampling rate ($f_s$)

$$\mathrm{SNR}_{\sigma^2} \approx \frac{\dot{N}_s\left(1+\dot{N}_p/f_s\right)\sqrt{f_s\Delta t}}{\left(\dot{N}_D+\dot{N}_p\right)\sqrt{2+f_s/\left(\dot{N}_D+\dot{N}_p\right)}}$$

- **Region I** ($\dot{N}_D < f_s,\ \dot{N}_p < f_s$)
  *Single photon detection (best SNR)*

$f_a = 10^9$ Hz, $f_s = 10^3$ Hz

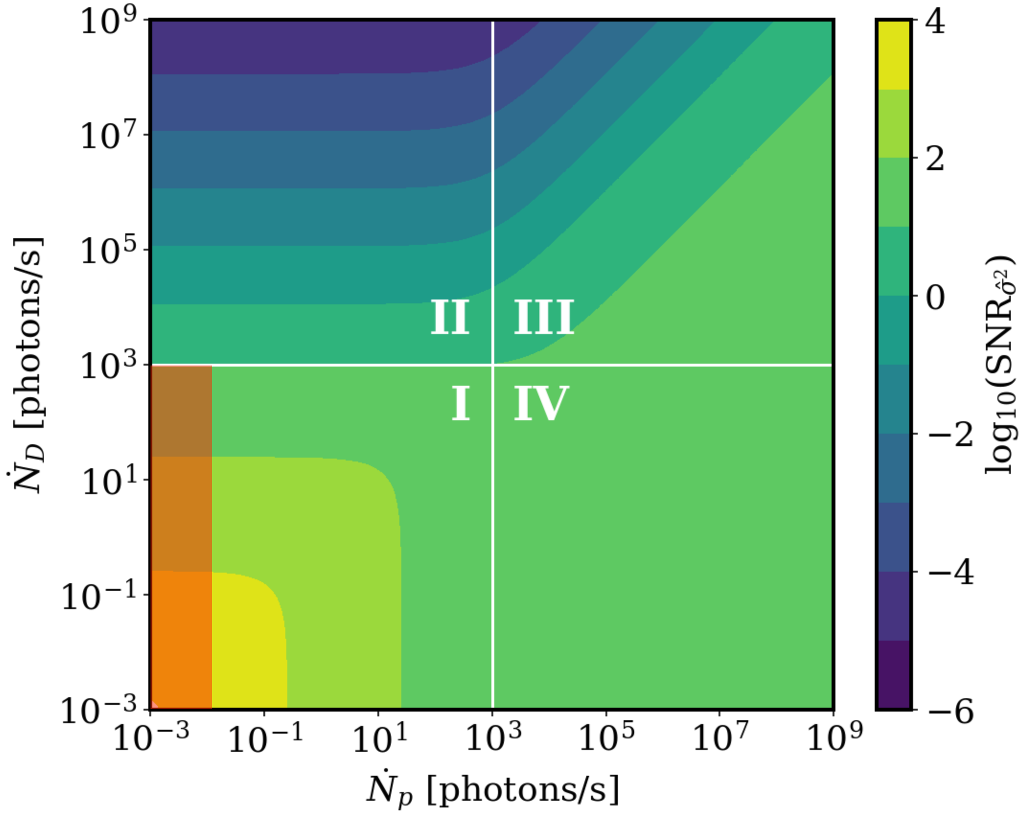

# Signal-to-Noise Retio

## In terms of photon rate,

Photon rate ($\dot{N}$) = Number of Photon ($N$) $\times$ Sampling rate ($f_s$)

$$\mathrm{SNR}_{\sigma^2} \approx \frac{\dot{N}_s\left(1+\dot{N}_p/f_s\right)\sqrt{f_s\Delta t}}{\left(\dot{N}_D+\dot{N}_p\right)\sqrt{2+f_s/\left(\dot{N}_D+\dot{N}_p\right)}}$$

- **Region I** ($\dot{N}_D < f_s,\ \dot{N}_p < f_s$)
  *Single photon detection (best SNR)*
- **Region II** ($\dot{N}_D > f_s,\ \dot{N}_p < f_s$)
  *Usual bolometer at microwaves*

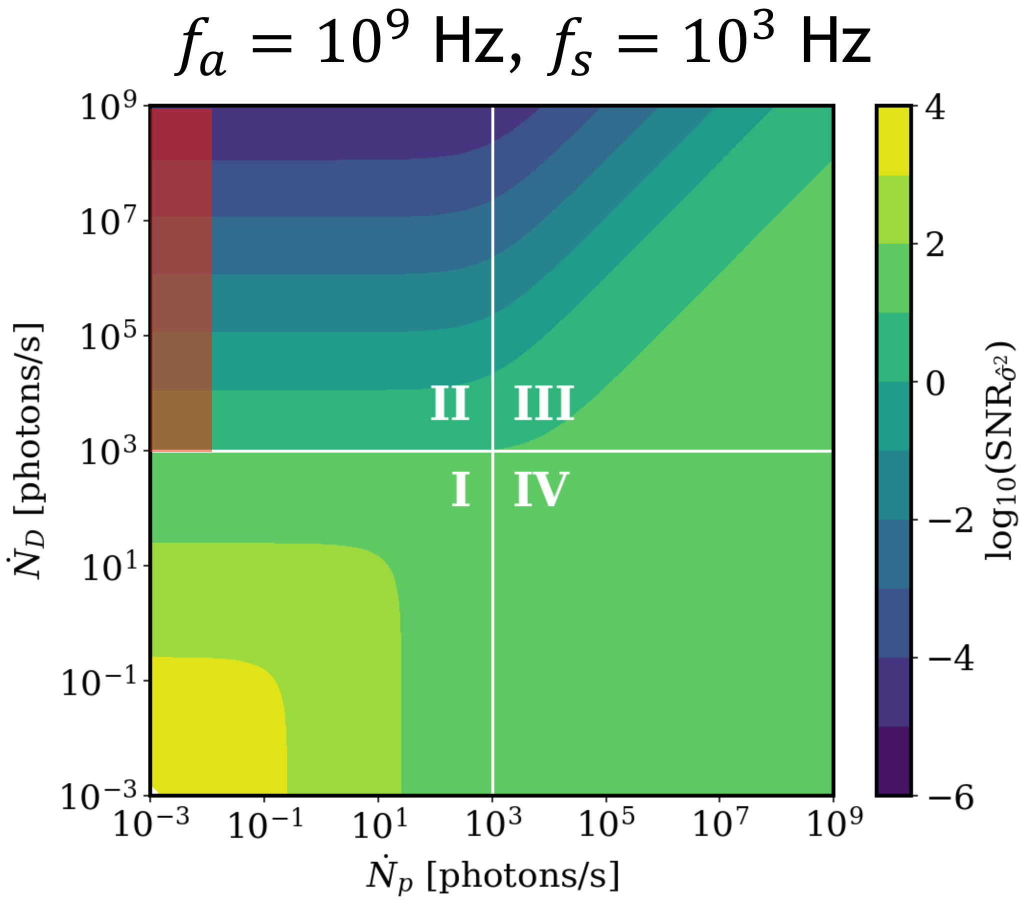

# Signal-to-Noise Retio

## In terms of photon rate,

Photon rate ($\dot{N}$) = Number of Photon ($N$) × Sampling rate ($f_s$)

$$\mathrm{SNR}_{\sigma^2} \approx \frac{\dot{N}_s\left(1+\dot{N}_p/f_s\right)\sqrt{f_s\Delta t}}{\left(\dot{N}_D+\dot{N}_p\right)\sqrt{2+f_s/\left(\dot{N}_D+\dot{N}_p\right)}}$$

- **Region I** ($\dot{N}_D < f_s,\ \dot{N}_p < f_s$)
  *Single photon detection (best SNR)*
- **Region II** ($\dot{N}_D > f_s,\ \dot{N}_p < f_s$)
  *Usual bolometer at microwaves*
- **Region III** ($\dot{N}_D > f_s,\ \dot{N}_p > f_s$)
  *Injecting probe enhances the SNR*
- **Region IV** ($\dot{N}_D < f_s,\ \dot{N}_p > f_s$)
  *Injecting probe reduces the SNR*

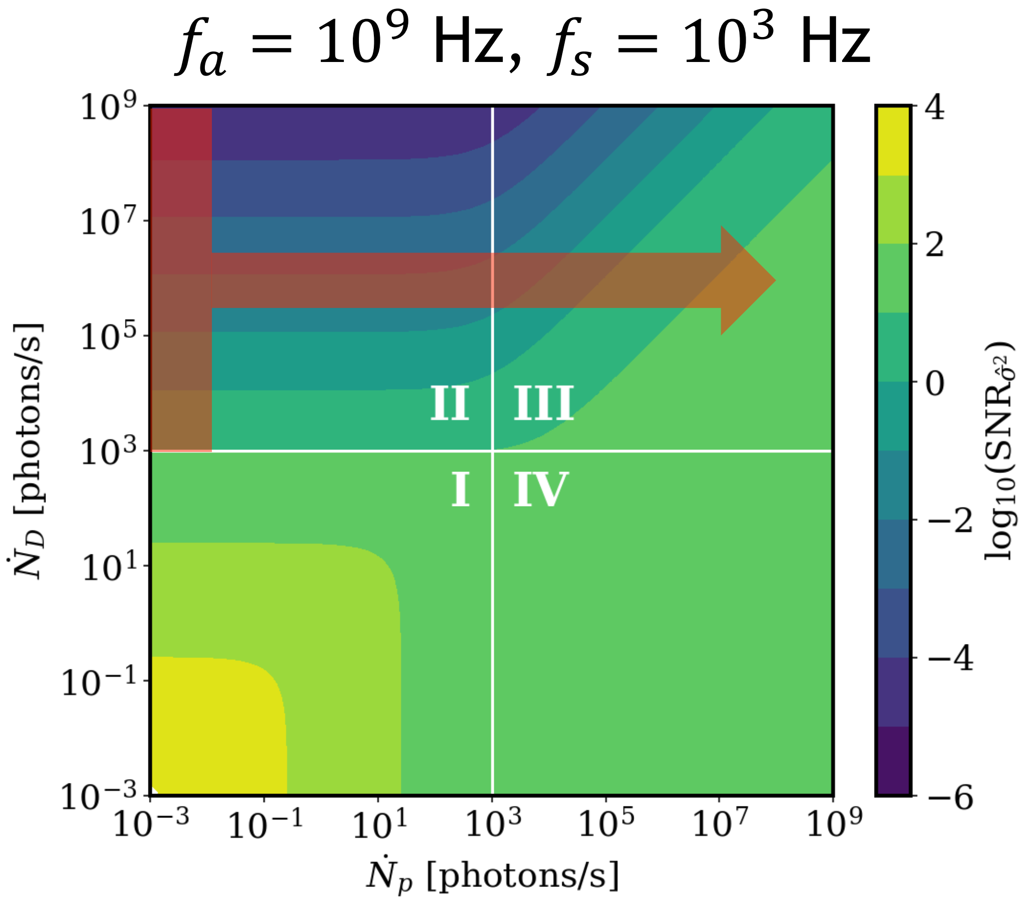

# SNR Comparison

**Variance method**

$$\mathrm{SNR}_{\sigma^2} \approx \frac{\dot{N}_s}{\sqrt{2f_s}}\sqrt{\Delta t}$$

**Single photon detector (Average)**

$$\mathrm{SNR}_{\mu} \approx \frac{\dot{N}_s}{\sqrt{\dot{N}_D}}\sqrt{\Delta t}$$

- The denominator chages from $\sqrt{\dot{N}_D}$ to $\sqrt{2f_s}$
- If $\dot{N}_D > 2f_s$, $\mathrm{SNR}_{\sigma^2} > \mathrm{SNR}_{\mu}$ (for known coherence)

# Scan rate

## Variance method

$$\mathrm{SNR}_{\sigma^2} \approx \frac{\dot{N}_s}{\sqrt{2f_s}}\sqrt{\Delta t}$$

## Linear Amplifier

$$\left.\frac{df}{dt}\right|_{\mathrm{lin.}} \approx \frac{\Delta f_c}{\Delta t}$$

$$= \frac{1}{\mathrm{SNR}_\mu}\left(\frac{P_s}{k_B(T_{\mathrm{th.}} + T_{\mathrm{amp}})}\right)^2 \frac{Q_a}{Q_l}$$

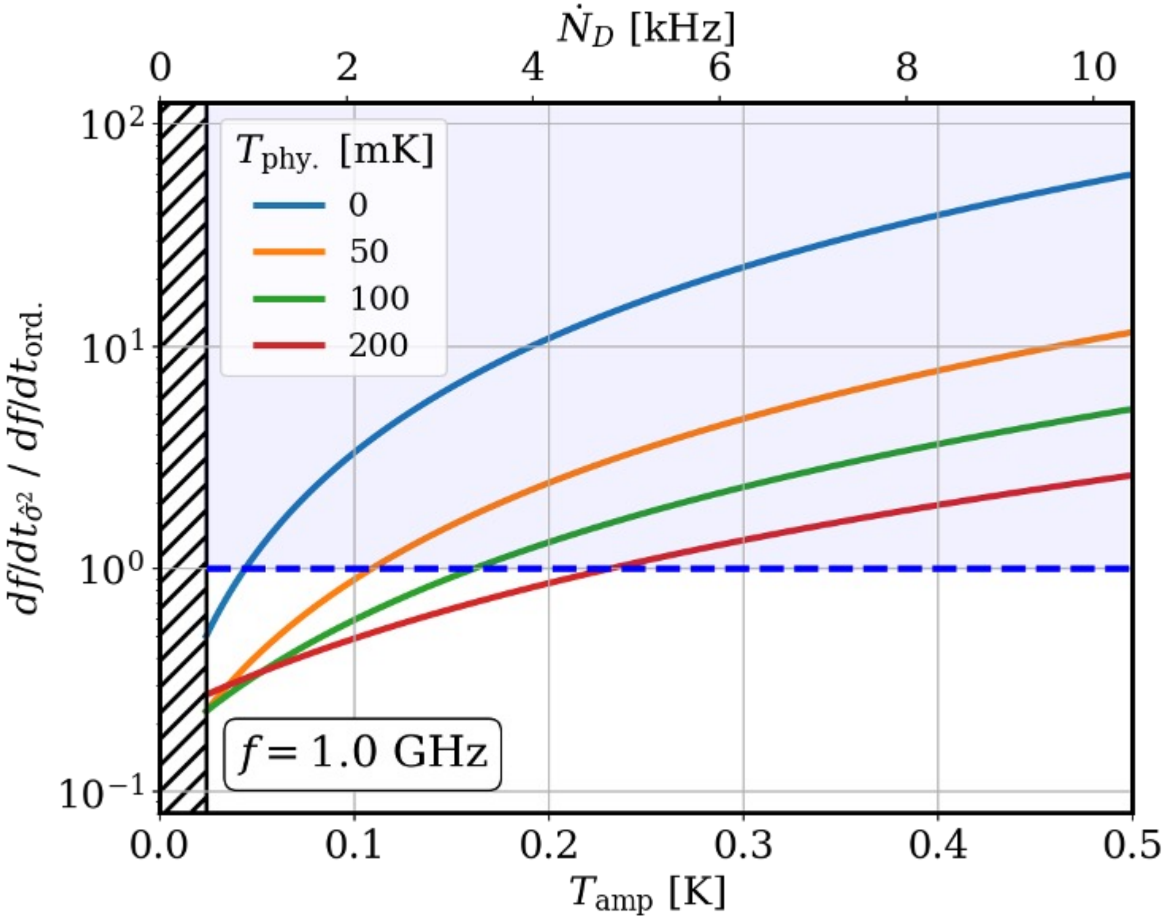

# Summary (1)

- CAPP has advanced high-mass axion searches through the development of three innovative cavity designs.
  - **Multiple-cell, Wheel tuning mechanism, Tunable photonic crystal**
- The effectiveness of the multiple-cell design was initially showcased using a 2-cell cavity.
- Further, **a near KSVZ run** was successfully executed **with an 8-cell cavity.**
- **A KSVZ run** was conducted using a **newly designed 3-cell cavity.**

- We introduced a **novel tuning method for photonic crystal cavities.**
- A proof-of-concept experiment is being prepared, employing a tunable 5x5 photonic crystal cavity.

- To extend the search to much higher frequencies, the concept of a **horn array haloscope has been proposed.**

# Summary (2)

- A new detection method, **heterodyne haloscope**, has been presented.
- It utilizes a probe tone to amplify weak signal power, effectively reducing the noise contribution from a power detector.
- The **variance estimator** with a **heterodyne interferometer** for a known coherence signal **provides effective noises near the Standard Quantum Limit**
- This technique is significant as it lays the groundwork for the development of a single photon detector